

การศึกษาโครงสร้างสำหรับการทำวิศวกรรมโปรตีน
ของเอนไซม์ไกลโคซิเนส

นางสาวสลิลา เฟ็งไธสง

วิทยานิพนธ์นี้เป็นส่วนหนึ่งของการศึกษาตามหลักสูตรปริญญาวิทยาศาสตรดุษฎีบัณฑิต

สาขาวิชาชีวเคมี

มหาวิทยาลัยเทคโนโลยีสุรนารี

ปีการศึกษา 2554

**STRUCTURAL ANALYSIS FOR PROTEIN
ENGINEERING OF A GLYCOSYNTASE**

Salila Pengthaisong

**A Thesis Submitted in Partial Fulfillment of the Requirements for the
Degree of Doctor of Philosophy in Biochemistry
Suranaree University of Technology
Academic Year 2011**

STRUCTURAL ANALYSIS FOR PROTEIN ENGINEERING OF A GLYCOSYNTHASE

Suranaree University of Technology has approved this thesis submitted in partial fulfillment of the requirements for the Degree of Doctor of Philosophy.

Thesis Examining Committee

(Asst. Prof. Dr. Kunwadee Rangriwatananon)

Chairperson

(Assoc. Prof. Dr. James R. Ketudat-Cairns)

Member (Thesis Advisor)

(Prof. Dr. M.R. Jisnuson Svasti)

Member

(Assoc. Prof. Dr. Wipa Suginta)

Member

(Assoc. Prof. Dr. Mariena Ketudat-Cairns)

Member

(Dr. Buabarn Kuaprasert)

Member

(Prof. Dr. Sukit Limpijumnong)

Vice Rector for Academic Affairs

(Assoc. Prof. Dr. Prapun Manyum)

Dean of Institute of Science

สลิลา เฟ็งไชสง : การศึกษาโครงสร้างสำหรับการทำวิศวกรรมโปรตีนของเอนไซม์
ไกลโคซินเทส (STRUCTURAL ANALYSIS FOR PROTEIN ENGINEERING OF A
GLYCOSYNTASE) อาจารย์ที่ปรึกษา: รองศาสตราจารย์ ดร.เจมส์ เกตุทัต-คาร์นส์,
172 หน้า.

เอนไซม์ BGlul1 เบตาไกลูโคซิเดสจากข้าวที่มีการดัดแปลงกรดอะมิโนกลูตามีนวาลิวอิล
ไพล์ตำแหน่งที่386 เป็นกรดอะมิโนไกลซีน (E386G) ซีรีน (E386S) และอะลานีน (E386A) ทำให้
เกิดเอนไซม์ไกลโคซินเทสที่สามารถสังเคราะห์ *p*-nitrophenyl (pNP) cellooligosaccharides ได้
ความยาวถึง 11 หน่วยน้ำตาลกลูโคสได้ปริมาณแตกต่างกัน โดยเอนไซม์กลายพันธุ์ไกลซีนสามารถ
ทำงานเป็นเอนไซม์ไกลโคซินเทสได้สูงสุด ในขณะที่เอนไซม์กลายพันธุ์อะลานีนมีความสามารถ
ต่ำสุด การวิเคราะห์โครงสร้างเชิงซ้อนของผลิตภัณฑ์ไกลโคซินเทสไกลซีน อะลานีน และซีรีน
ที่มีและไม่มี α -D-glucopyranosyl-fluoride (α -GlcF) พบว่าโมเลกุลของน้ำ อยู่ใกล้กับตำแหน่งของ
กรดอะมิโนวาลิวอิลไพล์ในโครงสร้างของเอนไซม์ BGlul1 ดั้งเดิม แม้ว่าพันธะไฮโดรเจนระหว่าง
น้ำกับซีรีนไฮดรอกซิล และน้ำกับซัลฟาฟลูออไรด์ที่เกิดขึ้นนี้อาจมีส่วนช่วยในการโยกย้ายฟลูออไรด์
ในระหว่างการเกิดปฏิกิริยาการสังเคราะห์สารของเอนไซม์ไกลโคซินเทสซีรีน ในขณะที่
ความสามารถในการเคลื่อนที่ที่มากกว่าของโมเลกุลน้ำในตำแหน่งเดียวกันพื้นเอนไซม์ไกลโคซิน
เทสไกลซีน อาจส่งผลให้เอนไซม์นี้มีความสามารถในการทำงานสูงกว่าเอนไซม์ไกลโคซินเทสอื่น
โครงสร้างเชิงซ้อนของเอนไซม์ไกลโคซินเทสไกลซีนกับ cellootetraose และเอนไซม์กับ
cellopentaose ยืนยันว่าโซ่ข้างของกรดอะมิโน N245 S334 และ Y341 จับกับหน่วยของน้ำตาล
กลูโคสของ cellooligosaccharide ที่ตำแหน่งจับ +2 +3 และ +4 ของเอนไซม์ นอกจากนี้ยังพบว่า
เอนไซม์กลายพันธุ์ที่ดัดแปลงกรดอะมิโนเหล่านี้มีประสิทธิภาพในการย่อย cellooligosaccharides
สายยาวได้ต่ำกว่าเอนไซม์เบตาไกลูโคซิเดสดั้งเดิมเพียงเล็กน้อย อย่างไรก็ตาม เอนไซม์ไกลโคซิน
เทสไกลซีนกลายพันธุ์ Y341A Y341L และ N245V สามารถสังเคราะห์ *p*NP-cellooligosaccharides
ได้สายสั้นกว่าเอนไซม์ไกลโคซินเทสไกลซีนและเอนไซม์ไกลโคซินเทสไกลซีนกลายพันธุ์ S334A
ซึ่งแสดงว่ากรดอะมิโน Y341 และ N245 มีบทบาทสำคัญในการสังเคราะห์ oligosaccharides สาย
ยาว

เอนไซม์ไกลโคซินเทสไกลซีนสามารถสังเคราะห์ cellooligosaccharides ได้เมื่อใช้
น้ำตาลหมู่ให้ชนิด α -GlcF และน้ำตาลหมู่รับชนิด *p*NP- β -D-cellobioside (pNPC2) หรือ
cellooligosaccharide ผลการทดสอบการทำงานของเอนไซม์ไกลโคซินเทสไกลซีนกับน้ำตาลหมู่
ให้และน้ำตาลหมู่รับชนิดอื่นๆ พบว่าเอนไซม์ไกลโคซินเทสไกลซีนชนิดแรก (BGlul1 E386G)

สามารถย่อย *pNP-β-D-glucopyranoside* (*pNPGlc*) และ *pNP-β-D-fucopyranoside* (*pNPFuc*) เป็น *pNP* และน้ำตาลกลูโคสและน้ำตาลฟูโคส ซึ่งเป็นผลมาจากกรปนเป็อนของเอนไซม์ BGlul เเบตากลูโคซิเดสตั้งเดิมในชั้นตอนการเตรียมเอนไซม์ ผลึกัณที่ที่เกิดจากปฏิกิริยาของ α -GlcF และ *pNPFuc* ได้แก่ $\text{Fuc-}\beta\text{-(1}\rightarrow\text{3)-Fuc-pNP}$ $\text{Glc-}\beta\text{-(1}\rightarrow\text{3)-Fuc-pNP}$ และ $\text{Fuc-}\beta\text{-(1}\rightarrow\text{4)-Glc-}\beta\text{-(1}\rightarrow\text{3)-Fuc-pNP}$ ซึ่งเป็นผลจากการการทำงานของทั้งเอนไซม์ BGlul เเบตากลูโคซิเดสและเอนไซม์ไกลโคซินเทส การยับยั้งการทำงานของเอนไซม์ BGlul เเบตากลูโคซิเดสโดยใช้ cyclophellitol ยืนยันว่าการเตรียมเอนไซม์ไกลโคซินเทสไกลซินชนิดแรกถูกปนเป็อนด้วยเอนไซม์ BGlul เเบตากลูโคซิเดส เอนไซม์ไกลโคซินเทสไกลซินจากข้าวชนิดที่สอง (BGlul E386G2) จึงถูกสร้างขึ้นมาเพื่อลดโอกาสการเปลี่ยนกลับไปเป็นเอนไซม์ BGlul เเบตากลูโคซิเดสตั้งเดิมโดยเปลี่ยนนิวคลีโอไทด์สองตัวในตำแหน่งกลายพันธุ์ผลการทดสอบพบว่าเอนไซม์ไกลโคซินเทสไกลซินชนิดที่สองมีการทำงานป็นเอนไซม์ไกลโคซินเทสเท่านั้น เอนไซม์ไกลโคซินเทสไกลซินชนิดที่สองสามารถเร่งปฏิกิริยาการโยกย้ายหมู่น้ำตาลจากน้ำตาลหมู่ให้ α -GlcF α -L-arabinosyl fluoride α -D-fucosyl fluoride α -D-galactosyl fluoride α -D-mannosyl fluoride และ α -D-xylosyl fluoride ไปยังน้ำตาลหมู่รับ *pNPC2* ผลึกัณที่สังเคราะห์ที่ได้จากปฏิกิริยาของน้ำตาลหมู่ให้ α -fucosyl fluoride และ α -mannosyl fluoride ได้รับการยืนยันว่าเป็นผลมาจากการเชื่อมต่อด้วยพันธะไกลโคซิดิก $\beta\text{-(1}\rightarrow\text{4)}$ ของหน่วยน้ำตาลกลูโคสนอกจากนี้ เอนไซม์ไกลโคซินเทสไกลซินสามารถโยกย้ายน้ำตาลกลูโคสจากน้ำตาลหมู่ให้ α -GlcF ไปยังน้ำตาลหมู่รับกลูโคส cellobiose *pNPGlc* *pNPFuc* *pNP-β-D-galactopyranoside* และ *pNP-β-D-xylopyranoside* ได้ ขณะที่สามารถโยกย้ายน้ำตาลกลูโคสไปยัง *pNP-β-D-mannopyranoside* ได้เพียงเล็กน้อย การผลิต oligosaccharides สายยาวส่วนใหญ่สามารถเกิดขึ้นได้กับน้ำตาลหมู่รับที่มี 4-OH แบบ equatorial ซึ่งความสามารถในการเร่งปฏิกิริยานี้ของเอนไซม์ BGlul ไกลโคซินเทสไกลซินเป็นไปได้อีกต่อเมื่อมีการกำจัดเอนไซม์เบตากลูโคซิเดสที่ปนเป็อนออกไปก่อนเท่านั้น

สาขาวิชาชีวเคมี

ปีการศึกษา 2554

ลายมือชื่อนักศึกษา _____

ลายมือชื่ออาจารย์ที่ปรึกษา _____

ลายมือชื่ออาจารย์ที่ปรึกษาร่วม _____

SALILA PENGTHAISONG : STRUCTURAL ANALYSIS FOR PROTEIN
ENGINEERING OF A GLYCOSYNTASE. THESIS ADVISOR :
ASSOC. PROF. JAMES R. KETUDAT-CAIRNS, Ph.D. 172 PP.

STRUCTURAL ANALYSIS FOR PROTEIN ENGINEERING OF A
GLYCOSYNTASE

Rice BGlu1 β -glucosidase nucleophile mutants E386G, E386S and E386A are glycosynthases that can synthesize *p*-nitrophenyl (*p*NP)-cellooligosaccharides of up to 11 residues with different efficiencies. The E386G mutant exhibits the highest glycosynthase activity and E386A the lowest. The X-ray crystal structures of the E386G, E386A and E386S glycosynthases with and without α -D-glucopyranosyl fluoride (α -GlcF) were solved and found to contain an ordered water molecule near the position of the nucleophile of the BGlu1 native structure. Strong hydrogen bonds between the water, the serine hydroxyl and the alpha-fluoride may aid fluoride departure in E386S, but the greater flexibility in the positioning of this water molecule in E386G may result in its yet higher activity. The structures of E386G glycosynthase in complex with cellotetraose and cellopentaose confirmed that the sidechains of N245, S334 and Y341 interact with glucosyl residues in cellooligosaccharide binding subsites +2, +3 and +4. Mutants in which these residues were replaced in BGlu1 β -glucosidase hydrolysed long cellooligosaccharides with only somewhat lower efficiency than does the wild type enzyme. However, the Y341A, Y341L and N245V mutants of the E386G glycosynthase synthesize shorter *p*NP-cellooligosaccharides than do the E386G glycosynthase and its S334A mutant, suggesting that Y341 and N245 play important roles in the synthesis of long oligosaccharides. X-ray structural studies revealed that cellotetraose binds to the Y341A mutant of the glycosynthase in a very different mode than it does the wild type enzyme, possibly explaining the similar hydrolysis, but poorer synthesis of longer oligosaccharides by Y341 mutants.

The E386G glycosynthase catalyzes the synthesis of cellooligosaccharides from α -GlcF donor and *p*NP- β -D-cellobioside (*p*NPC2) or cellooligosaccharide acceptors. When activity with other donors and acceptors was tested, the initial enzyme preparation cleaved *p*NP- β -D-glucopyranoside (*p*NPGlc) and *p*NP- β -D-fucopyranoside (*p*NPFuc) to *p*NP and glucose and fucose, suggesting contamination with wild type BGlu1 β -glucosidase. The products from reaction of α -GlcF and *p*NPFuc, included Fuc- β -(1 \rightarrow 3)-Fuc-*p*NP, Glc- β -(1 \rightarrow 3)-Fuc-*p*NP and Fuc- β -(1 \rightarrow 4)-Glc- β -(1 \rightarrow 3)-Fuc-*p*NP, suggesting the presence of both wild type BGlu1 and its glycosynthase. Inhibition of the BGlu1 β -glucosidase activity within this preparation by cyclophellitol confirmed that the E386G glycosynthase preparation was contaminated with wild type BGlu1. Rice BGlu1 E386G2, generated from a new construct designed with two nucleotide changes in the mutated codon to minimize back-mutation and misreading, showed glycosynthase activity without wild type hydrolytic or transglycosylation activity. E386G2 catalyzed transfer of glycosyl residues from α -GlcF, α -L-arabinosyl fluoride, α -D-fucosyl fluoride, α -D-galactosyl fluoride, α -D-mannosyl fluoride and α -D-xylosyl fluoride donors to *p*NPC2 acceptor. The synthetic products from the reactions of α -fucosyl fluoride and α -mannosyl fluoride donors were confirmed to result from addition of a β -(1 \rightarrow 4)-linked glycosyl residue. Moreover, the E386G glycosynthase transferred glucose from α -GlcF donor to glucose, cellobiose, *p*NPGlc, *p*NPFuc, *p*NP- β -D-galactopyranoside and *p*NP- β -D-xylopyranoside acceptors, but little to *p*NP- β -D-mannopyranoside. Production of longer oligosaccharides occurred most readily on acceptors with an equatorial 4-OH. This assessment of BGlu1 E386G glycosynthase catalytic abilities was possible only after the elimination of wild type contamination.

School of Biochemistry

Academic Year 2011

Student's signature _____

Advisor's signature _____

Co-advisor's signature _____

ACKNOWLEDGEMENTS

I would like to express my deepest appreciation to my advisor Assoc. Prof. Dr. James R. Ketudat Cairns for providing me the opportunity to study towards my Ph.D. degree in Biochemistry, and for his patient and continuous guidance, unconditional support, and encouragement. I am also deeply grateful to my co-advisor, Dr. Buabarn Kuaprasert at the Synchrotron Light Research Institute (Public Organization) of Thailand (SLRI) for her valuable guidance, advice on X-ray crystallography and helping me on the structural analysis.

I gratefully recognize the contribution of Prof. Dr. Stephen G. Withers for giving me a chance to do some parts of my research at Department of Chemistry, University of British Columbia, providing valuable suggestions, scientific discussions, and excellent guidance. Special thanks are extended to Chi-Fan Chen for NMR analysis, and all Withers lab members for providing synthetic α -glycosyl fluorides, research information and essential facilities and for their friendship. I also thank Kah-Yee Li and Prof. Dr. Herman S. Overkleeft, University of Leiden, for their generous gift of cyclophellitol.

I would like to thank Greanggrai Hommalai and Watchalee Chuenchor for generating the original E386A, E386G and E386S glycosynthase vectors, and I also thank Greanggrai Hommalai and Prof. Dr. M.R. Jisnuson Svasti for initiation of this work and for sharing preliminary data on galactoside production with BGlu1 E386S glycosynthase.

I would like to also express my deepest gratitude to Assoc. Prof. Dr. Jirundon Yuvaniyama for providing me the chance to learn X-ray crystallography and valuable technical skills, and his precious advice. I would like to thank Assoc. Prof. Dr. Chun-Jung

Chen, Dr. Phimonphan Chuankhayan and the protein crystallography beamline staff of the National Synchrotron Radiation Research Center (NSRRC), Hsinchu, Taiwan, for data collection and processing assistance, and the SLRI and its macromolecular X-ray crystallography staff, for providing in-house X-ray diffraction.

I would like to thank Prof. Dr. M.R. Jisnuson Svasti, Asst. Prof. Dr. Kunwadee Rangsiwatananon, Assoc. Prof. Dr. Wipa Suginta and Assoc. Prof. Dr. Mariena Ketudat-Cairns for patiently reading this dissertation and providing helpful comments.

I wish to express my special thanks to all my friends in the School of Biochemistry, Suranaree University of Technology and for their constant support and helping me throughout the project and in making this journey of mine relatively easy.

This Ph.D. dissertation was supported by a scholarship from the SLRI, the Suranaree University of Technology National Research University Project, the Thailand Research Fund and the Natural Sciences and Engineering Research Council of Canada through Discovery grants and a CREATE training grant to Prof. Dr. Steve Withers. Portions of this research were conducted at the NSRRC, a national user facility supported by the National Science Council of Taiwan, ROC. The NSRRC Synchrotron Radiation Protein Crystallography Facility is supported by the National Research Program for Genomic Medicine.

Finally, I would like to express my deepest gratitude to my family for their unconditional love, care, support, and encouragement. The usefulness of this thesis, I dedicate to my parents and my teachers who have taught me since my childhood.

Salila Pengthaisong

CONTENTS

	Page
ABSTRACT IN THAI.....	I
ABSTRACT IN ENGLISH	III
ACKNOWLEDGEMENTS	V
CONTENTS	VII
LIST OF TABLES	XIII
LIST OF FIGURES	XV
LIST OF ABBREVIATIONS	XX
CHAPTER	
I INTRODUCTION	1
1.1 Glycoside hydrolases	1
1.2 Glycoside hydrolase classification.....	1
1.3 Glycoside hydrolase families and clans.....	2
1.4 Glycosidase mechanism	3
1.5 β -Glucosidases.....	10
1.6 GH1 structures and substrate specificities.....	12
1.7 Oligosaccharide and glycoside synthesis	16
1.8 Glycosynthases	21
1.9 Improvement of glycosynthase activity	24
1.10 Rice BGlu1 β -glucosidase.....	32
1.11 Research objectives.....	38

CONTENTS (Continued)

	Page
II MATERIALS AND METHODS	39
2.1 Materials	39
2.1.1 Plasmids and bacterial strains	39
2.1.2 Oligonucleotides and mutagenic primers	39
2.1.3 Reagents and chemicals	41
2.2 General methods	43
2.2.1 Preparation of competent cells of <i>E. coli</i> strains XL-1 blue and Origami(DE3)	43
2.2.2 Transformation of plasmid DNA into competent cells	44
2.2.3 Mutagenesis with the QuikChange [®] Site-Directed Mutagenesis Kit ..	44
2.2.4 SDS-PAGE electrophoresis	45
2.3 Mutations	46
2.3.1 Mutation of rice BGlu1 and BGlu1 E386G	46
2.3.2 Generation of E386G2 mutant of rice BGlu1	46
2.4 Protein expression	47
2.5 Protein purification	47
2.5.1 Protein purification for crystallization	47
2.5.2 Protein purification for characterization	49
2.6 Protein crystallization	50
2.7 Data collection and processing	52
2.8 Structure solution and refinement	53

CONTENTS (Continued)

	Page
2.9 Oligosaccharide hydrolysis	54
2.10 Oligosaccharide synthesis by BGlu1 glycosynthase enzymes	55
2.11 Transglycosylation by BGlu1 E386G with various donors.....	56
2.12 Transglycosylation by BGlu1 E386G and 4 mutants to various acceptors.....	56
2.13 Transglycosylation by BGlu1 E386G2 mutant.....	57
2.14 NMR spectroscopy of glycosynthase products.....	57
2.15 Cyclophellitol inhibition.....	59
2.15.1 Time courses of cyclophellitol inhibition.....	59
2.15.2 Kinetic analysis	59
2.15.3 Cyclophellitol inhibition of transglycosylation	61
III RESULTS	62
3.1 Protein purification	62
3.2 Protein crystallization.....	66
3.2.1 BGlu1 E386G, E386S and E386A without and with α -GlcF	66
3.2.2 BGlu1 E386G with oligosaccharides	67
3.2.3 BGlu1 E386G mutants with oligosaccharides	67
3.3 3D structures of three glycosynthases in complexes with substrates.....	73
3.4 Oligosaccharide-binding residue mutants	87
3.5 Transglycosylation.....	89
3.6 Structures of oligosaccharide-binding site mutants	95

CONTENTS (Continued)

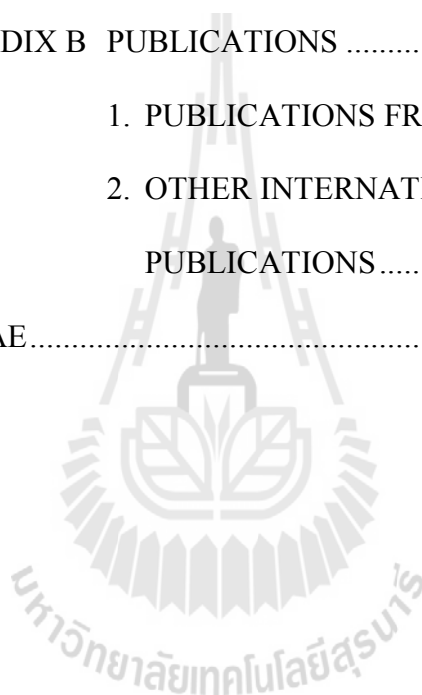
	Page
3.7 Donor specificity: transglycosylation activity of E386G using various donors	100
3.8 Acceptor specificity: transglycosylation activity of BGlu1 E386G and its mutants from α -glucosyl fluoride to various <i>p</i> NP-glycoside acceptors.....	102
3.9 NMR characterization of reaction product linkages	110
3.9.1 NMR and MS Spectra.....	111
3.9.1.1 4-Nitrophenyl [(2,3,4-tri- <i>O</i> -acetyl- β -D-fucopyranosyl)- (1 \rightarrow 4)- <i>O</i> -2,3,6-tri- <i>O</i> -acetyl- β -D-glucopyranosyl]- (1 \rightarrow 4)- <i>O</i> -2,3,6-tri- <i>O</i> -acetyl- β -D-glucopyranoside.....	111
3.9.1.2 4-Nitrophenyl [(2,3,4,6-tetra- <i>O</i> -acetyl- β -D- mannopyranosyl)-(1 \rightarrow 4)- <i>O</i> -2,3,6-tri- <i>O</i> -acetyl- β -D- glucopyranosyl]-(1 \rightarrow 4)- <i>O</i> -2,3,6-tri- <i>O</i> -acetyl- β -D- glucopyranoside	111
3.9.1.3 4-Nitrophenyl (2,3,4-tri- <i>O</i> -acetyl- α -D- fucopyranosyl)-(1 \rightarrow 3)-2,4-di- <i>O</i> -acetyl- β -D- fucopyranoside	112
3.9.1.4 4-Nitrophenyl (2,3,4,6-tetra- <i>O</i> -acetyl- α -D- glucopyranosyl)-(1 \rightarrow 3)-2,4-di- <i>O</i> -acetyl- β -D- fucopyranoside	112

CONTENTS (Continued)

	Page
3.9.1.5 4-Nitrophenyl [(2,3,4-tri- <i>O</i> -acetyl- β -D-fucopyranosyl)- (1 \rightarrow 4)- <i>O</i> -2,3,6-tri- <i>O</i> -acetyl- β -D-glucopyranosyl]- (1 \rightarrow 3)- <i>O</i> -2,4-di- <i>O</i> -acetyl- β -D-fucopyranoside	113
3.10 Cyclophellitol inhibition.....	115
3.11 Transglycosylation activity of BGlu1 E386G2	120
IV DISCUSSION	126
4.1 Protein expression and purification.....	126
4.2 Protein crystallization.....	127
4.3 3D structures of three glycosynthases in complexes with substrates.....	127
4.4 Structures of BGlu1 E386G glycosynthase complexed with cellooligosaccharides.....	130
4.5 Oligosaccharide-binding residue mutants	131
4.6 Transglycosylation.....	132
4.7 Structures of oligosaccharide-binding site mutants	133
4.8 Donor and acceptor specificities.....	134
4.9 NMR characterization of reaction product linkages	136
4.10 Cyclophellitol inhibition.....	137
4.11 Transglycosylation activity of BGlu1 E386G2	139
V CONCLUSION	142
REFERENCES.....	144
APPENDICES.....	165

CONTENTS (Continued)

	Page
APPENDIX A MOLECULAR MASS OF TRANGLUCOSYLATION PRODUCTS SYNTHESIZED BY THE RICE BGLU1 E386G USING α -GLCF AND PNPC2	166
APPENDIX B PUBLICATIONS	170
1. PUBLICATIONS FROM PH.D. THESIS	170
2. OTHER INTERNATIONAL PUBLICATIONS	170
CURRICULUM VITAE	172



LIST OF TABLES

Table		Page
2.1	Oligonucleotide primers used in mutagenesis	40
2.2	Internal oligonucleotide primers used for DNA sequencing of full-length rice <i>bglu1</i> and <i>bglu1 E386G</i>	41
3.1	Crystallization conditions and X-ray diffraction of protein crystals	68
3.2	Data collection statistics.....	76
3.3	Refinement statistics	78
3.4	Kinetic parameters of BGlu1 wild type and mutants for hydrolysis of cellotriose, cellotetraose and cellopentaose.....	88
3.5	Glycosynthase reaction products of BGlu1 E386G glycosynthase and its mutants with equal amounts of α -glucosyl fluoride donor and <i>pNPC2</i> acceptor.....	93
3.6	Products of glycosynthase reactions of BGlu1 E386G glycosynthase and its 4 glycosynthase mutants using α -glucosyl fluoride donor and <i>pNPFuc</i> acceptor	108
3.7	Products of glycosynthase reactions of BGlu1 E386G glycosynthase and its 4 mutants using α -glucosyl fluoride donor and <i>pNPGlc</i> acceptor.....	109
3.8	Structures of products of glycosynthase reactions of BGlu1 E386G and BGlu1 E386G/N245V	114
3.9	Products of glycosynthase reactions of BGlu1 E386G2 glycosynthase using different donors and <i>pNPC2</i> acceptor.....	123

LIST OF TABLES (Continued)

Table	Page
3.10 Products of glycosynthase reactions of BGlu1 E386G2 glycosynthase using α -glucosyl fluoride donor and different acceptors.....	124



LIST OF FIGURES

Figure	Page
1.1	Mechanisms of inverting and retaining glycosidases..... 5
1.2	A non-carboxylate residue (tyrosine) as a nucleophile 6
1.3	Schematic diagram showing active site structure of <i>Sinapis alba</i> myrosinase in a covalent glycosyl-enzyme intermediate 7
1.4	Mechanisms of azide rescue of the activity of a nucleophile mutant and an acid/base mutant 9
1.5	Rescue of catalytic activity in the acid/base mutant of <i>Agrobacterium</i> sp. β -glucosidase by substrate-assisted protonation..... 10
1.6	Structure of maize β -glucosidase Glu1 13
1.7	Active sites of ZmGlu1 β -glucosidase in complex with DIMBOA-Glc and SbDhr1 dhurrinase in complex with dhurrin 16
1.8	Mechanism of hydrolysis and transglycosylation by retaining <i>Agrobacterium</i> sp. β -glucosidase 19
1.9	Synthesis of a thioglycoside by a thioglycoligase 21
1.10	Mechanism of transglycosylation with a glycosynthase 22
1.11	Schematic diagram of the interactions of Man26A E320G with mannobiose 25
1.12	Overall model structure of the evolved <i>Agrobacterium</i> sp. glycosynthase 2F6 showing secondary structure elements and the positions of mutations. 27

LIST OF FIGURES (Continued)

Figure	Page
1.13 Schematic diagram of the Cel7B E197S-ligand interactions	29
1.14 Reaction mechanism of a glycosynthase derived from an inverting glycosidase.....	30
1.15 The synthesis of thioglycoside by a thioglycosynthase.....	31
1.16 Active site of the BGlu1-G2F complex and a covalent glycosyl-enzyme intermediate	35
1.17 Hydrogen bonding between the BGlu1 E176Q mutant active site residues and cellopentaose	37
2.1 Construct of the protein-coding sequence of recombinant pET32a(+) with the <i>bglu1</i> cDNA inserted after the enterokinase cleavage site	39
3.1 SDS-PAGE of purified BGlu1 E386G and its mutants	63
3.2 SDS-PAGE of purified BGlu1 E386A and BGlu1 E386S	64
3.3 SDS-PAGE of purified BGlu1 β -glucosidase and its mutants.....	65
3.4 SDS-PAGE of purified BGlu1 E386G2 from the purification steps.....	66
3.5 Crystals of BGlu1 glycosynthase enzymes with and without ligands.....	71
3.6 Crystals of BGlu1 glycosynthase mutants with celooligosaccharides	72
3.7 The electron densities of α -GlcF and water in the -1 subsite of BGlu1 E386G, BGlu1 E386A and BGlu1 E386S	80
3.8 Comparison of the active sites of rice BGlu1 E386G, E386A and E386S glycosynthases	81

LIST OF FIGURES (Continued)

Figure	Page
3. 9	Comparison of active sites of rice BGlu1 E386G, E386A and E386S glycosynthases and free BGlu1 and its 2-fluoroglucosyl enzyme intermediate..... 82
3. 10	The Fo-Fc electron density maps of oligosaccharides in the active sites of BGlu1 E386G 83
3. 11	The 2Fo-Fc electron densities of oligosaccharides in the active site of the BGlu1 E386G 84
3. 12	Comparison of cellotetraose and cellopentaose binding in the active site of BGlu1 E386G and BGlu1 E176Q 85
3. 13	Diagrams of the strong hydrogen bonds between oligosaccharides, surrounding amino acid residues and the network of water molecules in the active site of BGlu1 E386G 86
3. 14	Transglucosylation reactions between α -GlcF donor and <i>p</i> NPC2 acceptor at various molar ratios 91
3. 15	TLC detection of products of transglucosylation reactions between α -GlcF donor and <i>p</i> NPC2 acceptor at various molar ratios..... 92
3. 16	HPLC elution profiles of the transglucosylation products for reaction of α -GlcF donor and <i>p</i> NPC2 acceptor 94
3.1 7	The Fo-Fc electron density maps of cellotetraose in the active sites of BGlu1 E386G/S334A and BGlu1 E386G/S334A mutants..... 96
3. 18	The 2Fo-Fc electron densities of cellotetraose in the active sites of the BGlu1 E386G/S334A and BGlu1 E386G/S334A mutants 97

LIST OF FIGURES (Continued)

Figure	Page
3.19	Comparison of cellotetraose binding in the active site of BGlu1 E386G, BGlu1 E386G/S334A and BGlu1 E386G/Y341A 98
3. 20	Diagrams of the strong hydrogen bonds between cellotetraose, surrounding amino acid residues and the network of water molecules in the active sites of BGlu1 E386G/S334A and BGlu1 E386G/Y341A 99
3. 21	Products of transglycosylation catalyzed by BGlu1 E386G with various donors detected by thin layer chromatography 101
3. 22	TLC detection of transglycosylation catalyzed by BGlu1 E386G glycosynthase and its mutants using α -GlcF donor and <i>p</i> NPFuc, <i>p</i> NPGal or <i>p</i> NPXyl acceptors..... 104
3. 23	TLC detection of transglycosylation catalyzed by BGlu1 E386G glycosynthase and its mutants using α -GlcF donor and <i>p</i> NPGlc acceptor 105
3. 24	TLC detection of transglycosylation catalyzed by BGlu1 E386G glycosynthase and its mutants using α -GlcF donor and glucose or cellobiose acceptors..... 106
3. 25	TLC detection of transglycosylation catalyzed by 80 μ M BGlu1 E386G glycosynthase and its mutants with α -GlcF donor and <i>p</i> NPFuc, <i>p</i> NPGal or <i>p</i> NPXyl acceptors 107

LIST OF FIGURES (Continued)

Figure	Page
3. 26	Time course for cyclophellitol inactivation of rice BGlu1, BGlu1 E386G and BGlu1 E386G2 enzymes 117
3. 27	Cyclophellitol inhibition of rice BGlu1 118
3. 28	Effect of cyclophellitol inhibition on transglycosylation products of rice BGlu1, BGlu1 E386G and BGlu1 E386G2 with <i>p</i> NPFuc and α -GlcF 119
3. 29	TLC detection of transglycosylation catalyzed by BGlu1 E386G2 with various donors..... 121
3. 30	TLC detection of transglycosylation catalyzed by BGlu1 E386G2 with various acceptors..... 122
4.1	Reaction mechanisms of hydrolysis and transglycosylation catalyzed by rice BGlu1 β -glucosidase, covalent intermediate trapping of rice BGlu1 by cyclophellitol, and rice BGlu1 E386G glycosynthase..... 138
A1	Selected ion chromatograms of products synthesized by the rice BGlu1 E386G using α -GlcF and <i>p</i> NPC2 166
A2	Mass spectra of products synthesized by the rice BGlu1 E386G using α -GlcF and <i>p</i> NPC2 167

LIST OF ABBREVIATIONS

α -AraF	α -L-arabinosyl fluoride
α -FucF	α -D-fucosyl fluoride
α -GalF	α -D-galactosyl fluoride
α -GlcF	α -D-glucosyl fluoride
α -ManF	α -D-mannosyl fluoride
α -XylF	α -D-xylosyl fluoride)
Abs	Absorbance
ABTS	2,2'-azinobis-3-ethylbenthaiazolinesulfonic acid
(m, μ)l	(milli, micro) Liter(s)
(m, μ)g	(milli, micro) Gram(s)
(m, μ)M	(milli, micro) Molar(s)
(μ)mol	(micro) Mole(s)
$^{\circ}$ C	Degrees Celsius
bp	Base pairs
BSA	Bovine serum albumin
cDNA	Complementary deoxynucleic acid
CV	Column Volume
DMSO	dimethyl sufoxide
DNA	deoxynucleic acid
DNase	Deoxyribonuclease

LIST OF ABBREVIATIONS (Continued)

dNTPs	Deoxynucleoside triphosphates
DP	Degree of polymerization
EDTA	Ethylenediamine tetraacetate
ESI-MS	Electrospray ionization-mass spectrometry
EtOAc	Ethyl acetate
G2F	2-deoxy-2-fluoro- α -D-glucosyl moiety
GH	Glycoside hydrolase
GH1	Glycoside hydrolase family 1
Glc	Glucose
HPLC	High performance liquid chromatography
hr	Hour(s)
IMAC	Immobilized metal affinity chromatography
IPTG	Isopropyl thio- β -D-galactoside
kb	Kilo base pair(s)
kDa	Kilo Dalton(s)
LB	Luria-Bertani lysogeny broth
LC-MS	Liquid chromatography-mass spectrometry
MeOH	Methanol
min	Minute(s)
MME	Monomethyl ether
MW	Molecular weight

LIST OF ABBREVIATIONS (Continued)

nm	nanometer(s)
NMR	Nuclear magnetic resonance
OD	Optical density
PAGE	Polyacrylamide gel electrophoresis
PCR	Polymerase chain reaction
PEG	Polyethylene glycol
PMSF	Phenylmethylsulfonylfluoride
<i>p</i> NP	<i>para</i> -Nitrophenyl
<i>p</i> NP _{Ara}	<i>p</i> NP- α -L-arabinopyranoside
<i>p</i> NP _{C2}	<i>p</i> NP- β -D-cellobioside
<i>p</i> NP _{C3}	<i>p</i> NP- β -D-cellotrioside
<i>p</i> NP _{C4}	<i>p</i> NP- β -D-cellotetraoside
<i>p</i> NP _{C5}	<i>p</i> NP- β -D-cellopentaoside
<i>p</i> NP _{C6}	<i>p</i> NP- β -D-cellohexaoside
<i>p</i> NP _{C7}	<i>p</i> NP- β -D-celloheptaoside
<i>p</i> NP _{C8}	<i>p</i> NP β -D-cellooctaoside
<i>p</i> NP _{C9}	<i>p</i> NP β -D-cellonanaoside
<i>p</i> NP _{Fuc}	<i>p</i> NP- β -D-fucopyranoside
<i>p</i> NP _{Gal}	<i>p</i> NP- β -D-galactopyranoside
<i>p</i> NP _{Glc}	<i>p</i> NP- β -D-glucopyranoside
<i>p</i> NP _{Man}	<i>p</i> NP- β -D-mannopyranoside

LIST OF ABBREVIATIONS (Continued)

<i>p</i> NPXyl	<i>p</i> NP- β -D-xylopyranoside
PVDF	Polyvinylidene flouride
RNA	Ribonucleic acid
RNase	Ribonuclease
rpm	rotations per minute
s	second(s)
SDS	Sodium dodecyl sulfate
SgDhr1	Sorghum β -glucosidase (Dhurrinase)
TEMED	Tetramethylenediamine
TEV	Tobacco etch virus
TLC	Thin-layer chromatography
Tris	Tris-(hydroxymethyl)-aminoethane
UV	Ultraviolet
v/v	Volume/volume
w/v	Weight/volume
ZmGlu1	Maize β -D-glucosidase

CHAPTER I

INTRODUCTION

1.1 Glycoside hydrolases

Glycoside hydrolases (GH, EC 3.2, also called glycosyl hydrolases or glycosidases) are a widespread group of enzymes that catalyze the hydrolysis of the glycosidic bonds between two or more carbohydrates or between a carbohydrate and a non-carbohydrate residue. Glycoside hydrolases are found in all domains of living organisms, archaea, bacteria and eukaryotes. Glycoside hydrolases have many roles in nature that include digestion of carbohydrates in foods, degradation of biomass, such as cellulose and hemicellulose (Hrmova *et al.*, 1996; Sulzenbacher *et al.*, 1997), anti-bacterial defense (Henry *et al.*, 2000; Shawn and Skerrett, 2004), pathogenesis mechanisms (Duroux *et al.*, 1998; Mizutani *et al.*, 2002; Zhou *et al.*, 2009) and normal cellular functions e.g. glycoprotein synthesis (Jakob *et al.*, 2001; Gamblin *et al.*, 2009).

1.2 Glycoside hydrolase classification

Glycoside hydrolases have been classified either by activity or structural relationships. Enzyme Commission (EC) numbers comprise a numerical classification scheme for enzymes, based on the type of reaction that they catalyze and their substrate specificity. However, the EC classification is not appropriate for enzymes showing broad specificity, as is the case for many glycoside hydrolases.

Glycoside hydrolases include the enzymes catalyze hydrolysis of *O*-, *N*- and *S*-linked glycosides. However, the *S*-glycoside hydrolase (EC 3.2.3) thioglucosidase (formerly EC 3.2.3.1), has a sequence, molecular mechanism and 3D structure similar to β -glucosidases (EC 3.2.1.21) (Burmeister *et al.*, 1997). The substrate specificity and the structural features of these GH fail to group together in the EC system. Therefore, a new method to classify GH based on sequence similarities was developed by Henrissat (1991), and the thioglucosidase enzyme was reclassified in the same group as *O*-glycoside hydrolases with the EC 3.2.1.147 (Carbohydrate Active Enzymes, CAZy, database).

Glycoside hydrolases may catalyze the hydrolysis of glycosidic bonds via two different general mechanisms, which result either in retaining or in inverting the substrate anomeric configuration during the reaction (Davies and Henrissat, 1995; Sinnott, 1990). Therefore, they can be classified according to the stereochemical outcome of the hydrolysis reaction as retaining or inverting enzymes. GH can also be classified as *exo*- or *endo*-glycosidases, depending upon whether they cleave a substrate at the end (usually the nonreducing end) or in the middle, respectively, of an oligo- or polysaccharide chain. For example, most cellulases are *endo*-glycosidases, whereas LacZ β -galactosidase from *E. coli* is an *exo*-glycosidase.

1.3 Glycoside hydrolase families and clans

Glycoside hydrolases have been classified into a number of families based on their amino acid sequence similarities (Henrissat, 1991; Henrissat and Bairoch, 1993). As the number of 3D structures of GH increased, classification of families into larger groups, termed “clans” was proposed (Henrissat and Bairoch, 1996). A clan is a group

of families that have significant similarity in 3D structure, catalytic residues and mechanism. Recently, GH classification into families based on amino acid sequence, 3D structures and mechanism, and of families into the same clan by evolutionary relationship, overall structural fold, conserved arrangement of catalytic residues and mechanism of glycosidic bond hydrolysis has been maintained in the CAZy database (Henrissat and Davies, 1997; Naumoff, 2011; URL:www.cazy.org). So far, GH have been classified into 130 families and 14 clans (CAZy). The largest of the GH clans is clan GH-A, also called the 4/7 superfamily, in which the proton donor and the nucleophile residues are found on β -strands 4 and 7 of the $(\beta/\alpha)_8$ barrel structure, respectively (Jenkins *et al.*, 1995). It includes GH families 1 (GH1), GH2, GH5, GH10, GH17, GH26, GH30, GH35, GH39, GH42, GH50, GH51, GH53, GH59, GH72, GH79, GH86, GH113 and GH128.

1.4 Glycosidase mechanism

The hydrolysis of glycosidic bonds by GH takes place via general acid catalysis involving two acidic catalytic residues in the active site that act as a general acid or proton donor and a general base or nucleophile (Koshland, 1953; Sinnott, 1990). The reaction results in one of two possible stereochemical outcomes: either inversion or retention of anomeric configuration.

Inverting glycosidases (Figure 1.1A) catalyze hydrolysis via a single oxocarbenium ion-like transition state and lack a covalent enzyme intermediate formed during the catalysis. The mechanism generally involves the action of two carboxylic acid residues (Asp or Glu), which are located about 10.5 Å apart on opposite sides of the enzyme active site (Zechel and Withers, 2000; Rempel and

Withers, 2008). One carboxylic acid acts as a general base and deprotonates the incoming water nucleophile during its attack at the anomeric carbon. The other carboxylic acid acts as a general acid residue which protonates the leaving group, the aglycone, and assists in cleaving the glycosidic bond.

Retaining glycosidases (Figure 1.1B) differ in mechanism from inverting glycosidases by the formation of a covalently bound glycosyl-enzyme intermediate, and use two oxocarbenium ion-like transition states. The mechanism again has a pair of essential carboxylic acid residues (Asp or Glu) located on opposite sides of the enzyme active site, but they are normally closer together, at about 5.5 Å apart (Zechel and Withers, 2000; Rempel and Withers, 2008). In the first step (glycosylation), the glycosidic oxygen is protonated by one of the carboxylate residues, which acts as the general acid, while the other carboxylate group acts as a nucleophile and attacks the anomeric carbon, resulting in the formation of a covalently linked glycosyl-enzyme intermediate. In the second step (deglycosylation), the carboxylate residue that first acted as an acid catalyst acts as a base and deprotonates the incoming water molecule, which attacks at the anomeric center to cleave the covalent intermediate and displace the catalytic nucleophile from the sugar (Zechel and Withers, 2000). However, some glycosidases, sialidases (also called neuraminidases) and hyaluronidase, use a tyrosine as a catalytic nucleophile and an acidic amino acid in active site supports deprotonation of the Tyr and stabilizes the transition state during catalysis (Figure 1.2) (Watts *et al.*, 2003; Amaya *et al.*, 2004; Varrot *et al.*, 2005; Zhang *et al.*, 2009). Another variation on this theme is the substrate-assisted catalysis of certain enzymes with N-acetylglucosamine-containing substrates, such as GH18 and GH20 β -hexosaminidases and chitinases, in which the N-acetyl group acts as a nucleophile to

form a cyclic intermediate (Terwisscha van Scheltinga *et al.*, 1995; Knapp *et al.*, 1996; Zechel and Withers, 2000).

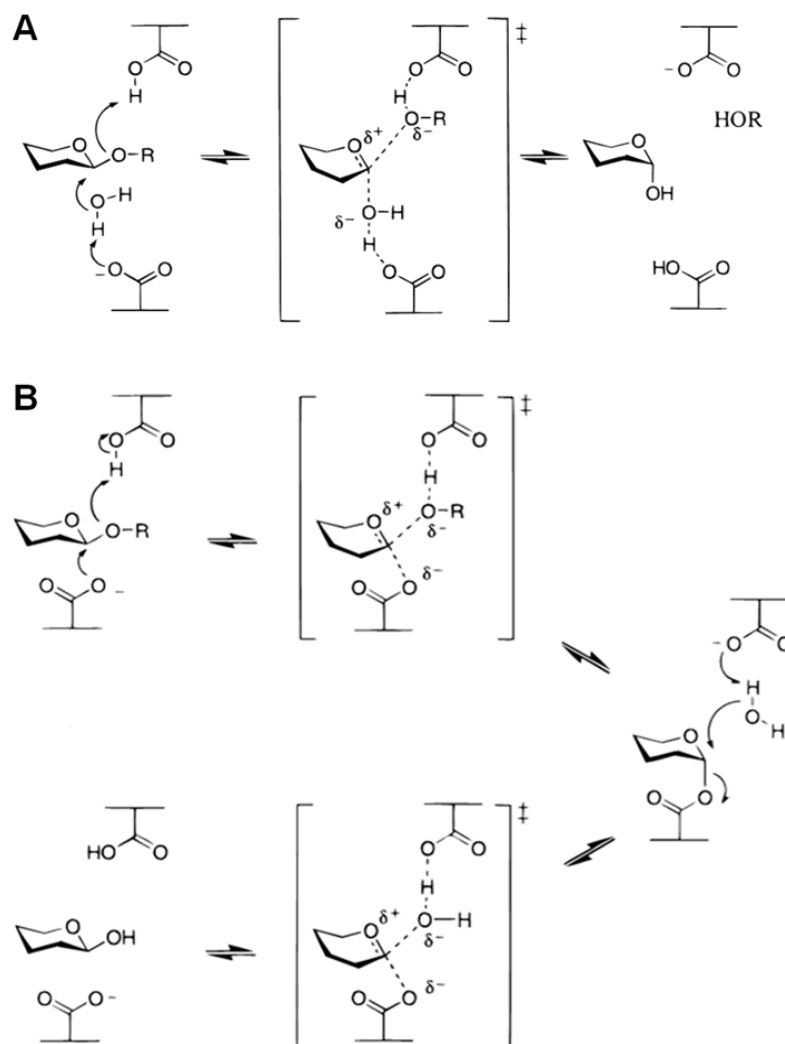


Figure 1.1 Mechanisms of inverting and retaining glycosidases. **(A)** Mechanism for inverting glycosidases. **(B)** Mechanism for retaining glycosidases (Zechel and Withers, 2000). A covalent glycosyl-enzyme intermediate is formed and displaced, with general acid/base assistance, via oxocarbenium ion-like transition states.

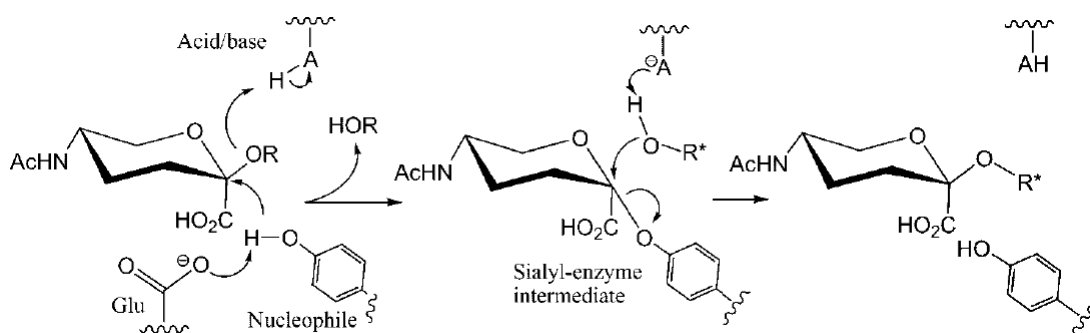


Figure 1.2 A non-carboxylate residue (tyrosine) as a nucleophile. With support of an anionic carboxylate from a glutamate, the tyrosine attacks at the anomeric center of the substrate (Vuong and Wilson, 2010). The covalent intermediate is broken down by the attack of a nucleophile (HOR*), where R* is H in the case of hydrolysis.

The two catalytic amino acids, the acid/base and nucleophile, in β -glycosidases have been investigated by mechanism-based labeling of catalytic amino acid residues, X-ray crystallography and site-directed mutagenesis studies. Covalent labeling with 2,4-dinitrophenyl-2-deoxy-2-fluoroglucoside has been successfully used in identification of the catalytic nucleophile of several β -glycosidases (Withers and Street, 1988; Street *et al.*, 1992; Withers and Aebersold, 1995; Dan *et al.*, 2000). Substitution of the 2-OH group of the substrate with fluorine destabilizes the accumulation of a partial positive charge on C1 and O5 in the transition states for glycosyl enzyme formation and hydrolysis. Therefore, the presence of the 2-fluoride leads to formation of stable covalent glycosyl-enzyme intermediates. The glycone product is released very slowly, but the glycosylation half-reaction can occur more quickly when a reactive leaving group, dinitrophenolate, is incorporated into the 2-fluoroglucoside. The formation of the covalent intermediate was confirmed by proteolytic digestion and mass spectrometry. This technique was first employed to

identify the catalytic nucleophile in a GH family 1 β -glucosidase from *Agrobacterium* (Withers *et al.*, 1987; Withers and Street, 1988). The crystal structures of the covalent intermediates of *O*-glycosidases and a *S*-glycosidase have also been solved (Figure 1.3) (Burmeister *et al.*, 1997; Chuenchor *et al.*, 2008; Noguchi *et al.*, 2008). In addition, site-directed mutagenesis has been widely used to verify the acid/base and nucleophile residues based on sequence alignment, X-ray crystallography or homology modeling (Trimbur *et al.*, 1992; Wang *et al.*, 1994; 1995; Sue *et al.*, 2006).

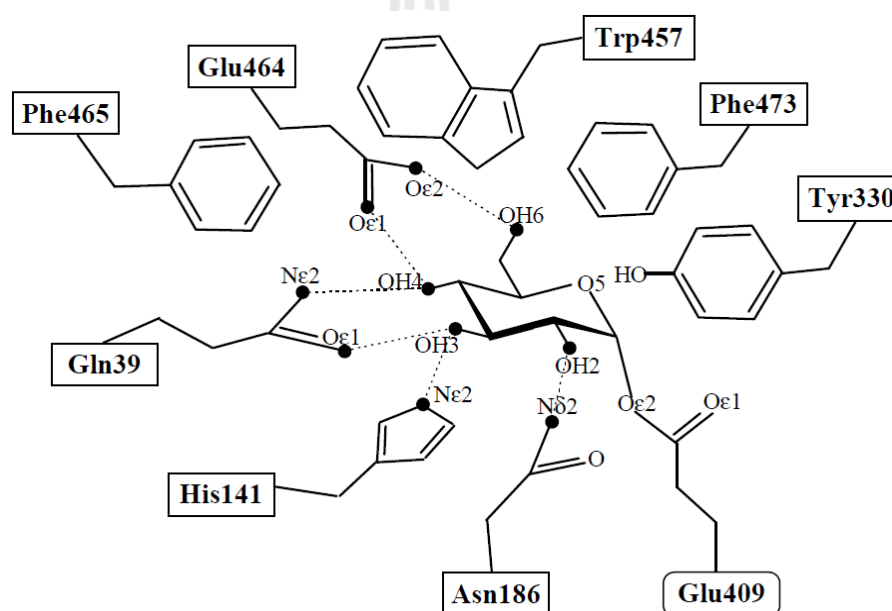


Figure 1.3 Schematic diagram showing active site structure of *Sinapis alba* myrosinase in a covalent glycosyl-enzyme intermediate (Burmeister *et al.*, 1997).

Rescue of activity by small nucleophiles has been used to identify the acid/base and nucleophile residues (Wang *et al.*, 1994; 1995; Vallmitjana *et al.*, 2001; Bravman *et al.*, 2003). An Ala mutant of the nucleophile of the *Agrobacterium* sp. β -glucosidase, which completely lacks activity, can be reactivated for hydrolysis of

dinitrophenyl glycoside by azide, formate or acetate with formation of a glycoside with inverted anomeric configuration, e.g. α -glucosyl azide (Figure 1.4A) (Wang *et al.*, 1994). In contrast, the same anomeric configuration as the substrate, β -glucosyl azide, was obtained when the activity of an *Agrobacterium* sp. β -glucosidase acid/base mutant was rescued (Figure 1.4B) (Wang *et al.*, 1995). In this case, the good leaving group, which has a low pK_a and therefore it does not require protonation, eliminates the requirement for acid catalysis in the glycosylation step, while the azide does not require basic assistance in the deglycosylation step. Surprisingly, catalytic activity can be restored to the acid/base mutant of *Agrobacterium* sp. β -glucosidase (E170G) by the inclusion of a suitably positioned carboxyl group into the substrate without an external nucleophile (Figure 1.5) (Zechel and Withers, 2000). The rescue activity has been observed with mutant species of other retaining β -glycosidases, such as *Cellulomonas fimi* β -(1 \rightarrow 4)-glycanase, *Geobacillus stearothermophilus* T6 β -xylosidase and *Streptomyces* sp. β -glucosidase (MacLeod *et al.*, 1996; Bravman *et al.*, 2003; Vallmitjana *et al.*, 2001).

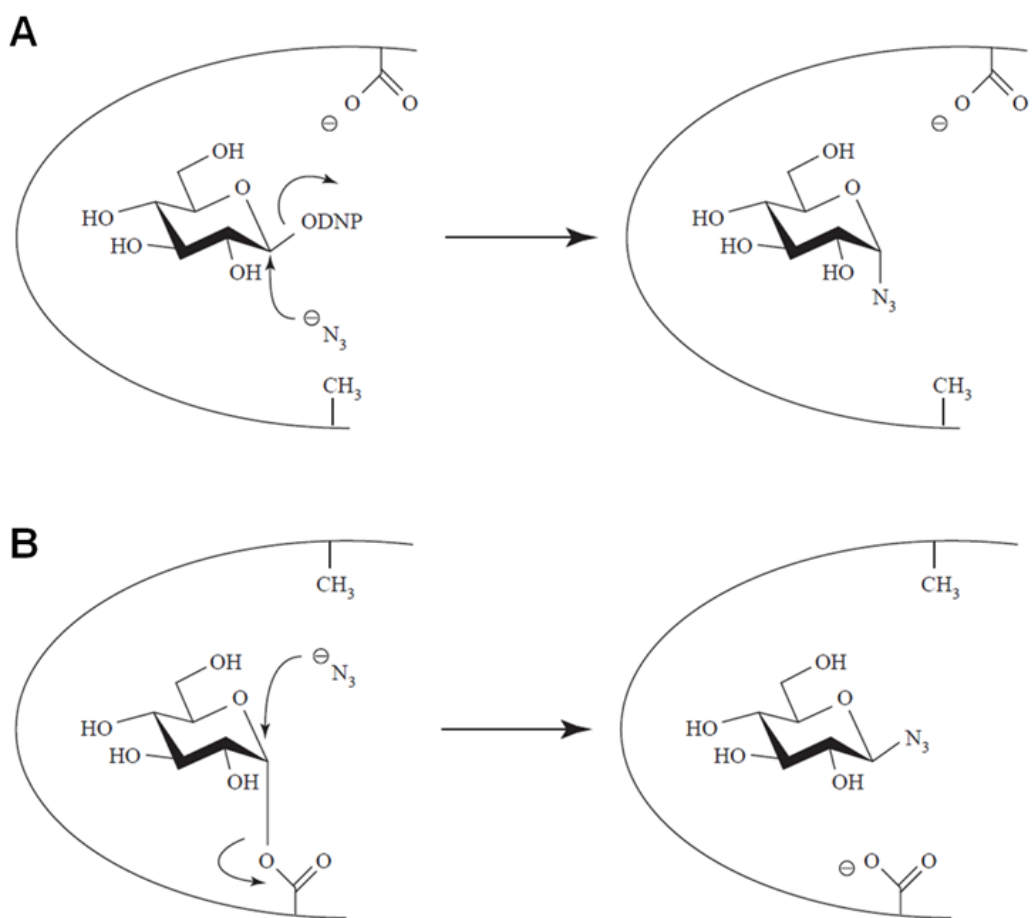


Figure 1.4 Mechanisms of azide rescue of the activity of a nucleophile mutant (A) and an acid/base mutant (B) (Ly and Withers, 1999).

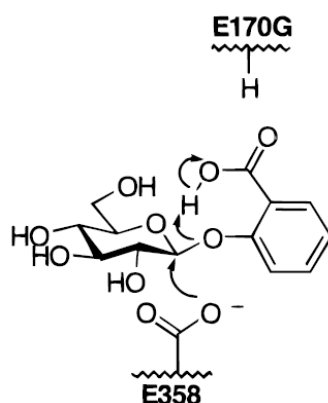


Figure 1.5 Rescue of catalytic activity in the acid/base mutant of *Agrobacterium* sp. β -glucosidase by substrate-assisted protonation (Zechel and Withers, 2000).

1.5 β -Glucosidases

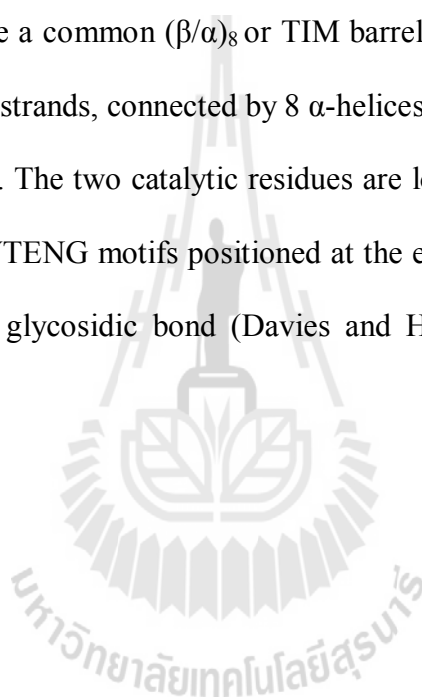
β -Glucosidases (β -D-glucoside glucohydrolases; EC 3.2.1.21) are a widespread group of enzymes that catalyze the hydrolysis of β -glucosidic bonds of disaccharides, oligosaccharides or glucosides to release terminal nonreducing glucosyl residues (Rempel and Withers, 2008). In addition to hydrolysis, many β -glucosidases catalyze transglucosylation to synthesize different β -glucosides. They occur widely in all domains of living organisms, Archaea, prokaryotes and eukaryotes and play important roles in biological and biotechnological processes. β -Glucosidases are grouped into GH1, GH3, GH5, GH9, GH30 and GH116 from the CAZY database (Henrissat, 1991; Henrissat and Bairoch, 1993; 1996; Naumoff, 2011). Plant β -glucosidases that have been characterized can be classified into GH1, GH3 and GH5 (Ketudat Cairns and Esen, 2010).

In microorganisms, bacteria and fungi, β -glucosidases involved in cellulose and cellobiose catabolism are used in the process of biomass conversion to produce

glucose, or in breaking down plant cell walls to establish pathogenic or symbiotic relationships (Ketudat Cairns and Esen, 2010). In mammals, β -glucosidases are involved in metabolism of glycolipids and dietary glucosides and may have signaling functions. For example, human β -glucosidase (lactase phlorizin hydrolase) is involved in flavonoid metabolism (Day *et al.*, 2000) and in the metabolism of dietary lactose (Naim *et al.*, 2001). Mammalian cytoplasmic β -glucosidase has also been implicated in breakdown of exogenous flavonoid glycosides, along with glycolipid metabolism, which is a known role of lysosomal acid β -glucosidase and bile acid β -glucosidase (Ketudat Cairns and Esen, 2010). In addition, deficiency of lysosomal acid β -glucosidase (glucocerebrosidase), which belongs to GH30, results in accumulation of glucocerebrosides in the lysosomes of some cells, which causes Gaucher's disease (Michelin *et al.*, 2004). In plants, β -glucosidases have been found to be involved in numerous functions, including cell wall metabolism: degradation of oligosaccharides in cell wall turnover and release of monolignols from their glycosides to stabilize secondary cell walls by lignification, defense against pathogens and herbivores by release of HCN, hydroxamic acids and other toxic compounds from their nontoxic glucosides, regulation of the biological activity of plant phytohormones, including auxin, cytokinin and gibberellin, by release of active forms from inactive hormone-glucoside conjugates, release of glycosyl blocking groups from metabolic intermediates and release of aroma compounds from nonvolatile glucosides (Dharmawardhana *et al.*, 1995; Leah *et al.*, 1995; Hakulinen *et al.*, 2000; Vetter, 2000; Haberer and Kieber, 2002; Barleben *et al.*, 2007; Zagrobelny *et al.*, 2008, Ketudat Cairns and Esen, 2010).

1.6 GH1 Structures and substrate specificities

Currently, structures of 35 GH1 enzymes and their mutants have been investigated and are available in the Protein DataBank (PDB), including 4 from archaea, 14 from bacteria, 3 from animals, 2 from fungus and 12 from plants (CAZY). In addition, several complexes of these enzymes with inhibitors or substrates are available, which provide insights into the mechanisms of both catalysis and substrate recognition. They have a common $(\beta/\alpha)_8$ or TIM barrel fold, which consists of a core of 8 twisted parallel β -strands, connected by 8 α -helices, which form the outer layer of the barrel (Figure 1.6). The two catalytic residues are located in the highly conserved T(F/L/M)NEP and I/VTENG motifs positioned at the end of the active site pocket on opposite sides of the glycosidic bond (Davies and Henrissat, 1995; Henrissat and Bairoch, 1996).



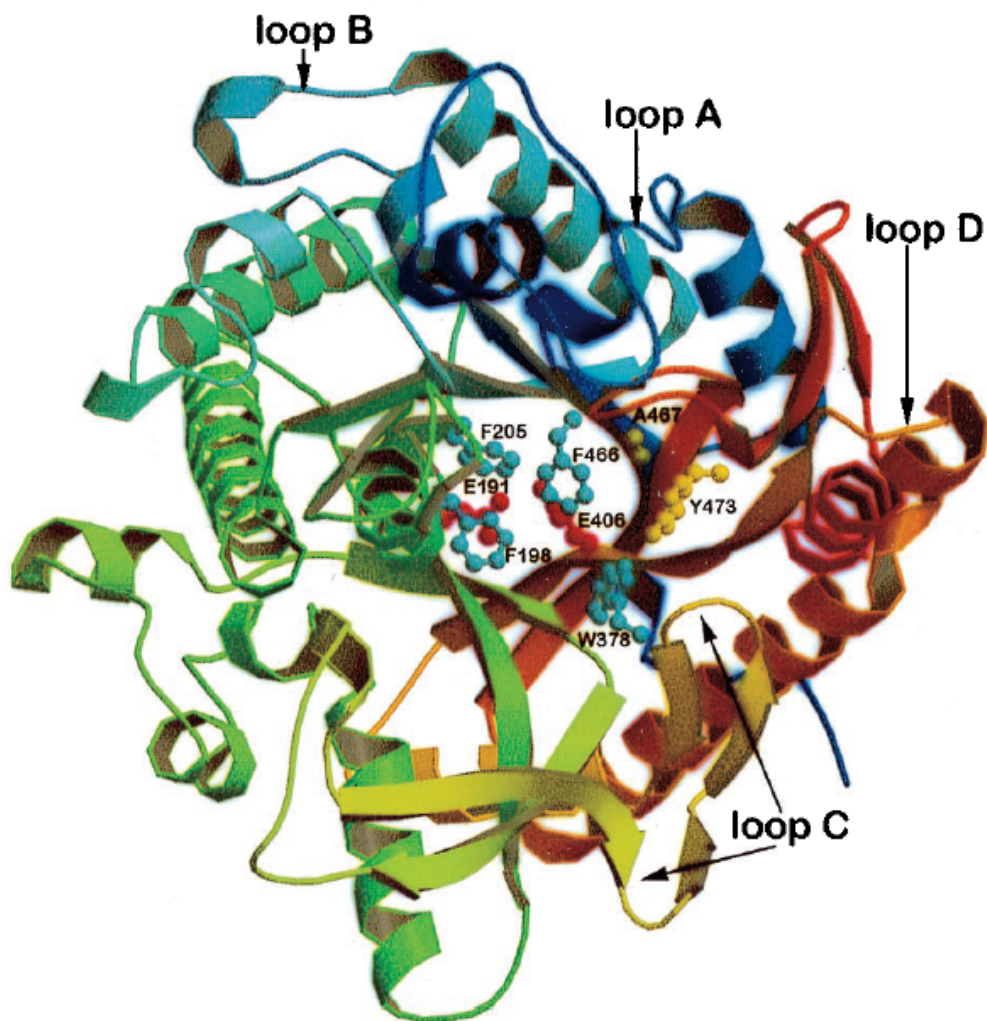


Figure 1.6 Structure of maize β -glucosidase Glu1. Ball and stick side chains are showed for the catalytic residues E191 (D191 in the inactive Glu1 E191D mutant) and E406 (red), four residues (F198, F205, W378 and F466) forming the aglycone-binding pocket (blue), and two other residues (A467 and Y473) that are probably important for aglycone recognition (yellow). Different colors and the color transitions in α -helices and β -strands trace the polypeptide backbone in the barrel-shaped three-dimensional structure from the N-terminus (dark blue) to the C-terminus (dark red) (Czjzek *et al.*, 2000). The variable loops (A, B, C and D) around the active site are labeled.

The most common enzymatic activities for GH1 glycoside hydrolases are β -D-glucosidases, β -D-fucosidases and β -D-galactosidases, which are often found within the same enzymes. However, other commonly found activities include 6-phospho- β -D-glucosidase and 6-phospho- β -D-galactosidase, β -D-mannosidase, β -D-thioglucosidase and β -D-glucuronidase. Thus, GH1 enzymes may have specificity to one or a few glycone sugars. The hydrogen bonding network of the glycone moiety at subsite -1 has been reported in several GH1 structures with covalently bound inhibitors, or other ligands (Burmeister *et al.*, 1997; Wiesmann *et al.*, 1997; Sanz-Aparicio *et al.*, 1998; Czjzek *et al.*, 2000; Zechel *et al.*, 2003; Verdoucq *et al.*, 2004; Isorna *et al.*, 2007; Chuenchor *et al.*, 2008). All hydrogen bonds between the glucose hydroxyl groups and the enzyme active site are conserved in GH1 structures. However, a conserved glutamate interacts with the 4-OH and 6-OH in most GH1 enzymes, but this glutamate residue is replaced by serine (S428), lysine (K435) and tyrosine (Y437) for hydrogen bonding with the 6-phosphate group in 6-phospho- β -galactosidase (Wiesmann *et al.*, 1997). Nevertheless, differences are still seen in the glycone specificity in this family, which apparently relate to the different contacts with the OH in the sugar substrate and transition state (Namchuck and Withers, 1995).

Since the glycone moiety is conserved in GH1 β -glucosidases, substrate specificity is mainly determined by high diversity in specificity for the aglycone part. The maize β -glucosidase isoenzyme Glu1 (ZmGlu1) hydrolyzes a broad spectrum of substrates in addition to its natural substrate 2- β -D-glucosyl-2,4-dihydroxy-7-methoxy-1,4-benzoxazine-3-one (DIMBOA-Glc), but not dhurrin, whereas the sorghum β -glucosidase isoenzyme Dhr1 (SbDhr1) hydrolyzes only its natural substrate dhurrin. These two plant β -glucosidases, ZmGlu1 and SbDhr1, which

shared 70% amino acid sequence identity, have been crystallized and the binding of their natural substrates compared (Czjzek *et al.*, 2000; 2001; Verdoucq *et al.*, 2004). The structures of inactive mutants of ZmGlu1 and SbDhr1 with DIMBOA-Glc and dhurrin, respectively, showed distinctly different aglycone binding pockets. The high substrate specificity of SbDhr1 is reflected in tighter binding of the aglycone moiety than ZmGlu1. Two residues, S462 and N259, form indirect hydrogen bonds with the phenolic hydroxyl group of dhurrin via water molecules, which act together with hydrophobic interactions from V196 and L203 (Verdoucq *et al.*, 2004). In contrast, the aglycone moiety was bound with only hydrophobic interactions with W378 on one side and F198, F205, and F466 on the other side in ZmGlu1 (Czjzek *et al.*, 2000). More flexibility in binding of the aglycone moiety for the ZmGlu1 results in the enzyme hydrolyzing a broader range of substrates, including several artificial substrates. In addition, the three amino acids: F198, F205 and F466, that form the aglycone binding pocket in ZmGlu1 are replaced by smaller residues: V196, L203 and S462, respectively, in SbDhr1. Thus, the active site of ZmGlu1 is narrow, while that of SbDhr1 is wider (Figure 1.7). Changing the substrate specificity between these two enzymes was investigated by exchanging segments between them and site-directed mutagenesis (Cicek *et al.*, 2000; Verdoucq *et al.*, 2003). Interestingly, replacement of residues that affect the orientation of the aglycone aromatic platform residue (W378 for ZmGlu1; W376 for SbDhr1) changed substrate specificity. For example, the Y473F change in ZmGlu1, which removed a hydrogen bond with W378, increased its efficiency and allowed it to bind with the aglycone moiety of dhurrin (Verdoucq *et al.*, 2003).

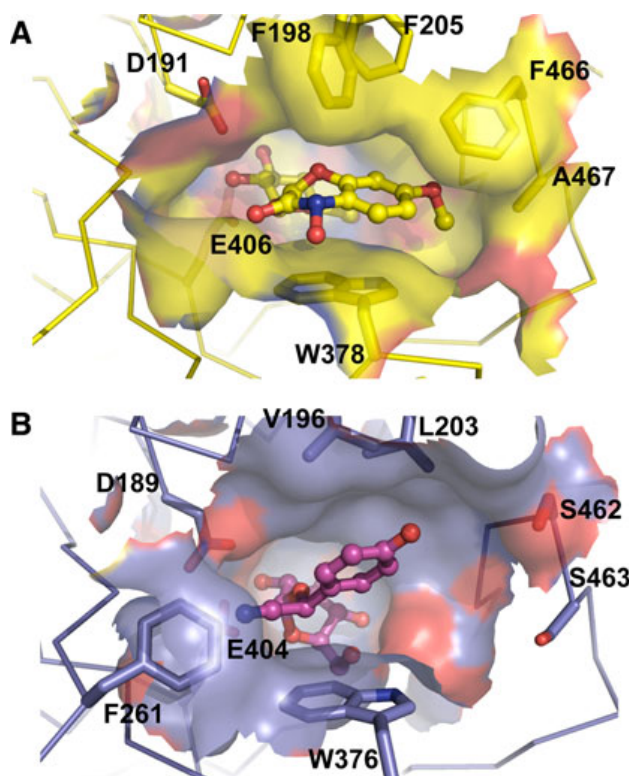


Figure 1.7 Active sites of ZmGlu1 β -glucosidase in complex with DIMBOA-Glc (A) and SbDhr1 dhurrinase in complex with dhurrin (B). The inactive acid/base mutants ZmGlu1 E191D and SbDhr1 E189D are shown in complexes with the ligands. The sidechains of residues interact with the aglycone are shown in stick representation behind the active site surface, which is colored as the underlying residues. These residues are colored with carbon in yellow for Glu1 and purple for Dhr1, nitrogen in blue, and oxygen in red. The ligands are shown in ball and stick representation with similar coloration. The F261 residue, which narrows the active site in Dhr1, is also shown in front of the catalytic nucleophile E404 (Ketudat Cairns and Esen, 2011).

1.7 Oligosaccharide and glycoside synthesis

Carbohydrates and polysaccharides play important cellular functions in all living organisms, including energy storage, cell wall structure, host-pathogen

interactions, cell-cell interactions, signaling, and protein glycosylation (Dwek *et al.*, 1996; Davies *et al.*, 1997; Wells *et al.*, 2002; Ducros *et al.*, 2003). Of medical interest, these biomolecules are involved in a variety of molecular recognition processes in intercellular communication and signal transduction, which have implications for cancer and other diseases. Toxic glycosides have also been shown to be effective anticancer drugs, when combined with targeted β -glucosidase gene therapy (Cortés *et al.*, 1998). In addition, oligosaccharides have potential therapeutic applications as anti-infective agents, and some are probiotics that can promote growth of protective gastrointestinal flora and are therefore used as supplements in infant formula (Zopf and Roth, 1996; Euler *et al.*, 2005). Therefore, glycoside and oligosaccharide synthesis is increasingly important in the pharmaceutical industry (Perugino *et al.*, 2004). Cellooligosaccharides also have applications to synthesis of artificial cellulose for use in wound dressings, high-quality additives to paper, fiber glass filter sheets, chewing gum, food stabilizers, and acoustic diaphragms for audio instruments (Ross *et al.*, 1991). However, a major limitation to the use of oligosaccharides and glycoconjugates for application as therapeutic agents is the difficulty in producing large quantities of these molecules efficiently.

Cellooligosaccharides and polysaccharides from natural sources are very heterogeneous, their use often requires extensive processing and purification (Klemm *et al.*, 2001). The chemical synthesis of these compounds is difficult because the manipulation needed to control the stereospecificity (glycosidic bond formation of only one anomer) and regiospecificity (formation of (1→2), (1→3), (1→4) or (1→6) glycosidic bonds) of the products limits the efficient production of oligosaccharides (Crout and Vic, 1998; Hanson *et al.*, 2004). Therefore, techniques for the analysis and

synthesis of oligosaccharides are of interest, as they can be used for development of enzymes that hydrolyze these oligosaccharides in biomass conversion and fuel production, as well as the applications noted above.

Enzymatic synthesis can produce oligosaccharides in large-scale, because the formation of the glycosidic linkages in the reaction can be controlled (Crout and Vic, 1998). Enzymatic synthesis of oligosaccharides can be done by glycosyltransferases and glycosidases. Glycosyltransferases catalyze the transfer of the sugar from activated nucleotide phosphosugar donor to a suitable acceptor (Thiem, 1995). However, the limited availability of glycosyltransferases, their membrane association and the high cost of their substrates limits their use (Perugino *et al.*, 2004; Shaikh and Withers, 2008). Glycosidases catalyze reverse hydrolysis or transglucosylation to form glycosidic linkages by transferring the glycone of the glycosyl enzyme to an acceptor sugar rather than to water (Figure 1.8). Therefore, retaining glycosidases can be used to synthesize glycosides. However, glycosidases produce poor yields from synthetic reactions, because of their hydrolysis of the products (Perugino *et al.*, 2004; Shaikh and Withers, 2008).

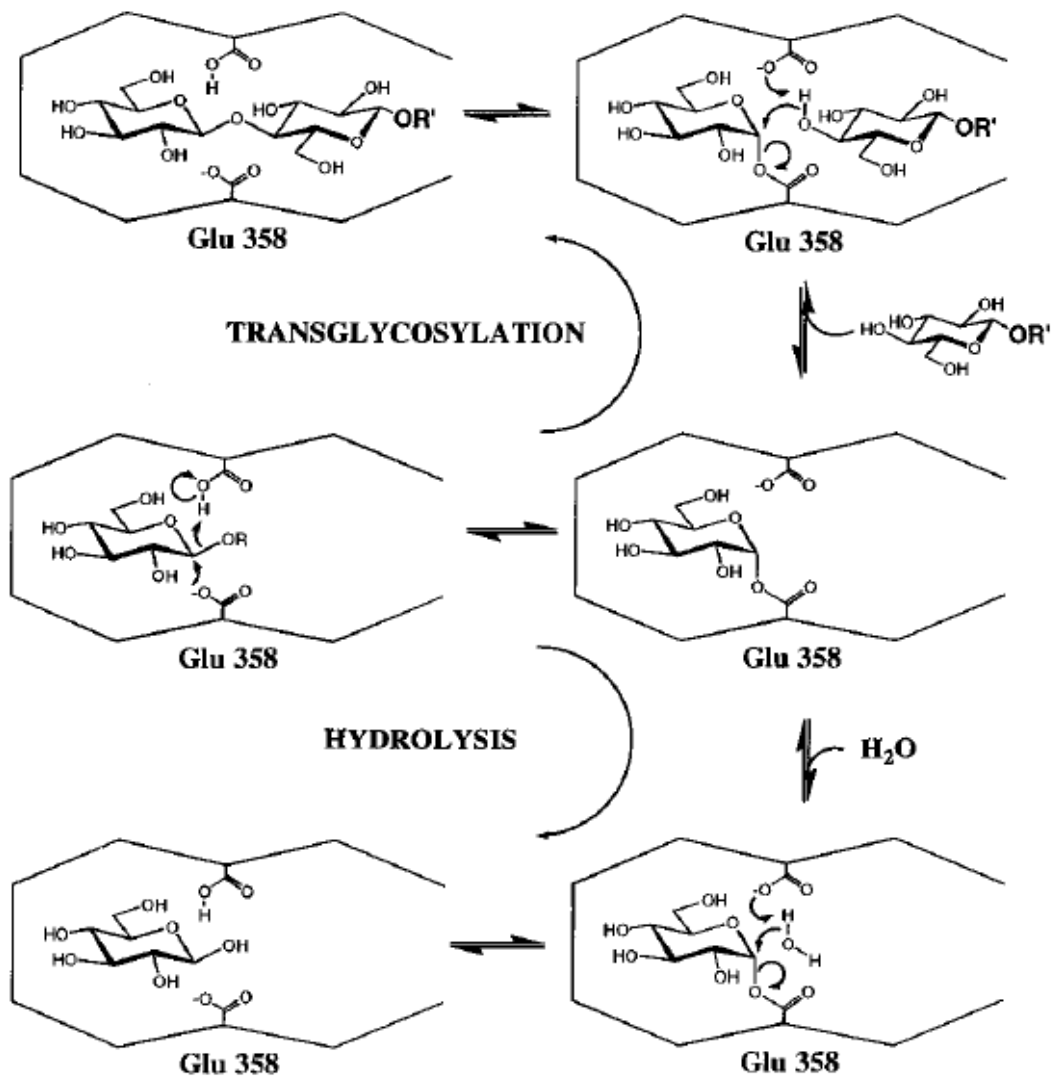


Figure 1.8 Mechanism of hydrolysis and transglycosylation by retaining *Agrobacterium* sp. β -glucosidase (Mackenzie *et al.*, 1998).

Recently, glycosidases have been mutated to glycosynthases that efficiently synthesize oligosaccharides, but do not hydrolyse them, by mutation of the catalytic nucleophile to small, nonnucleophilic residues, including alanine, glycine and serine. These nucleophile mutants have hydrolysis rates at least 10^5 -fold lower than the wild type enzyme (Wang *et al.*, 1994). Moreover, a glycosynthase has been derived from an inverting glycoside hydrolase by mutating the catalytic base aspartate to cysteine,

but the mutant still retained 0.02% hydrolytic activity comparing with the wild type (Honda and Kitaoka, 2006). Regardless, enzymatic synthesis offers the advantage of potentially producing much more homogeneous oligosaccharides, which require less purification and processing than those prepared from natural sources (Klemm *et al.*, 2001).

Thioglycosides are resistant to hydrolytic cleavage by most glycosidases and have proved useful as competitive inhibitors of glycosidases (Legler, 1990), in the formation of stable complexes for X-ray crystallography (Driguez, 2001), and have potential as therapeutics. Thus, they are of interest as metabolically stable glycoside analogues or inhibitors (Rakić and Withers, 2009; Vuong and Wilson, 2010). The general acid/base residue in retaining glycosidases has been mutated to generate thioglycoligases, which can synthesize thioglycosides from highly activated substrates with excellent leaving groups such as 2,4-dinitrophenyl glycosides in the presence of highly nucleophilic thiosugar acceptors that do not require catalysis by the missing base residue (Figure 1.9) (Jahn *et al.*, 2003a; Müllegger *et al.*, 2005; Rakić and Withers, 2009; Vuong and Wilson, 2010). The retaining acid/base mutants from *Agrobacterium* sp. β -glucosidase (Abg), *Cellulomonas fimi* β -mannosidase (Man2A), *Thermotoga maritima* β -glucuronidase, *Bacillus circulans* xylanase (Bcx), *Escherichia coli* α -xylosidase (YicI), *Sulfolobus solfataricus* α -glucosidase (MalA) and *Xanthomonas manihotis* β -galactosidase (BgaX) have been generated to synthesize glycosidase inhibitors (Cobucci-Ponzano *et al.*, 2011). Moreover, the α -thioglycoligases derived from *Escherichia coli* α -xylosidase and *Sulfolobus solfataricus* α -glucosidase can catalyze reactions using α -glycosyl fluoride donors and deoxythioglycoside acceptors in yields up to 86% (Kim *et al.*, 2006). Another

advanced strategy of thioglycosynthases is to produce double mutants of both the acid/base and nucleophile residues. This type of enzyme was produced to synthesize thioglycosides using activated glycosyl fluoride donors and nucleophile thiosugars (Jahn *et al.*, 2004).

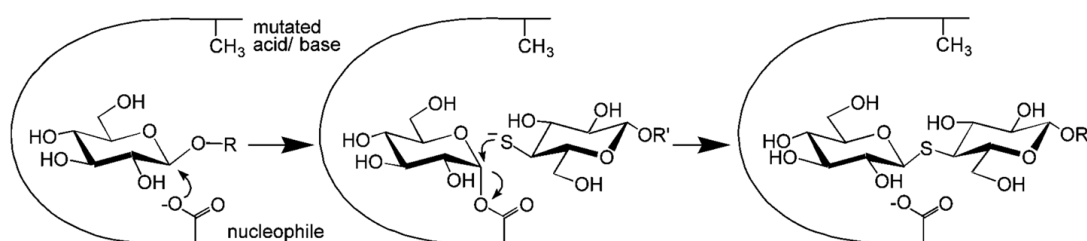


Figure 1.9 Synthesis of a thioglycoside by a thioglycosylase (Jahn *et al.*, 2004). Replacement of the catalytic acid/base with a nonionizing amino acid allows the glycosylation half reaction to proceed for substrates with good leaving groups, such as 2,4-dinitrophenolates. Ionized nucleophiles, such as a thiosugar, can then displace the sugar from the enzyme to produce thio-linked products.

1.8 Glycosynthases

As noted in section 1.7, glycosynthases are nucleophile mutants of glycosidases that can be used for synthesis of specific oligosaccharides in appropriate quantities for many desired applications. These mutants cannot form a reactive α -glycosyl-enzyme intermediate for transglycosylation. However, when an α -glycosyl fluoride is present as a glycosyl donor, the mutant enzymes can transfer the glycosyl moiety to acceptor alcohols without hydrolysis of the products, as shown in Figure 1.10 (Shaikh and Withers, 2008). The first glycosynthase was derived from the $\text{exo-}\beta$ -glucosidase from

Agrobacterium sp., in which case the wild type enzyme has an efficient transglycosylation activity (Withers *et al.*, 1990; Kempton and Withers, 1992). The nucleophile mutant E358A was inactive for hydrolysis and could synthesize high yields of β -(1 \rightarrow 4)-linked cellooligosaccharides, using α -glucosyl fluoride and α -galactosyl fluoride as donors with various acceptors.

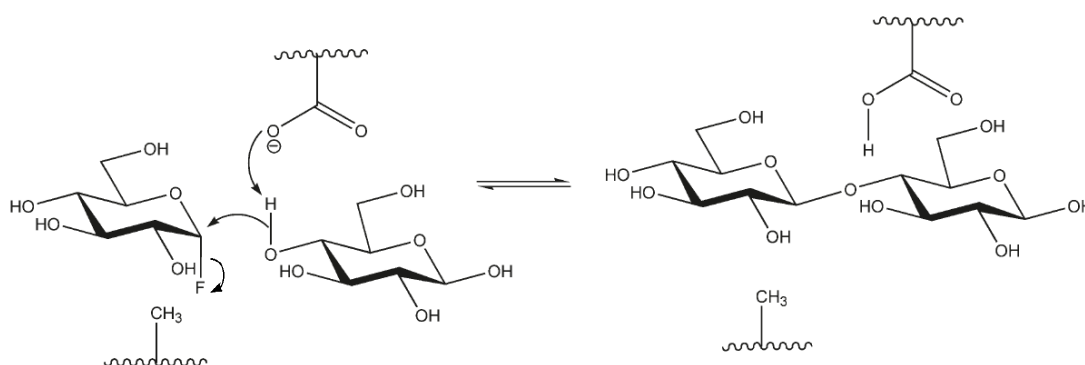


Figure 1.10 Mechanism of transglycosylation with a glycosynthase (Shaikh and Withers, 2008).

Recently, several glycosynthases have been obtained from different families of glycosidases, including exoglycosidases and endoglycosidases, to synthesize many oligosaccharides of interest (Perugino *et al.*, 2004; Hancock *et al.*, 2006; Shaikh and Withers, 2008; Cobucci-Ponzano *et al.*, 2011). The exoglycosynthases have moderate substrate specificity and regioselectivity and can synthesize short chain oligosaccharides (di-, tri- and tetra-oligosaccharides) that have various glycosidic linkages. For instance, a glycosynthase derived from *Sulfolobus solfataricus* β -glucosidase synthesized β -(1 \rightarrow 3)- or β -(1 \rightarrow 6)-linked tetrasaccharides (Trincone *et al.*, 2000), which are used for the defense against pathogens in plants and invertebrates (Skriver *et al.*, 1991; Duvic and Soderhall, 1992; Zagrobelny *et al.*,

2008). In each case, these β -glucosidase-derived glycosynthases synthesize short oligosaccharides of 2-4 glycosyl residues, as do other exoglycosidase-derived glycosynthases. However, rice BGlu1 glycosynthase can synthesize long chains of β -(1 \rightarrow 4)-linked oligosaccharides to at least 11 residues (Hommalai *et al.*, 2007), presumably because rice β -glucosidase has a long aglycone-binding site (Opassiri *et al.*, 2004).

Glycosynthases have also been derived from exoglycosidases with other glycone specificities as well. A β -galactosynthase developed from *Escherichia coli* LacZ gene β -galactosidase synthesized β -(1 \rightarrow 6) linkages with yields of 80% (Jakeman and Withers, 2002). A β -mannosynthase derived from *Cellulomonas fimi* β -mannosidase could produce β -(1 \rightarrow 3)- or β -(1 \rightarrow 4)-linked hexamannosides. Although the β -mannosidic linkage is the most difficult glycosidic linkage to synthesize by chemical processes, due to the steric effect of the axial 2-hydroxyl of mannose, yields of 70% were obtained (Alais and David, 1990; Gunther and Kunz, 1992; Nashiru *et al.*, 2001). The glycosynthase enzyme developed from the *Thermotoga maritima* β -glucuronidase synthesized β -(1 \rightarrow 4)-linked glucuronic and galacturonic acid conjugates, which are found in plant and bacterial cell walls and mammalian glycosaminoglycans (Müllegger *et al.*, 2006). Moreover, the first glycosynthase to be derived from an inverting glycosidase, an exo-xylanase from *Bacillus halodurans*, which hydrolyzes the glycosidic bond by a single displacement mechanism, was obtained by saturation random mutagenesis of the catalytic base aspartate, which was changed to cysteine in the most efficient glycosynthase (Honda and Kitaoka, 2006).

Endoglycosynthases have high regioselectivity and can catalyze the synthesis of specific glycosidic linkages. They can synthesize longer oligosaccharides than exoglycosynthases, because they have long glycone-binding sites, which accommodate longer glycosyl donor substrates, such as α -cellobiosyl fluoride or α -cellotriosyl fluoride (Perugino *et al.*, 2004; Hancock *et al.*, 2006). The β -endoglucansynthase from *Bacillus licheniformis* β -(1 \rightarrow 3),(1 \rightarrow 4)-glucanase produced β -(1 \rightarrow 3)- or β -(1 \rightarrow 4)-linked glycans with yields of 76% containing galactosyl and glucosyl residues (Fairweather *et al.*, 2002). The glucansynthase from *Humicola insolens* produced high yields of oligosaccharides containing only β -(1 \rightarrow 4) linkages by the regio- and stereoselective glycosylation using lactosyl fluoride as donor, and glucoside, xyloside, mannoside, cellobioside and laminaribioside as acceptors (Fort *et al.*, 2000). An endoglycosynthase derived from *Cellulomonas fimi* endo- β -(1 \rightarrow 4)-xylanase, which can synthesize long chains of xylo-oligosaccharides (4-12 residues) using xylobiosyl fluoride as donor, has also been reported (Kim *et al.*, 2005).

1.9 Improvement of glycosynthase activity

Yield and selectivity of the glycosynthase reaction are key features of the oligosaccharide synthesis for optimization, therefore, mutagenesis of glycosynthases has been important in the improvement and alteration of the catalytic activities of glycosynthases. The E358S mutant from *Agrobacterium* sp. exo- β -glucosidase was found to have improved glycosynthase activity (Mayer *et al.*, 2000), with 24-fold higher synthetic rates and higher product yields, and could synthesize other glycosides that were not obtained with the E358A mutant. However, the E358G mutant had even

higher glycosynthase activity than the E358S mutant (Mayer *et al.*, 2001). The 3D-structure of E320G β -mannanase Man26A from *Cellvibrio japonicus* in complex with mannobiose (Figure 1.11; Jahn *et al.*, 2003b) suggested an explanation for these higher rates. A water molecule situated at the position of the nucleophile of the wildtype enzyme makes a hydrogen bond to the α -anomeric O1 atom and may play a role similar to that proposed for the serine hydroxyl group in assisting departure of the fluoride leaving group (Mayer *et al.*, 2000). Flexible positioning of the water molecule may optimize the interaction between the water and fluoride to stabilize the departing fluoride better than occurs with the relatively rigid hydrogen bond formed with serine (Ducros *et al.*, 2003).

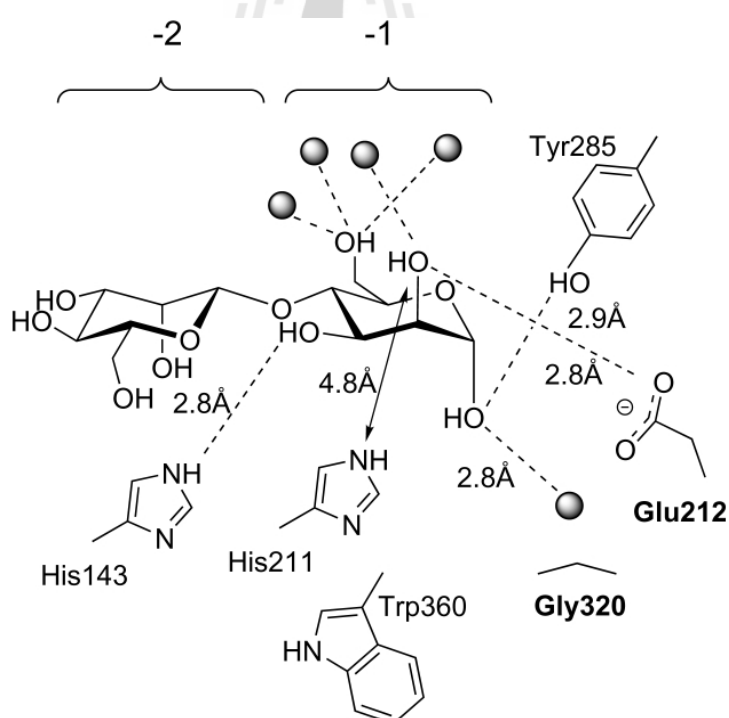


Figure 1.11 Schematic diagram of the interactions of Man26A E320G with mannobiose. Only the -1 subsite interactions are included, with distances given where relevant. Water molecules are shown as shaded spheres (Jahn *et al.*, 2003b).

Moreover, glycosynthase technology can be improved, in terms of the catalytic activity and substrate specificity, by directed evolution of glycosynthases with point mutations within the catalytic site for synthesis of novel glycosides and oligosaccharides (Shaikh and Withers, 2008). Random mutagenesis of the *Agrobacterium* sp. β -glucosidase E358G mutant was performed by two rounds of error-prone PCR to improve efficiency (Kim *et al.*, 2004). The E358G glycosynthase mutant 2F6, which contained three additional amino acid mutations (A19T, Q248R and M407V), had a 27-fold higher glycosynthase activity than the E358G mutant itself. A homology model of the *Agrobacterium* sp. glycosynthase mutant 2F6 structure (Figure 1.12) showed that the locations of the mutations were far from the active site, which indicated that the A19T and M407V mutations do not interact directly with substrates but have their effects by changing the conformation of the active site. Moreover, the A19T mutation seems to cause favorable interactions with the equatorial C2-OH group of substrates such as galactose, glucose and xylose, thus the 2F6 mutant showed rate enhancements on a variety of donors and acceptors.

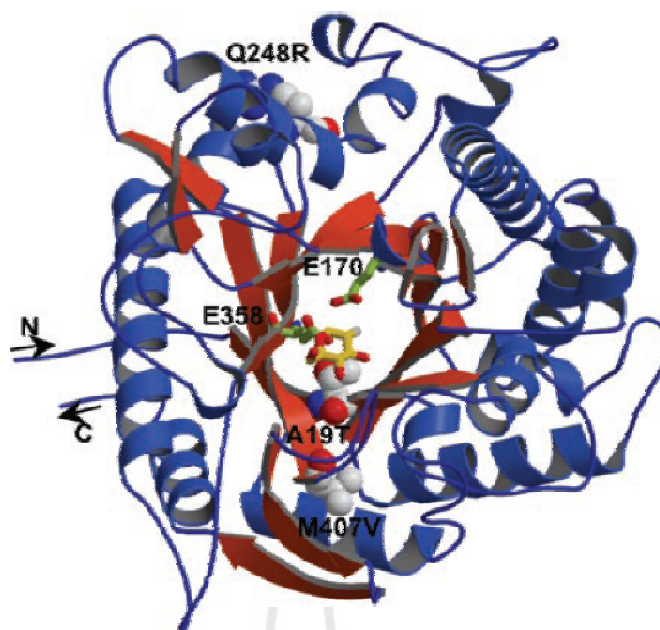
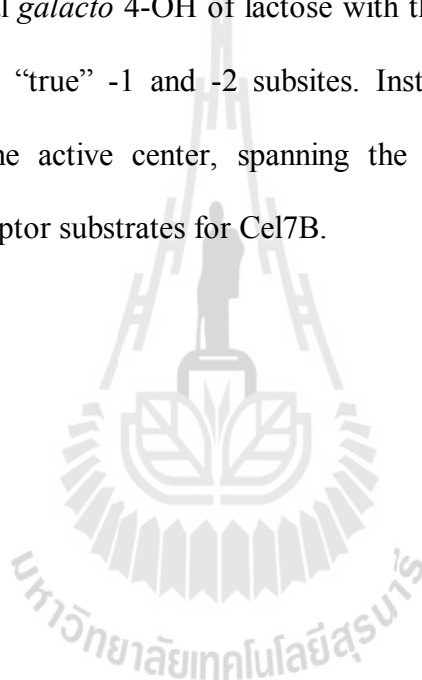


Figure 1.12 Overall model structure of the evolved *Agrobacterium* sp. glycosynthase 2F6 showing secondary structure elements and the positions of mutations. The catalytic amino acids of wild type are represented in stick style, colored yellow-green. Three positive mutations are depicted in CPK coloring with carbon atoms in white, nitrogen atoms in blue, and oxygen atoms in red (Kim *et al.*, 2004). Note: This is a homology model, since there is no experimentally derived structure of *Agrobacterium* sp. glycosynthase.

The Cel7B E197A endoglycosynthase derived from *Humicola insolens* endoglucanase Cel7B produced oligosaccharides with α -lactosyl fluoride donor and a variety of acceptors in high yields (Ducros *et al.*, 2003). The E197S mutant had a 34-fold higher catalytic efficiency than the E197A mutant, using α -lactosyl fluoride as donor and *p*-nitrophenyl β -cellobioside as acceptor. The 3D structures of Cel7B E197S complexes with cellobiose and lactose revealed the locations and interaction in

donor and acceptor subsites (Figure 1.13). Both cellobiose and lactose complexes display essentially identical interactions in the donor -2 and -1 subsites, which have hydrophobic “stacking” with W347 and Y147. The E197S mutant generated sufficient space to accommodate the axial anomeric hydroxyl of an α -glycoside, and the serine hydroxyl did not make a direct interaction with the anomeric hydroxyl. In the acceptor subsites, the lactoside and cellobioside complexes were not equivalent. The potential clash between the axial *galacto* 4-OH of lactose with the side-chain of Q175, prevent lactose binding in the “true” -1 and -2 subsites. Instead, it is rotated slightly and displaced “out” of the active center, spanning the “-1.5 to -2.5” subsites, thus lactosides are not acceptor substrates for Cel7B.



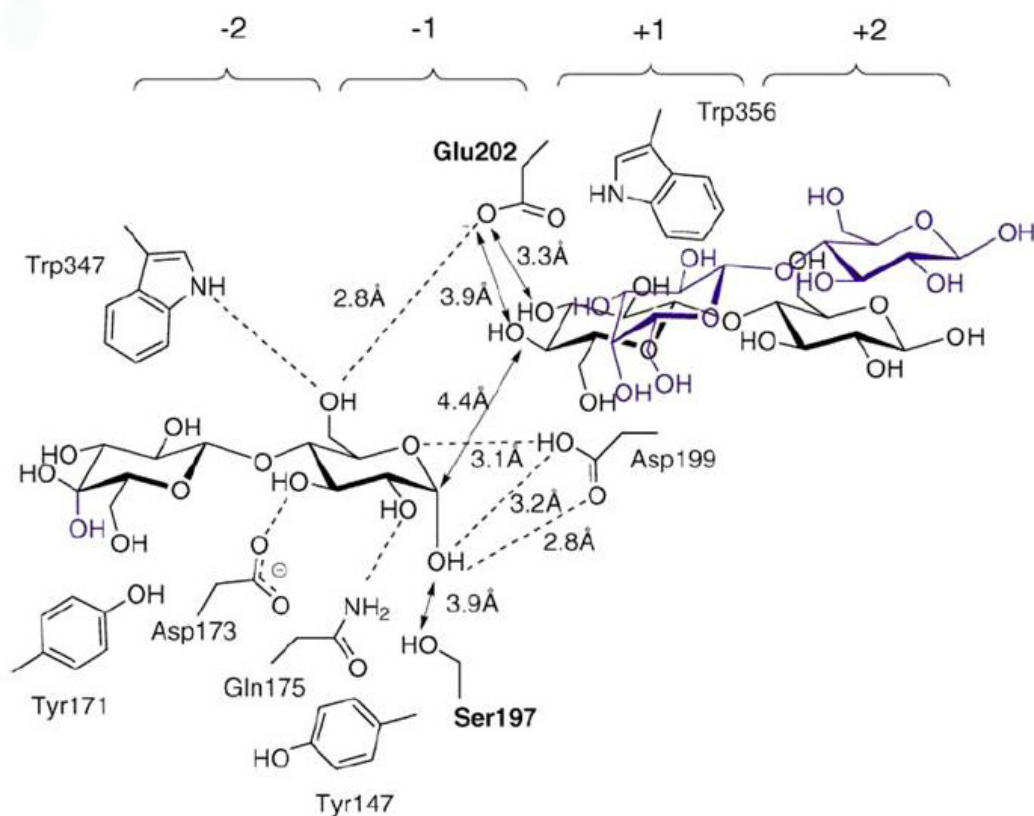


Figure 1.13 Schematic diagram of the Cel7B E197S-ligand interactions. Only the -1 subsite interactions (from the cellobiose complex) are given in their entirety, and the approximate position of the lactose moieties is shown for reference in blue (Ducros *et al.*, 2003).

Glycosynthases derived from exooligoxylanase, an inverting glycosidase from *Bacillus halodurans* which hydrolyzes xylooligosaccharides, were generated with mutations of the catalytic base D263 to Gly, Ala, Val, Thr, Leu, Asn, Cys, Pro or Ser by saturation random mutagenesis. The mutants were found to possess glycosynthase activity forming β -(1 \rightarrow 4)-linked xylotriose from α -xylobiosyl fluoride and xylose. The D263C mutant showed the highest level of xylotriose production (Figure 1.14), because the mutant showed 10-fold lower hydrolytic activity than D263N, which

exhibited the fastest consumption of α -xylobiosyl fluoride (Honda and Kitaoka, 2006).

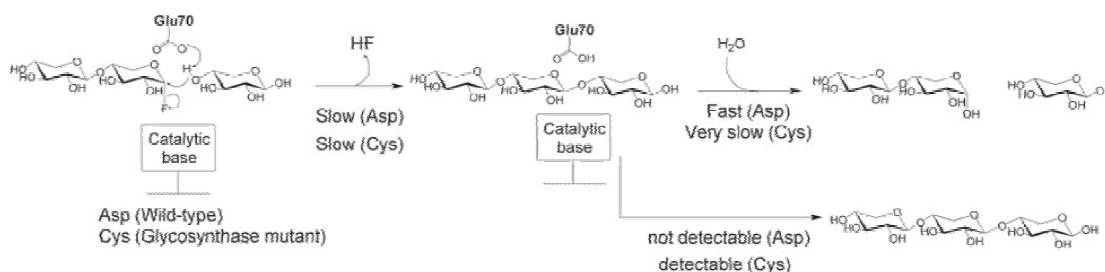


Figure 1.14 Reaction mechanism of a glycosynthase derived from an inverting glycosidase (Honda and Kitaoka, 2006).

The regioselectivity of glycosidic linkages can be altered by changing the stereochemistry of the acceptors (Cobucci-Ponzano *et al.*, 2011). The mutant E383A β -glucosidase from *Streptomyces* sp. is an efficient glycosynthase enzyme, catalyzing the condensation of α -glucosyl and α -galactosyl fluoride donors to a variety of acceptors. In glycosynthase reactions with aryl monosaccharide acceptors, β -(1 \rightarrow 3)-linked disaccharides were obtained in good to excellent yields. In the reaction with xyloside acceptor, regioselectivity was poorer and resulted in the formation of a mixture of β -(1 \rightarrow 3) and β -(1 \rightarrow 4) linkages. In contrast, disaccharide acceptors produced exclusively β -(1 \rightarrow 4) linkages, because the presence of a glycosyl unit in subsite +2 redirects regioselectivity from β -(1 \rightarrow 3)- to β -(1 \rightarrow 4)-linked (Fajjes *et al.*, 2006).

Thioglycosynthase is a double mutant of the nucleophile and the catalytic acid/base residues of a retaining glycosidase can catalyzes transglycosylations with glycosyl fluorides of inverted anomeric configuration and thiosugar acceptors to

synthesize thioglycosides (Figure 1.15) (Jahn *et al.*, 2004; Bojarová and Kren, 2009). The thioglycosynthase combines the two approaches of thioglycoligase and glycosynthase, and has two major advantages over the thioglycoligase for synthesis of thioglycosidic linkages in oligosaccharides. Firstly, nucleophile mutants are completely hydrolytically inactive, whereas acid/base mutants used in the thioglycoligase strategy can slowly hydrolyse the donor. Secondly, glycosyl fluoride donors are more easily synthesized than dinitrophenyl glycosides (Jahn *et al.*, 2004). The double mutant E171A/E358G *Agrobacterium* sp. β -glucosidase has been successfully generated the thioglycosynthase enzyme to synthesize β -glycosidase inhibitors (Jahn *et al.*, 2004; Cobucci-Ponzano *et al.*, 2011). However, this approach has not been further developed yet, possibly for the difficulties in the chemical synthesis of suitable donors and acceptors, but it has promising possibilities for the production of specific inhibitors.

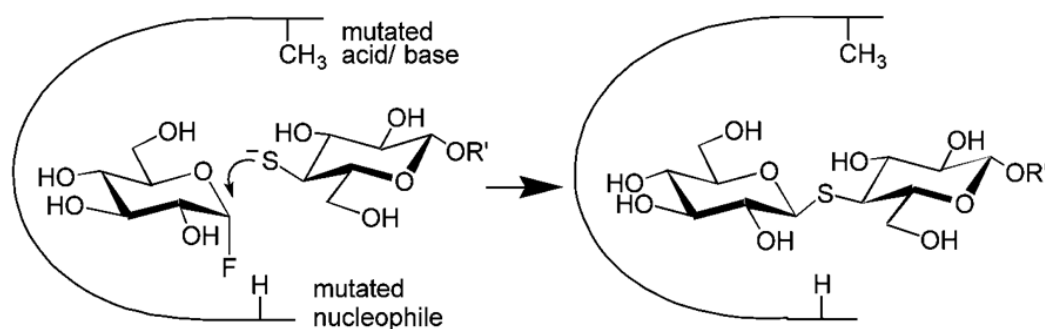


Figure 1.15 The synthesis of thioglycoside by a thioglycosynthase (Jahn *et al.*, 2004).

1.10 Rice BGlu1 β -glucosidase

A GH1 β -glucosidase (BGlu1, also called Os3BGlu7) from rice (*Oryza sativa* L.) has been characterized and expressed in *E. coli* (Opassiri *et al.*, 2003; 2004; 2006). The rice BGlu1 acts as an exo- β -glucanase on oligosaccharides and can hydrolyze sophorose (β -(1 \rightarrow 2)-linked glucobiose), gentiobiose (β -(1 \rightarrow 6)-linked glucobiose), laminarioligosaccharides (β -(1 \rightarrow 3)-linked glucooligosaccharides) and celooligosaccharides (β -(1 \rightarrow 4)-linked glucooligosaccharides). The BGlu1 enzyme had lower K_m and high k_{cat} values for laminaribiose, but had high K_m and low k_{cat} values for cellobiose, sophorose and gentiobiose. For β -(1 \rightarrow 4)-linked oligosaccharides, the K_m decreased with increasing chain length of the substrate, and catalytic efficiency (k_{cat}/K_m) increased with increasing chain length of the celooligosaccharides from degree of polymerization (DP) 2 to 6. In contrast, the k_{cat}/K_m value for β -(1 \rightarrow 3)-linked oligosaccharides decreased from DP 2 to 3, and the enzyme could not hydrolyze the β -(1 \rightarrow 3)-linked oligosaccharides with a DP longer than 3 (Opassiri *et al.*, 2004). The BGlu1 also hydrolyzed several *p*NP- β -D-glycosides and *p*NP- α -L-arabinoside, while the BGlu1 could not hydrolyze *p*NP- α -D-glucoside, *p*NP- β -L-fucose, *p*NP- β -D-thiogluconoside or *p*NP- β -D-thiofucoside. The enzyme had low K_m and high k_{cat} values for both *p*NP- β -D-glucoside (*p*NPGlc) and *p*NP- β -D-fucoside. However, the BGlu1 hydrolyzed *p*NP- β -D-galactopyranoside, *p*NP- β -D-mannoside, *p*NP- β -D-xyloside, *p*NP- α -L-arabinoside and *p*NP- β -D-cellobioside with much lower catalytic efficiency than *p*NPGlc (Opassiri *et al.*, 2004). Compared to *p*NPGlc, the enzyme had lower catalytic efficiency against some natural and artificial glucosides, and pyridoxine 5'-*O*- β -D-glucoside was the most efficiently hydrolyzed natural glycoside substrate tested. Moreover, the BGlu1 had high transglucosylation

activity with only *p*NPGlc substrate, and *p*NPGlc donor and pyridoxine acceptor to synthesize pyridoxine 5'-O- β -D-glucoside (Opassiri *et al.*, 2004). In addition, the BGlu1 had transglucosylation activity toward cellotriose, cellotetraose, laminaribiose and laminaritriose substrates (Opassiri *et al.*, 2003).

Subsite affinity analysis of BGlu1 β -glucosidase for glucose residues in cellooligosaccharides, calculated by the equations of Hiromi *et al.* (1973), showed productive binding at glucose residues 1 and 3-6 from the non-reducing end (subsites -1, and +2 to +5). Highest affinity was seen at the +2 subsite, which had negative binding affinity in barley β II β -glucosidase (Hrmova *et al.*, 1998). In contrast, the +1 subsite has highest affinity in barley β II β -glucosidase, which had negative binding affinity in BGlu1, corresponding, BGlu1 had higher preference for cellotriose than barley β II β -glucosidase, but lower preference for cellobiose (Hrmova *et al.*, 1998; Opassiri *et al.*, 2004). In addition, the binding energies of interaction for different subsites, based on competitive inhibition constants of oligosaccharides in a mutant that hydrolyzes *p*NPGlc but not oligosaccharides, are similar to those calculated from the subsite affinity analysis (Chuenchor *et al.*, 2011).

Rice BGlu1 has been mutated to form glycosynthases. (Hommalai *et al.*, 2007). Three glycosynthases, E386G, E386A and E386S, catalyzed the synthesis of mixed length oligosaccharides by transglucosylation, using α -glucosyl fluoride donor and *p*NP-cellobioside acceptor. In this study, it was found that the E386G mutation had approximately 3- and 19-fold higher glycosynthase activity in terms of k_{cat} values than E386S and E386A, respectively. The E386G glycosynthase can synthesize long chains of β -(1 \rightarrow 4)-linked glucose residues to at least 11 residues. Moreover, the E386G synthesized longer oligosaccharide products when it used cellotriose and

cellotetraose as acceptors, but no transglucosylation products were observed when *p*NPGLc and cellobiose were used as acceptors. The unique property of this enzyme compared to previous glycosynthases is that previous glycosynthases that were derived from exoglycosidases did not synthesize such long oligosaccharide products. This was presumed to be due to the fact that rice BGlu1 has an extended active site with subsites for binding up to at least 6 residues, as calculated from the subsite mapping (Opassiri *et al.*, 2004) and the binding energies of interaction (Chuenchor *et al.*, 2011).

The X-ray crystal structures of the BGlu1 wild type protein and of its E176Q acid/base mutant in complexes with oligosaccharides have recently been determined (Chuenchor *et al.*, 2008; 2011). The structures of BGlu1 showed a deep, narrow and straight binding cleft, which contained negatively charged amino acids around the deepest and narrowest part, compatible with the hydrolysis of long β -(1 \rightarrow 4)-linked oligosaccharides. The covalent glycosyl-enzyme intermediate of BGlu1 in complex with 2-deoxy-2-fluoro-glucoside (G2F) inhibitor showed five hydrogen bonds between G2F and amino acids at the -1 subsite (Figure 1.16) (Chuenchor *et al.*, 2008). The O4 and O6 interact with E440, which is conserved with other GH1 β -glucosidases, and the glucosyl residue stacked upon the indole ring of the conserved W433 residue. A glycerol molecule located at the +1 subsite was in position to act as an acceptor for transglycosylation. The structure of BGlu1 E176Q acid/base mutant covalent intermediate with G2F showed similar glucosyl binding compared to the wild type enzyme (Chuenchor *et al.*, 2011).

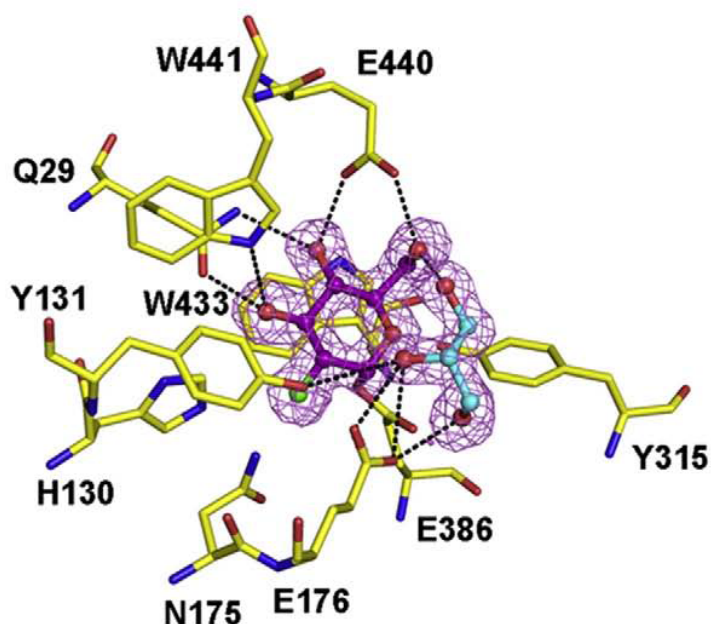


Figure 1.16 Active site of the BGlu1-G2F complex and a covalent glycosyl-enzyme intermediate. The amino acid residues surrounding the G2F moiety are presented in stick representation, with carbon in yellow, nitrogen in blue, oxygen in red, and fluoride in green. G2F and glycerol are drawn in ball and stick representation in the same colors, except that the carbon atoms are purple and cyan, respectively. Hydrogen bonds between the protein and the glycone at subsite -1 and glycerol at subsite +1 are drawn as dashed black lines (Chuenchor *et al.*, 2008).

The amino acids and glucosyl residues in the active sites of BGlu1 E176Q in complexes with cellotetraose and cellopentaose were placed at similar positions to those in the native enzyme structure (Chuenchor *et al.*, 2011). No water molecules interacting with Glc1 (from nonreducing end) were found in the -1 subsite. In contrast, nearly all of the polar interactions are mediated by water molecules at all other subsites. The only direct hydrogen bond between the protein and ligand at subsites +1 to +4 was found between N δ of N245 and O3 of Glc3 in the structures

with cellotetraose and cellopentaose, which may help explain the strong binding at +2 subsite (Chuenchor *et al.*, 2011; Opassiri *et al.*, 2004). The interactions between the five glucosyl residues of cellopentaose with the surrounding amino acids are diagrammed in Figure 1.17. The Glc2 and Glc3 residues in subsites +1 and +2 are aligned to stack onto the indole ring of W358, and the Glc4 and Glc5 at subsites +3 and +4 are stacked along the face of the Y341 phenol ring. In the structure of BGlu1 E176Q with laminaribiose, the nonreducing end sugar at the -1 subsite is placed in a position similar to that seen with cellotetraose and cellopentaose. The ring of Glc2 was flipped 180° compared that of the cellooligosaccharides, which allowed formation of a hydrogen bond between Glc2 O1 and N245 (Chuenchor *et al.*, 2011).

To understand the properties of the rice BGlu1 E386G, BGlu1 E386A and BGlu1 E386S glycosynthases, the structures of the protein with and without substrates were determined by X-ray crystallography. In order to probe the contributions of binding cleft residues, the glucose binding subsites (+3 and +4) of the wild type BGlu1 and BGlu1 E386G were disrupted by site-directed mutagenesis and the functional and structural effects of these mutations on cellooligosaccharide hydrolysis, glycosynthase activity and cellooligosaccharide binding determined.

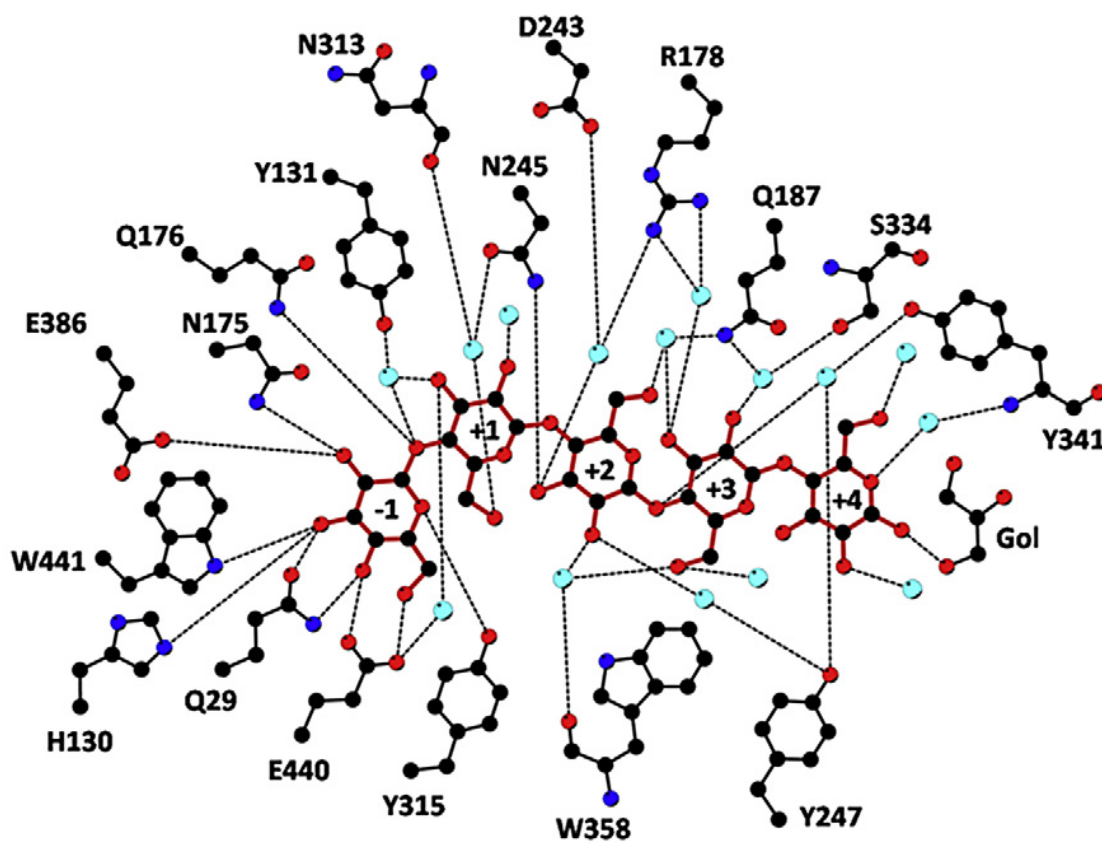


Figure 1.17 Hydrogen bonding between the BGlu1 E176Q mutant active site residues and cellopentaose. The diagram shows the apparent hydrogen bonds with measured distances of 3.2 Å or less as dotted lines to indicate hydrophilic interactions. Water molecules involved in the hydrogen-bonding network are shown as light blue balls (Chuenchor *et al.*, 2011).

1.11 Research objectives

1. To determine X-ray crystal structures of the BGlu1 E386G, E386A and E386S with and without substrates for determination of the structural adaptation leading to an efficient glycosynthase and the binding sites of sugars by X-ray crystallography.
2. To change specific glucose binding sites of oligosaccharides for wild type BGlu1 and BGlu1 E386G to test for production of specific oligosaccharides and/or synthesis with shorter acceptors.
3. To compare the hydrolysis and synthesis reaction of mutants to see if the glycosynthases produce oligosaccharides of different length, compared to the original glycosynthase.
4. To crystallize and determine the structures of the glucose binding site mutants with and without oligosaccharides in order to determine what structural changes have occurred and how they may have caused the changes in hydrolysis and glycosynthase activity for oligosaccharide synthesis.

CHAPTER II

MATERIALS AND METHODS

2.1 Materials

2.1.1 Plasmids and bacterial strains

The *bglu1*, *bglu1 E386G*, *bglu1 E386A* and *bglu1 E386S* cDNA were previously cloned into pET32a(+) expression vector to produce fusion proteins that contain thioredoxin and His₆ tags and an enterokinase cleavage site N-terminal to the BGlul protein, as shown in Figure 2.1 (Opassiri *et al.*, 2003, Hommalai *et al.*, 2007). Bacterial host cells used included *Escherichia coli* strains XL-1 blue for cloning and Origami(DE3) for recombinant protein expression.

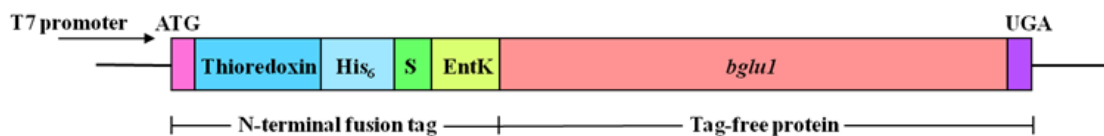


Figure 2.1 Construct of the protein-coding sequence of recombinant pET32a(+) with the *bglu1* cDNA inserted after the enterokinase cleavage site.

2.1.2 Oligonucleotides and mutagenic primers

All mutagenic primers (Table 2.1) used for site-directed mutagenesis were ordered from Sigma-Aldrich (St. Louis, MO, USA), except the primers for N245V mutant were ordered from Prologo Singapore Pty Ltd. (Singapore) and for

BGlu1 E386G2 were ordered from Bio Basic Inc. (Markham, Ontario, Canada). Oligonucleotide primers used for DNA sequencing (Table 2.2) were provided by Prof. Asim Esen, Virginia Tech, VA, USA.

Table 2.1 Oligonucleotide primers used in mutagenesis.

Mutation	Primer name	Sequence	Length (bp)	T_m (°C)
S334A	S334A_f	5'-G ACA CCG ACG AGT TAC <u>GCA</u> GCC GAT TGG CAG-3'	31	84.9
	S334A_r	5'-CTG CCA ATC GGC TGC <u>GTA</u> ACT CGT CGG TGT C-3'	31	84.9
Y341A	Y341A_f	5'-C GAT TGG CAG GTT ACC <u>GCT</u> GTT TTT GCG AAA AAC GGC-3'	37	84.3
	Y341A_r	5'-GCC GTT TTT CGC AAA AAC <u>AGC</u> GGT AAC CTG CCA ATC G-3'	37	84.3
Y341L	Y341L_f	5'-CC GAT TGG CAG GTT ACC <u>CTT</u> GTT TTT GCG AAA AAC GGC-3'	38	84.2
	Y341L_r	5'-GCC GTT TTT CGC AAA AAC <u>AAG</u> GGT AAC CTG CCA ATC GG-3'	38	84.2
N245V	N245V_f	5'-AA GTT GGA ATA GTT CTG GAC TTC <u>GTA</u> TGG TAT GAA GCT CTT TCC AAC TC-3'	49	84.5
	N245V_r	5'-GA GTT GGA AAG AGC TTC ATA CCA <u>TAC</u> GAA GTC CAG AAC TAT TCC AAC TT-3'	49	84.5
E386G2	E386G2_f	5'-G ACA GTC GTC ATA ACT <u>GGC</u> AAC GGA ATG GAT CAA C-3'	35	82.1
	E386G2_r	5'-G TTG ATC CAT TCC GTT <u>GCC</u> AGT TAT GAC GAC TGT C-3'	35	82.1

*The mutated nucleotides are underlined.

**The T_m was calculated with the QuikChange calculator.

(<http://www.stratagene.com/QPCR/tmCalc.aspx>).

Table 2.2 Internal oligonucleotide primers used for DNA sequencing of full-length rice *bglu1* and *bglu1 E386G*.

Primer name	Direction	Sequence	Length (bp)	T_m (°C)
40F	Forward	5'-CTTGAGAAGAAGTACGG-3'	17	61.1
42F	Forward	5'-ACGGCAAACCAATTGGACC-3'	19	67.6
41R	Reverse	5'-CCGAGTAATTTACATTTGGT-3'	20	62.1
58R	Reverse	5'-TAGCTCCTGTAGAAATGAAC-3'	20	64.2
128R	Reverse	5'-GGTGAGCTTCAACAGGTCCTCT CTGGT-3'	27	79.3

2.1.3 Reagents and Chemicals

Chelating sepharose fast flow resin, lysozyme, *N,N'*-methylene-bis-acrylamide, *N,N',N'',N'''*-tetramethylethylenediamine (TEMED) and Triton X-100 were purchased from GE Healthcare (Uppsala, Sweden). Bromophenol blue, Coomassie Brilliant Blue R-250, sodium acetate, sodium carbonate, sodium chloride (NaCl), sodium dodecyl sulfate (SDS), sodium hydroxide, disodium ethylenediamine tetraacetate (Na₂-EDTA), sulfuric acid, Tris base, methanol (MeOH), ethanol, glacial acetic acid, glycine and ethyl acetate (EtOAc) were purchased from Carlo ERBA (Milano, Italy). Acrylamide, imidazole, bovine serum albumin (BSA), dichlorodimethylsilane, polyethylene glycol monomethyl ether (PEG MME) 5000, 2-(*N*-morpholino)-ethanesulfonic acid (MES) and ethidium bromide were purchased from Fluka (Steinheim, Switzerland). Ammonium sulfate, calcium chloride and thin layer chromatography silica gel 60 aluminum F₂₅₄ plates for oligosaccharide detection were purchased from Merck (Darmstadt, Germany). Isopropyl thio-β-D-galactoside

(IPTG) was purchased from United States Biological (Swampscott, MA, USA). 2,2'-azino-bis(3-ethylbenzothiazoline-6-sulfonic acid) (ABTS), ammonium persulfate, ampicillin, tetracycline, DNase I, Bis-Tris, 2-mercaptoethanol, *p*-nitrophenyl β -D-glucopyranoside (*p*NP_{Glc}), *p*NP- β -D-fucopyranoside (*p*NP_{Fuc}), *p*NP- α -L-arabinopyranoside (*p*NP_{Ara}), *p*NP- β -D-galactopyranoside (*p*NP_{Gal}), *p*NP- β -D-xylopyranoside (*p*NP_{Xyl}), *p*NP- β -D-mannopyranoside (*p*NP_{Man}), *p*NP- β -D-cellobioside (*p*NP_{C2}), sophorose, gentiobiose, cellobiose and phenylmethylsulfonyl fluoride (PMSF) were purchased from Sigma (St. Louis, MO, USA). Cellooligosaccharides of degree of polymerization (DP) 3-5 were purchased from Seikagaku Kogyo Co. (Tokyo, Japan). Kanamycin sulfate was purchased from Amresco (Solon, OH, USA). Agarose was purchased from Invitrogen (Carlsbad, CA, USA). Deoxynucleoside triphosphates (dNTPs) were purchased from Promega (Madison, WI, USA). Peptone, yeast extract and bacto-agar were purchased from Hi-Media (Mumbai, India). Ultrafiltration membranes (Centricon, 30 kDa MW and 10 kDa MW cut off) and Ultrafree MC 0.22 μ m filters were purchased from Millipore Corporation (Bedford, MA, USA). High vacuum grease was purchased from Dow Corning (Midland, MI, USA). The QuikChange[®] Site-Directed Mutagenesis Kit was purchased from Stratagene (La Jolla, CA, USA) and QIAprep spin miniprep plasmid extraction kit was purchased from QIAGEN (Hilden, Germany). HPLC-grade distilled water and acetonitrile were purchased from RCI Labscan (Bangkok, Thailand). α -D-glucosyl fluoride (α -GlcF), α -L-arabinosyl fluoride (α -AraF), α -D-fucosyl fluoride (α -FucF), α -D-galactosyl fluoride (α -GalF), α -D-mannosyl fluoride (α -ManF) and α -D-xylosyl fluoride (α -XylF) were provided by Prof. Stephen G. Withers, University of British Columbia, whose group synthesized these by the

Yokoyama (2000) method. Cyclophellitol was a generous gift from Kah-Yee Li and Prof. Dr. Herman Overkleeft, University of Leiden. Other chemicals and molecular reagents used but not listed here were purchased from a variety of suppliers.

2.2 General methods

2.2.1 Preparation of competent cells of *E. coli* strains XL-1 blue and Origami(DE3)

Bacteria from glycerol stocks were streaked onto a Lennox broth (LB, 10 g/l tryptone, 5 g/l yeast extract, 5 g/l sodium chloride) agar plates containing 15 µg/ml kanamycin and 12.5 µg/ml tetracycline for Origami(DE3) or without antibiotic for XL-1 blue. A single colony was picked into 5 ml LB media containing antibiotics as listed above. The cells were grown at 37°C for 16-18 hr with shaking at 200 rpm. Then, 0.5 ml of starter culture was inoculated into 50 ml LB in a 250 ml flask and incubated at 37°C with shaking until the OD₆₀₀ reached 0.3-0.4. The culture was cooled on ice for 15 min, then transferred to pre-cooled centrifuge tubes, and the cells were collected by centrifugation at 3,000 rpm for 10 min. Cells were gently and slowly resuspended with 10 ml of cold 0.1 M CaCl₂ and placed on ice for 20 min. The cells were centrifuged as before and resuspended with 0.5 ml of cold 0.1 M CaCl₂ and placed on ice for 1 hr. Finally, cold glycerol was added to the cells to the final concentration of 15%. Then, they were resuspended and 50 µl aliquots were stored in pre-cooled tubes at -80°C.

2.2.2 Transformation of plasmid DNA into competent cells

Super coiled plasmid DNA (50 ng) was added into the 50 µl of competent cells, mixed by tapping and immediately place on ice for 30 min. The cells were heat shocked at 42°C for exactly 45 s and then immediately put on ice for 2-3 min. Then, 0.5 ml of LB medium was added into the cell mixture and the tube was incubated in a 37°C shaker for 1 hr. Then, 100-200 µl of the cells were spread on an LB plate containing the appropriate antibiotics and incubated at 37°C overnight.

2.2.3 Mutagenesis with the QuikChange[®] Site-Directed Mutagenesis Kit

The QuikChange[®] Site-Directed Mutagenesis Kit (Stratagene) was used to construct the mutants of BGlu1 and BGlu1 E386G. The pET32a(+) *bglu1* or *bglu1 E386G* plasmid (containing the *bglu1* or *bglu1 E386G* cDNA, respectively) was used as a template for amplification of full-length plasmid strands using two overlapping oligonucleotide primers containing the desired mutation (Table 2.1). The mutagenic oligonucleotide primers were specifically designed according to the criteria of the QuikChange manual to have lengths of 25-45 bases with $T_m \geq 78^\circ\text{C}$. The T_m was calculated from following formula:

$$T_m = 81.5 + 0.41 (\%GC) - 675/N - \%mismatch, \text{ where}$$

- N is the primer length in nucleotides,
- %GC and %mismatch are whole numbers.

PfuTurbo DNA polymerase (with proofreading activity) was used to polymerize the mutated plasmid DNA during the temperature cycling, which included step 1, 95°C 30 s; step 2, 95°C 30 s; step 3, 55°C 1 min and step 4, 68°C 7.5 min, with steps 2 to 4 repeated for 16 cycles. The PCR products were treated with *DpnI* endonuclease to

eliminate methylated and hemimethylated DNA of the parental DNA template. Repair of the nicked circular dsDNA products was performed by transformation into competent XL-1 blue cells. The transformants were selected on agar plates containing ampicillin and were expected to contain the target mutation, but were sequenced to confirm the presence of these mutations and the absence of any others.

2.2.4 SDS-PAGE electrophoresis

SDS-PAGE was performed by the method of Laemmli (1970). The 12% separating gel was prepared for 2 mini-gels containing 3.345 ml of distilled water, 2.5 ml of 1.5 M Tris-HCl, pH 8.8, 4 ml of 30% (2.67% C) acrylamide/bisacrylamide solution, 100 μ l of 10% (w/v) SDS, 50 μ l of 10% (w/v) ammonium persulfate, and 5 μ l TEMED. The 4% stacking gel was prepared by mixing 3 ml of distilled water, 1.25 ml of 0.5 M Tris-HCl, pH 6.8, 0.67 ml of 30% acrylamide/bisacrylamide solution, 50 μ l of 10% (w/v) SDS, 25 μ l of 10% (w/v) ammonium persulfate, and 5 μ l of TEMED. The two gel polymerizations were done in a Hoeffer gel electrophoresis cassette (GE Healthcare). Sixteen microliters of protein sample was mixed with 4 μ l of 5x denaturing sample buffer (0.05 M Tris-HCl pH 6.8, 10% (w/v) SDS, 50% (v/v) glycerol, 0.5 mg/ml bromophenol blue, 20% (v/v) 2-mercaptoethanol) and boiled at 100°C for 5 min. The sample was spun down and loaded onto the gel under running buffer (25 mM Tris, 192 mM glycine, 0.1% (w/v) SDS) and placed in an electric field of 150 volts for 1 hr and 30 min. The protein bands were detected with Coomassie brilliant blue staining solution (0.1% (w/v) Coomassie brilliant blue R-250, 40% (v/v) MeOH, 10% (v/v) glacial acetic acid) and the blue background was washed out with destaining solution (40% (v/v) MeOH, 10% (v/v) glacial acetic acid). The migration

distance of the protein band was compared to the low molecular weight calibration electrophoresis standards (GE Healthcare); phosphorylase b (97 kDa), bovine serum albumin (66 kDa), ovalbumin (45 kDa), bovine carbonic anhydrase (30 kDa), soy bean trypsin inhibitor (20.1 kDa), and bovine milk α -lactalbumin (14.4 kDa).

2.3 Mutations

2.3.1 Mutation of rice BGlu1 and BGlu1 E386G

The production of the mutations for BGlu1 N245V, and the BGlu1 glycosynthases, BGlu1 E386G, BGlu1 E386A and BGlu1 E386S, which were previously designated E414G, E414A and E414S based on their positions in the BGlu1 precursor protein, has been described previously (Chuenchor *et al.*, 2008, Hommalai *et al.*, 2007). The mutations S334A, Y341A, Y341L and N245V of the rice *bglu1* and rice *bglu1 E386G* cDNA (Opassiri *et al.*, 2003, Hommalai *et al.*, 2007) were constructed with the QuikChange site-directed mutagenesis kit as described in Section 2.2.3. The primers used are shown in Table 2.1 and the presence of all desired mutations and lack of undesired mutations were confirmed by DNA sequencing.

2.3.2 Generation of E386G2 mutant of rice BGlu1

BGlu1 E386G2 was constructed by changing the DNA codon for GAG to GGC by QuikChange mutagenesis (Section 2.2.3) with the E386G2_f and E386G2_r primers (shown in Table 2.1) and the pET32a/BGlu1 expression vector as template. The presence of the desired mutation and lack of additional mutations were confirmed by DNA sequencing.

2.4 Protein expression

The circular super coiled recombinant pET32a(+) plasmids containing the *bgluI* cDNA and the *bgluI* cDNA with the mutants described above were transformed into *E. coli* Origami(DE3) competent cells by heat shock and the cells were selected on LB plates containing 15 µg/ml kanamycin, 12.5 µg/ml tetracycline and 50 µg/ml ampicillin at 37°C overnight. Single colonies of transformed cells were picked and inoculated into 50 ml LB broth containing the same antibiotics and grown at 37°C overnight. A 1% starter culture was inoculated in a large scale culture in the same medium for 5-6 hr, at 37°C, until the OD₆₀₀ reached 0.5. Then, IPTG was added to a final concentration of 0.4 mM for induction, and the culture was grown for 18 hr at 20°C. The cultures were precooled on ice, the bacterial cells were collected by centrifugation at 5,000 rpm for 20 min, and the cell pellets were kept at -80°C.

2.5 Protein purification

2.5.1 Protein purification for crystallization

The cell pellets were extracted in extraction buffer; containing 50 mM sodium phosphate buffer, pH 7.0, 150 mM NaCl, 1% (v/v) Triton-X 100, 200 µg/ml lysozyme, 1 mM PMSF and 5 µg/ml DNase I and incubated at room temperature for 30 min. Cell debris was removed by centrifugation (12,000 rpm, 20 min, 4°C) and the soluble fusion protein was purified by immobilized metal-affinity chromatography (IMAC) on cobalt resin (Chelating Sepharose Fast Flow, GE Healthcare, loaded with 100 mM CoCl₂). To bind the His₆-tagged proteins to the cobalt resin, 5 ml of cobalt resin, which had been equilibrated with equilibration buffer (50 mM sodium

phosphate buffer, pH 7.0, 150 mM sodium chloride) were added to 40 ml of soluble protein extract and then gently shaken on ice for 1 hr. The resin-bound protein was centrifuged at 1,000 rpm for 5 min at 4°C, the supernatant was removed, and the resin was loaded into a column. The protein-bound resin was washed with 10 column volumes (CV) of equilibration buffer, 5 CV of wash buffer 1 (5 mM imidazole in equilibration buffer) and 5 CV of wash buffer 2 (10 mM imidazole in equilibration buffer). Finally, the bound protein was eluted with elution buffer (150 mM imidazole in equilibration buffer). The fractions were checked for protein patterns by SDS-PAGE (Laemmli, 1970), then the fractions containing purified fusion protein were pooled, and imidazole was removed by buffer exchange with 20 mM Tris-HCl, pH 8.0, via gel filtration chromatography on a Sephadex G-25 column (GE Healthcare) on an ÄKTA Protein Purifier (GE Healthcare) or repeated filtration in a 30 kDa molecular weight cut-off (MWCO) Centricon centrifugal filter (Millipore, Beverly, MA, USA).

To remove the N-terminal fusion tag, the fusion protein was cleaved with 1 µl enterokinase (12.5 units/µl, New England Biolabs, Beverly, MA, USA) per milligram of protein in 20 mM Tris-HCl, pH 8.0, at 23°C for 16 hr. To remove the cleaved fusion tag and uncleaved fusion protein from the tag-free enzyme, the digest was loaded onto a cobalt IMAC column with 1 ml cobalt resin per 2 milligrams of protein and the resin was washed with equilibration buffer. The purity of the protein in the unbound fractions containing tag-free BGlul was checked by SDS-PAGE and the most pure fractions combined. The buffer was changed to 20 mM Tris-HCl, pH 8.0, and the protein was concentrated in a 10 kDa MWCO Centricon centrifugal filter. To purify the tag-free protein to homogeneity, it was loaded onto a Superdex 200 gel

filtration chromatography column (HR10/30, GE Healthcare) on an ÄKTA Protein Purifier. The column was equilibrated and eluted with 20 mM Tris-HCl, pH 8.0, 150 mM NaCl at a flow rate of 0.25 ml/min. The protein sample was centrifuged at 12,000 rpm for 10 min to remove dust, then 0.5 ml was injected to the system, and 0.5 ml fractions were collected. The purified protein fractions were pooled, concentrated and stored at -20°C.

The purified protein concentration was determined by measuring absorbance at 280 nm. Extinction coefficients ϵ_{280} of 113320 M⁻¹cm⁻¹ for most of the BGlu1 proteins and ϵ_{280} of 112040 M⁻¹cm⁻¹ for BGlu1 Y341A and Y341L calculated, by the method of Gill and von Hippel (1989), were used to calculate the enzyme concentrations. Rice BGlu1 contains 12 tryptophan (Trp) residues, 35 tyrosine (Tyr) residues and 2 cystine residues. The equation of Gill and von Hippel is:

$$\epsilon_{\text{protein}} (\text{M}^{-1} \text{cm}^{-1}) = a \epsilon_{\text{trp}} + b \epsilon_{\text{tyr}} + c \epsilon_{\text{cystine}},$$

where $\epsilon_{\text{trp}} = 5690 \text{ M}^{-1} \text{cm}^{-1}$, $\epsilon_{\text{tyr}} = 1280 \text{ M}^{-1} \text{cm}^{-1}$, $\epsilon_{\text{cys}} = 120 \text{ M}^{-1} \text{cm}^{-1}$;

a = amount of tryptophan residues

b = amount of tyrosine residues

c = amount of cystine residues

2.5.2 Protein purification for characterization

Wild type BGlu1 and mutant BGlu1 enzymes of BGlu1 S334A, BGlu1 Y341A, BGlu1 Y341L and BGlu1 N245V were purified by immobilized metal affinity chromatography (IMAC), enterokinase digestion and IMAC, as described in

the preceding section, and the buffer was exchanged with 20 mM Tris-HCl, pH 8.0, and then the proteins were used for kinetic analysis of oligosaccharide hydrolysis.

The BGlu1 E386G glycosynthase and its 4 mutants, BGlu1 E386G/S334A, BGlu1 E386G/Y341A, BGlu1 E386G/Y341L and BGlu1 E386G/N245V, and BGlu1 E386G2 were purified as the other proteins described above and the buffer was exchanged with 50 mM phosphate buffer, pH 6.0, and then the proteins were used for transglycosylation.

2.6 Protein crystallization

Before crystallization, the protein solution was filtered through an Ultrafree-MC 0.22 μm filter (Millipore) at 8,000 rpm for 5 min to eliminate microbial contamination, dust, micro-crystals, and precipitated protein. The BGlu1 E386G and its mutants were crystallized alone and with ligands, including 10 mM α -glucosyl fluoride (α -GlcF), 10 mM *p*NP- β -D-cellobioside (*p*NPC2), both 10 mM α -GlcF and 10 mM *p*NPC2, 2 mM cellotetraose and 2 mM cellopentaose by hanging drop vapor diffusion with microseeding in a 24 well TC-plate (Greiner Bio-One, Germany). Conditions for the crystallization were optimized from the conditions used for crystallization of BGlu1 (Chuenchor *et al.*, 2006; 2008), by varying the concentrations of polyethylene glycol monomethyl ether (PEG MME) 5000 over the range of 16-26%, $(\text{NH}_4)_2\text{SO}_4$ between 0.12-0.26 M, and protein between 2-6 mg/ml in 0.1 M MES, pH 6.7, at 15°C. For seed stock preparation, BGlu1 crystals were washed in 10 μl of reservoir solution three times. The crystals were crushed with a cat whisker, and then the suspension was added to a 1.5 ml microcentrifuge tube containing 100 μl of

reservoir solution. The microcrystal stock was diluted with mother liquor to 1/100 and stored at 4°C. Glass cover slips (18 mm x 18 mm, Menzel-Glaser, Braunschweig, Germany) were siliconized to reduce surface tension and prevent nonspecific binding. For siliconization, the glass cover slides were washed with a solution of 1 part 0.1 M HCl and 3 parts absolute MeOH for 30 min, and then washed with deionized water three times. Finally, 300 µl of dimethyldichlorosilane (Fluka, Switzerland) were added and the glass slides were put in the oven at 70°C overnight. High vacuum grease (Dow Corning, Michigan, USA) was applied to the edges of each well of the TC-plate, and 0.5 ml of reservoir solution containing appropriate amounts of precipitant was added to each well. Then, 1 µl of precipitant solution was pipetted onto the center of a siliconized cover slip, and 2 µl of pure protein was placed on the precipitant drop without mixing. The cover slip was carefully inverted, so the crystallization drop faced the reservoir solution and the cover slip was sealed with the grease layer. The plates were equilibrated against the reservoir solution in a 15°C incubator. The rice BGl1 crystal seeds (Chuenchor *et al.*, 2006; 2008) were microseeded by streak seeding with a cat whisker into pre-equilibrated hanging drops after pre-equilibration of the drop and precipitant for 2 hr, and incubated further at the same temperature. The crystallization drops were carefully checked under a Zeiss Stemi 2000-C stereo microscope (Zeiss Corp, NJ, USA).

Before flash cooling in liquid nitrogen, the crystals with 10 mM α -GlcF, 10 mM *p*NPC2, and both 10 mM α -GlcF and 10 mM *p*NPC2 were soaked in cryo solution (18% (v/v) glycerol in precipitant solution) containing the same concentrations of ligands for 1-5 min, while the crystals with cellotetraose and cellopentaose were soaked in the cryosolution saturated with the ligands (approx. 75-100 mM

cellotetraose or 25 mM cellopentaose). Then, the crystals were scooped up in a nylon loop and flash vitrified in liquid nitrogen for diffraction.

2.7 Data collection and processing

Preliminary diffraction experiments were done under a nitrogen cryostream from a 700 series Cryostream Cooler (Oxford Cryosystems, Oxford, England), using a Cu K α rotating anode source mounted on a MicroSTAR generator operating at 45 kV and 60 mA connected to Rayonix SX-165 CCD detector at the Synchrotron Light Research Institute (Public Organization) (SLRI, Nakhon Ratchasima, Thailand). Promising crystals were used to diffract 1.0 Å wavelength X-rays on the BL13B1 beamline at the National Synchrotron Radiation Research Center (NSRRC in Hsinchu, Taiwan), and reflections were recorded with an ADSC Quantum 315 CCD detector. The crystals were maintained at 105 K during diffraction with a nitrogen cold stream (Oxford Instruments). The mounted crystal was translated and rotated using the goniometer head to center the crystal in the X-ray beam. During X-ray diffraction, data frames were collected over 0.5° oscillations, and an exposure time of 5-15 s for 180° rotation or until the data were complete. The distance between the crystal and the detector was in the range of 160-300 mm, depending on the highest resolution of the data and spot overlap. Data were processed and scaled with the HKL-2000 package (Otwinowski and Minor, 1997). The maximum resolution for each data set was determined by choosing the outer shell that gave a ratio of measured intensity to its standard deviation ($I/\sigma(I)$) >2-fold. Moreover, the completeness, redundancy, and R_{linear} after merging (R_{merge}) were considered for evaluating the

resolution of the data set. The cut off for the linear R_{merge} was generally ≤ 0.5 in the outer shell, depending on redundancy.

2.8 Structure solution and refinement

The crystals of glycosynthases were isomorphous with wild type BGlu1 crystals (Chuenchor *et al.*, 2008), allowing the structures to be solved by rigid body refinement with the free BGlu1 structure (PDB: 2RGL) in REFMAC5 (Murshudov *et al.*, 1999) with the two molecules in the asymmetric unit refined as independent domains. The refinement was executed with the same program with tight noncrystallographic symmetry (NCS) restraints and model building was done with Coot (Emsley and Cowtan, 2004). The two Fourier electron density maps 2Fo-Fc and Fo-Fc were calculated after each round of refinement for rebuilding. The ligands were added based on these maps, and then water molecules were added with the Coot and ARP/wARP programs in the CCP4 suite. The water molecules were added or deleted based on the electron density (2Fo-Fc map sculpted at 1.2σ), temperature factors (B-factors) and hydrogen bonding distances between the water molecules and the neighboring amino acid residues. Glucosyl residues were built into the electron densities in the shapes that fit the densities best (4C_1 relaxed chairs or 1S_3 skew boats) and refined. The refined sugar residue coordinates were assigned their final conformation designation according to their Cremer-Pople parameters (Cremer and Pople, 2004), as calculated by the Cremer-Pople parameter calculator of Dr. Shinya Fushinobu (University of Tokyo, <http://www.ric.hi-ho.ne.jp/asfushi/>). The occupancy of cellopentaose binding in the active site of BGlu1 E386G was refined to 0.7 by setting at different values and refining to find the occupancy that minimized the

values of the B-factors of the ligand and the free residual factor (R_{free}). The final models were analyzed with PROCHECK (Laskowski *et al.*, 1993) and MolProbity (Davis *et al.*, 2007). The criteria for any good quality model is root mean square (R.M.S.) deviations of not more than 0.014 Å for bond distance and 3° for bond angles. The figures of protein structures were generated in PyMol (Schrödinger LC).

2.9 Oligosaccharide hydrolysis

The activities of wild type and mutant BGl1 enzymes were assayed against the specific substrates cellotriose, cellotetraose and cellopentaose. To determine the kinetic parameters, wild type and mutant BGl1 proteins were assayed in 50 mM sodium acetate buffer, pH 5.0, at 30°C for a time to which the initial velocity (v_0) was maintained (15 min), as determined by initial time course experiments. The reactions were stopped by heating at 90°C for 5 min and the amount of glucose generated was analyzed by a glucose oxidase/peroxidase (PGO) coupled assay. The 50 µl reaction mixture was transferred to a microtiter plate well containing 50 µl of 1 mg/ml 2,2'-azino-bis(3-ethylbenzothiazoline-6-sulfonic acid) (ABTS), and 100 µl of PGO enzyme (Sigma). The PGO reaction assay was incubated at 37°C for 30 min. The glucose release was measured as the absorbance at 405 nm with an iEMS Reader MF microtiterplate photometer (Labsystems iEMS Reader MF, Finland). The kinetic parameters V_{max} and K_m were calculated by nonlinear regression of Michaelis-Menten plots with the Grafit 5.0 computer program (Erithacus Software, Horley, UK) and divided by the protein concentrations to determine the apparent k_{cat} and k_{cat}/K_m . Relative subsite affinities were determined by the method of Hiromi *et al.* (1973), which assumes an intrinsic k_{cat} . Subsite affinities were calculated as follows: $A_{n-1} =$

$-\Delta G = RT \ln[(k_{\text{cat}}/K_m)_n / (k_{\text{cat}}/K_m)_{n-1}]$, where n designates the length of the oligosaccharide in glucosyl residues, R is the gas constant ($8.314 \text{ J mol}^{-1} \text{ K}^{-1}$) and T the absolute temperature (303 K).

2.10 Oligosaccharide synthesis by BGlu1 glycosynthase enzymes

The BGlu1 E386G glycosynthase and its 4 mutants, BGlu1 E386G/S334A, BGlu1 E386G/Y341A, BGlu1 E386G/Y341L and BGlu1 E386G/N245V were incubated with α -GlcF donor and p NPC2 acceptor in 150 mM ammonium bicarbonate buffer, pH 7.0, at 30°C for 16 hr. (Hommalai *et al.*, 2007). The reaction mixture was centrifuged at 12,000 rpm for 5 min. The enzymes in the supernatant were removed by centrifugal filtration (Microcon YM-10, Millipore, USA) and the soluble products were analyzed by electrospray ionization-mass spectrometry (ESI-MS). The 5 μl of samples were diluted in 200 μl of 20% (v/v) MeOH, 0.1% (v/v) formic acid and 5 μl of the solution was injected to ESI-MS (Waters, Alliance HPLC, Micromass ZQ ESCi, USA). The quadrupole mass analyzer was scanned over a range of 100-1,000 m/z and 500-1500 m/z . Moreover, 1 μl of the soluble products were monitored by thin-layer chromatography (TLC, silica gel 60 F₂₅₄, Merck, Darmstadt, Germany) using 7:2.5:1 (v/v/v) EtOAc-MeOH-water as solvent. Plates were visualized under ultraviolet (UV) light and by exposure to 10% (v/v) sulfuric acid in ethanol followed by charring. Five microliters of the products from the reactions with 1:1 molar ratios of α -GlcF donor: p NPC2 acceptor were loaded onto a ZORBAX carbohydrate column (4.6 mm x 250 mm, Agilent, USA) connected to an Agilent 1100 series LC-MSD. The column was eluted with a linear gradient from 90% to 50% (v/v) acetonitrile in water over 30 min at a flow rate of 1 ml/min. The eluted peaks

were detected at 300 nm with a UV-visible diode array detector. Reaction yields were determined by integration of the product UV peaks within the HPLC profile, and the molecular masses of the eluted products were determined by mass spectrometry.

2.11 Transglycosylation by BGlu1 E386G with various donors

The BGlu1 E386G glycosynthase was incubated at 40 μ M with 10 mM of one of the donors α -AraF, α -FucF, α -GalF, α -ManF and α -XylF and 10 mM *p*NPC2 acceptor in 150 mM ammonium bicarbonate buffer, pH 7.0, at 30°C for 16 hr (Hommalai *et al.*, 2007). The products were analyzed by TLC with EtOAc-MeOH-water (7:2.5:1, v/v/v) as solvent. Plates were visualized under UV light and by exposure to 10% sulfuric acid in ethanol, followed by charring. Samples of 5 μ l were diluted to 200 μ l of 20% (v/v) MeOH, 0.1% (v/v) formic acid and 5 μ l of the solution was injected to ESI-MS (Waters), as described in Section 2.10.

2.12 Transglycosylation by BGlu1 E386G and 4 mutants to various acceptors

The BGlu1 E386G glycosynthase and the E386G double mutants of BGlu1 E386G/S334A, BGlu1 E386G/Y341A, BGlu1 E386G/Y341A and BGlu1 E386G/N245V described above were incubated at a concentration of 40 μ M with 10 mM α -GlcF donor and 10 mM of one of the possible acceptors: glucose, cellobiose, *p*NPGlc, *p*NPFuc, *p*NPGal, *p*NPMan or *p*NPXyl in 150 mM ammonium bicarbonate, pH 7.0, at 30°C for 16 hr. The products were analyzed by TLC with EtOAc-MeOH-water at 7:2.5:1 (v/v/v) as solvent for glucose and *p*NP-oligosaccharides, and 2:1:1

(v/v/v) for cellobiose. The products were further verified by ESI-MS (Waters), as described in Section 2.10. Three microliters of the products from the reactions with 1:1 molar ratios of α -GlcF:*p*NPGlc or α -GlcF:*p*NPFuc were loaded onto a ZORBAX carbohydrate column, as described in Section 2.10, and the column was eluted with a linear gradient from 90% to 60% (v/v) acetonitrile in water over 30 min at a flow rate of 0.8 ml/min.

2.13 Transglycosylation by BGlu1 E386G2 mutant

The transglycosylation activity of the glycosynthase with the new mutation (codon: GGC, BGlu1 E386G2) was compared to the original BGlu1 E386G glycosynthase (codon: GGG, Hommalai *et al.*, 2007) toward various donors, including α -AraF, α -FucF, α -GalF, α -GlcF, α -ManF and α -XylF with *p*NPC2 acceptor, and α -GlcF donor with various acceptors, including glucose, cellobiose, *p*NPGlc, *p*NPC2, *p*NPFuc, *p*NPGal, *p*NPMan and *p*NPXyl in 150 mM ammonium bicarbonate, pH 7.0, at 30°C for 16 hr. The products were analyzed by TLC with EtOAc-MeOH-water at 7:2.5:1 (v/v/v) as solvent.

2.14 NMR spectroscopy of glycosynthase products

To characterize the linkages in glycosynthase products, *p*NP-oligosaccharide products from reactions of α -FucF and *p*NPC2, and α -ManF and *p*NPC2 synthesized with BGlu1 E386G glycosynthase and from reactions of α -GlcF and *p*NPFuc synthesized with both BGlu1 E386G and BGlu1 E386G/N245V were purified. Reactions of α -FucF or α -ManF (14.6 mg, 4 equivalents) and *p*NPC2 (9.2 mg, 1

equivalent); α -GlcF (48 mg, 1 equiv.) and *p*NPFuc (75 mg, 1 equiv.) and 40 μ M of the enzyme were incubated at 30°C in 150 mM ammonium bicarbonate, pH 7.0, (2-10 ml total reaction volume) for 24-48 hr. The reaction mixtures were filtered and loaded onto a reverse-phase column (Sep-Pak tC18, sorbent weight 2 g, Waters, USA), which was eluted with a gradient of 5% steps from 0-30% (v/v) MeOH in water. Eluted fractions were checked by TLC, as described above. Fractions containing the compounds of interest were pooled, dried on a rotary evaporator, and further purified by silica gel TLC with EtOAc-MeOH-water at 7:2:0.5 (v/v/v) as solvent. Silica gel containing each compound was scratched from TLC plate and the separated compounds were eluted with 30% (v/v) MeOH, then the MeOH was evaporated and the sample solution was dried by lyophilization. Their masses were determined by ESI-MS (Waters).

A mixture of pyridine and acetic anhydride (5 ml, $V_{\text{pyridine}} : V_{\text{acetic anhydride}} = 3:2$) was added to the purified glycoside products at room temperature and the reaction mixture was stirred overnight. Ice water was added to quench the unreacted acetic anhydride and the reaction was stirred for another 10 min. After evaporation of the solvent, the residue was dissolved in EtOAc and washed successively with ice water, 1 M HCl, NaHCO₃ and brine (saturated NaCl), and dried with MgSO₄. The organic solvent was removed *in vacuo*, and the resulting residue was purified by flash chromatography on a silica gel column using 1:1 (v/v) EtOAc:petroleum ether as eluent.

All ¹H and ¹H COSY nuclear magnetic resonance (NMR) spectra were recorded on a Bruker Avance-400 inv spectrometer (400 MHz) and chemical shifts were reported in δ units (p.p.m.) and were calibrated based on the deuterium solvent

chemical shift (CDCl_3). Multiplicity of signals was described as the following: br-broad, s-singlet; d-doublet; t-triplet; m-multiplet.

2.15 Cyclophellitol inhibition

2.15.1 Time courses of cyclophellitol inhibition

The time courses of cyclophellitol inhibition of wild type BGlu1, BGlu1 E386G and BGlu1 E386G2 activities were determined for kinetic analysis. Solutions of 0.2 μM BGlu1, 40 μM BGlu1 E386G and 40 μM BGlu1 E386G2 in 50 mM sodium acetate, pH 5.0, were pre-incubated with 1 μM cyclophellitol at 30°C for different times (10, 20, 30, 60 and 120 min) and then β -glucosidase activity against *p*NPGlc was assayed. Ten microliters of the enzyme, 70 μl of 10 mM *p*NPGlc and 60 μl of 50 mM sodium acetate, pH 5.0, were transferred to a microtiter plate well and the plate was incubated at 30°C for 15 min and the reactions were stopped by adding 70 μl of 0.4 M NaCO_3 . The liberated *p*NP was measured at 405 nm absorbance and the relative inhibition was quantified by comparison to a control reaction of the enzymes without cyclophellitol.

2.15.2 Kinetic analysis

Inactivation of wild type BGlu1 by cyclophellitol was performed by incubating the BGlu1 enzyme in 50 mM sodium acetate, pH 5.0, at 30°C in the presence of different cyclophellitol concentrations (0.5, 0.75, 1, 1.25 and 1.5 μM). Aliquots (10 μl) were removed at appropriate time intervals (0, 5, 10, 15, 20, 30, 40, 50, 70 and 90 min) and assayed for enzyme activity against *p*NPGlc, as described above. A Semi-logarithmic plot of the β -glucosidase activity versus time was

generated for first order kinetics and their slopes gave the apparent first order rate constants for inactivation at each inhibitor concentration. The apparent first order rate constant, k_{app} , is related to the inhibitor concentration [I] by the following reaction scheme and equations (Lalégerie *et al.*, 1982; Tai *et al.*, 1995).



Where, E is free enzyme, I is inhibitor, E*I is the noncovalently bound enzyme-inhibitor complex, and E-I is enzyme-inhibitor covalent complex.

Most experimental results obtained with covalent inhibitors of glycosidases can be adequately explained with this scheme. The ratio of residual activity /initial activity (V/V_0) is proportional to E/E_0 ratio, which is time (t) dependent according to:

$$\ln \frac{E}{E_0} = -k_{app} \cdot t \quad (1)$$

k_{app} is the apparent experimental kinetic inhibition constant defined by:

$$k_{app} = k_i \frac{[E^*I]}{[E] + [E^*I]} \quad \text{with} \quad K_i = \frac{[E][I]}{[E^*I]}$$

Therefore, substituting for [E*I] leads to:

$$k_{app} = k_i \frac{[I]}{K_i + [I]} \quad (2)$$

Since k_{app} remains constant during the course of inactivation when $[E_0] \ll [I_0]$, Equation (1) will give a linear plot of $\ln(E/E_0) = \ln(V/V_0)$ vs time, which was used to determine k_{app} at each concentration of inhibitor.

Taking the reciprocal of Equation (2), gives a linear equation of the various parameters:

$$\frac{1}{k_{app}} = \frac{K_i}{k_i} \frac{1}{[I]} + \frac{1}{k_i} \quad (3)$$

Thus, a replot of the reciprocal of k_{app} versus the reciprocal of $[I]$ was generated, and the equilibrium constant for initial binding, K_i , and the inactivation rate constant, k_i , obtained from the graph, where the y-intercept = $1/k_i$ and x-intercept = $-1/K_i$.

2.15.3 Cyclophellitol inhibition of transglycosylation

The β -glucosidase activity was inactivated by pre-incubating 0.2 μ M BGlu1, 40 μ M BGlu1 E386G or 40 μ M BGlu1 E386G2 with 2 mM cyclophellitol for 2 hr and then the transglycosylation reactions were set-up with 10 mM *p*NPFuc and 10 mM α -GlcF in 150 mM NH_4HCO_3 , pH 7.0, at 30°C for 16 hr. The transglycosylation products were analyzed by TLC, with EtOAc-MeOH-water (7:2.5:1, v/v/v) as solvent. The TLC plate was visualized under UV light and by exposure to 10% sulfuric acid in ethanol followed by charring.

CHAPTER III

RESULTS

3.1 Protein purification

In this study, rice BGlu1 proteins, including β -glucosidase enzymes: wild type BGlu1 and its mutants, BGlu1 S334A, BGlu1 Y341A, BGlu1 Y341L and BGlu1 N245V; glycosynthase enzymes: BGlu1 E386G, BGlu1 E386A and BGlu1 E386S; glycosynthase mutant enzymes: BGlu1 E386G/S334A, BGlu1 E386G/Y341A, BGlu1 E386G/Y341L and BGlu1 E386G/N245V; and the new construct glycosynthase enzyme BGlu1 E386G2, were studied. All enzymes were purified by an initial IMAC step, enterokinase cleavage and a 2nd IMAC step for characterization, while the glycosynthase and its mutant enzymes were further purified by Superdex 200 gel filtration chromatography for crystallization.

The recombinant BGlu1 proteins from two to four liters of bacterial culture were conveniently prepared by purification of the fusion protein over an IMAC column, followed by cleavage of the fusion proteins by enterokinase protease and removal of the fusion tags by binding them to the IMAC column. Moreover, gel filtration chromatography was required to further purify the tag-free proteins for crystallization. The purity of the proteins after the 2nd IMAC and S200 gel filtration steps appeared similar, based on SDS-PAGE (Figure 3.1), although better crystallization was achieved after gel filtration. The resulting soluble 55 kDa proteins

were >95% pure (Figures 3.1, 3.2, 3.3 and 3.4), and could be concentrated to a final concentration of 10-20 mg/ml.

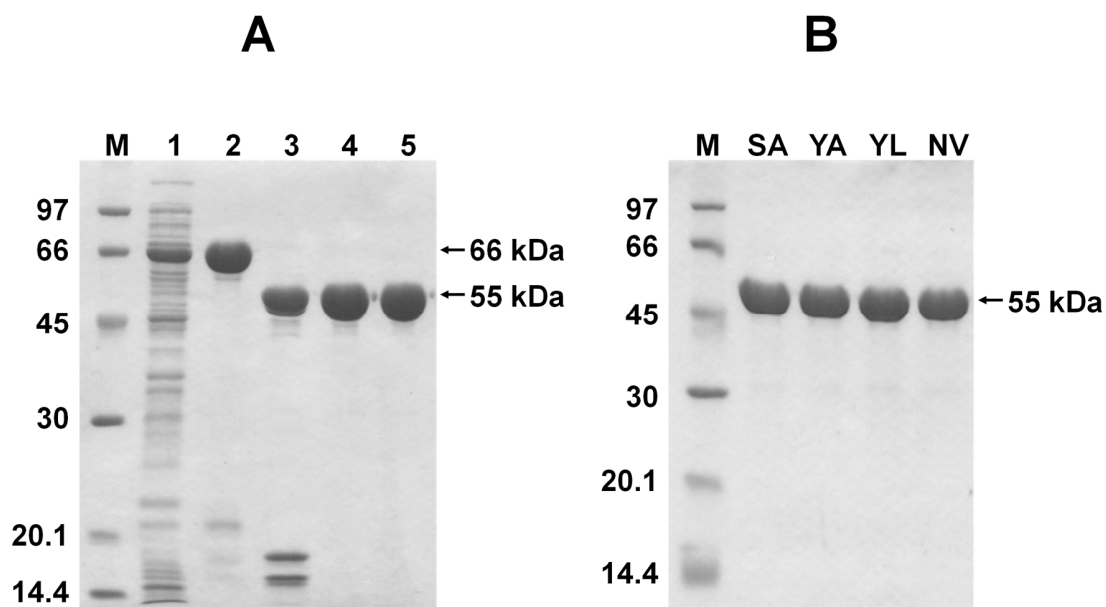


Figure 3.1 SDS-PAGE of purified BGlul1 E386G and its mutants. (A) BGlul1 E386G fractions from the purification steps and (B) BGlul1 E386G mutants after the final purification step of S200 gel filtration. Lane M, Low molecular weight markers (kDa); Lane 1, soluble extract of *E. coli* cells; Lane 2, fusion protein after the 1st IMAC step; Lane 3, enterokinase digest; Lane 4, BGlul1 E386G after the 2nd IMAC step; Lane 5, BGlul1 E386G after the final S200 purification. Mutant enzymes in B are SA, BGlul1 E386G/S334A; YA, BGlul1 E386G/Y341A; YL, BGlul1 E386G/Y341L and NV, BGlul1 E386G/N245V.

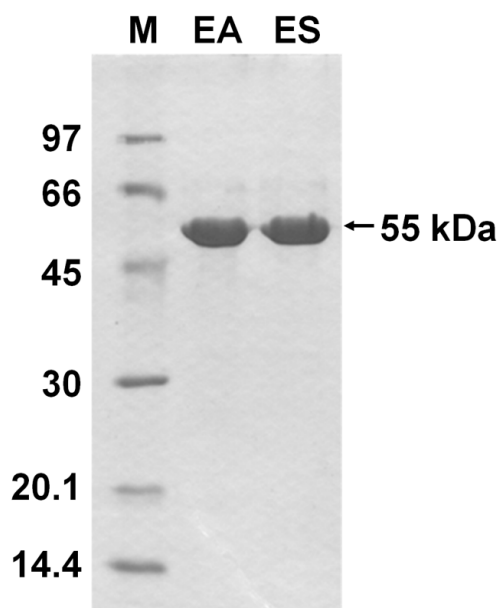
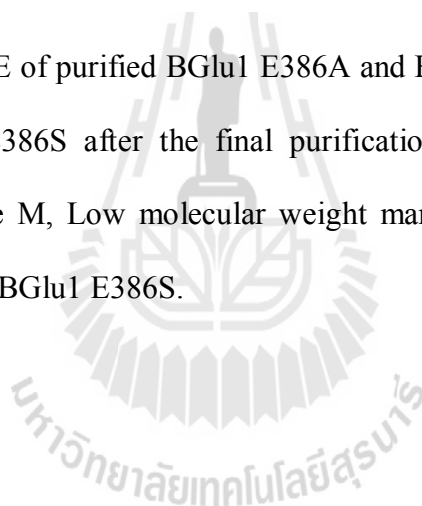


Figure 3.2 SDS-PAGE of purified BGLu1 E386A and BGLu1 E386S. Purified BGLu1 E386A and BGLu1 E386S after the final purification step of S200 gel filtration chromatography. Lane M, Low molecular weight markers (kDa); Lane EA, BGLu1 E386A; and Lane ES, BGLu1 E386S.



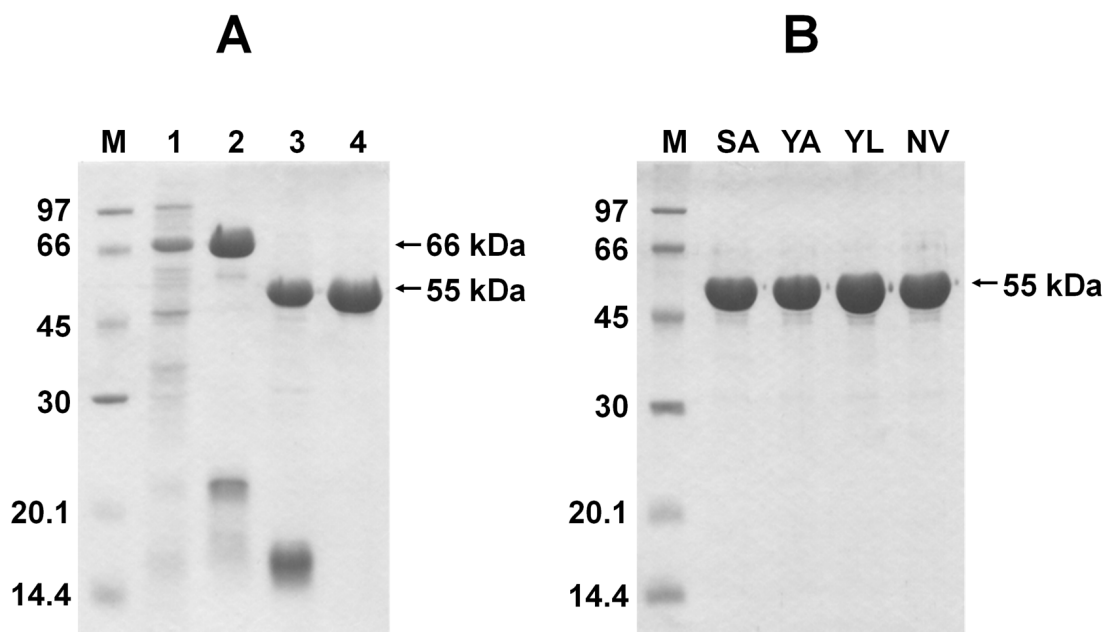


Figure 3.3 SDS-PAGE of purified BGLu1 β -glucosidase and its mutants. (A) BGLu1 pools from the purification steps and its mutants (B) purified after the 2nd IMAC step. Lane M, Low molecular weight markers (kDa); Lane 1, soluble extract of *E. coli* cells; Lane 2, fusion proteins after the 1st IMAC; Lane 3, enterokinase digest; Lane 4, BGLu1 protein after the 2nd IMAC. Mutant enzymes in B are SA, BGLu1 S334A; YA, BGLu1 Y341A; YL, BGLu1 Y341L; and NV, BGLu1 N245V.

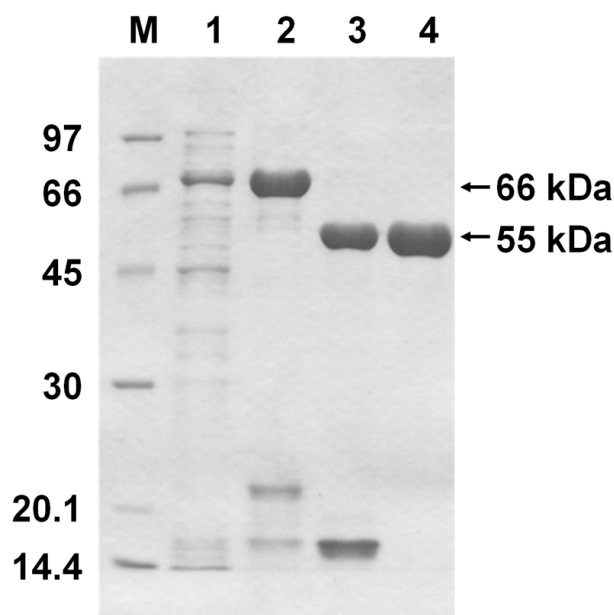


Figure 3.4 SDS-PAGE of purified BGlul1 E386G2 from the purification steps. Lane M, Low molecular weight markers (kDa); Lane 1, soluble extract of *E. coli* cells; Lane 2, fusion proteins after the 1st IMAC; Lane 3, enterokinase digest; and Lane 4, protein after the final step of the 2nd IMAC.

3.2 Protein crystallization

3.2.1 BGlul1 E386G, E386S and E386A without and with α -GlcF

Crystallization of BGlul1 E386G, E386S and E386A without and with 10 mM α -GlcF was optimized by hanging drop vapor diffusion with microseeding and varied around the conditions used for crystallization of BGlul1 (Chuenchor *et al.*, 2006; 2008). Small tetragonal crystals with various sizes appeared after 3-5 days under several conditions, as shown in Table 3.1 and Figure 3.5. After 1-2 months, larger crystals developed under some conditions. High quality crystals, with good size and shape, were soaked in the cryo solutions in Table 3.1, flash-frozen in liquid

nitrogen and preliminary diffraction data was collected at an in-house X-ray diffraction system facility at SLRI.

3.2.2 BGlu1 E386G with oligosaccharides

Crystallization of BGlu1 E386G with 2 mM cellotetraose and 2 mM cellopentaose was optimized from the conditions used for crystallization of BGlu1 (Chuenchor *et al.*, 2006; 2008), by hanging drop vapor diffusion with microseeding. High quality crystals were obtained from several conditions (Table 3.1 and Figure 3.5) and preliminary diffraction data were collected at SLRI.

3.2.3 BGlu1 E386G mutants with oligosaccharides

Crystallization of BGlu1 E386G/S334A, BGlu1 E386G/Y341A, BGlu1 E386G/Y341L and BGlu1 E386G/N245V with 2 mM cellotetraose and 2 mM cellopentaose was optimized from the conditions used for crystallization of BGlu1 (Chuenchor *et al.*, 2006; 2008), by hanging drop vapor diffusion with microseeding. The development of the crystals was slower than the BGlu1 E386G, resulting in smaller crystals (Table 3.1 and Figure 3.6). The crystals were assessed for X-ray diffraction at SLRI.

Table 3.1 Crystallization conditions and X-ray diffraction of protein crystals.

Crystals	Crystallization condition					Cryo solution					Resolution* (Å)
	Protein (mg/ml)	Ligand (mM)	PEG MME 5000 (%)	(NH ₄) ₂ SO ₄ (M)	MES pH 6.7 (M)	Ligand (mM)	PEG MME 5000 (%)	(NH ₄) ₂ SO ₄ (M)	MES pH 6.7 (M)	Glycerol (%)	
BGlul E386G	4	None	24	0.16	0.1	None	27.6	0.184	0.115	18	2.20
BGlul E386G with α -GlcF**	2	10	18	0.12	0.1	10	20.7	0.138	0.115	18	1.95
BGlul E386G with <i>p</i> NPC2	2	10	22	0.20	0.1	10	25.3	0.253	0.115	18	1.85
BGlul E386G with α -GlcF and <i>p</i> NPC2	3	10, 10	22	0.22	0.1	10, 10	25.3	0.253	0.115	18	1.75
BGlul E386G with cellotetraose**	3	2	22	0.22	0.1	100	25.3	0.250	0.115	18	1.60
BGlul E386G with cellopentaose**	3	2	22	0.18	0.1	25	25.3	0.207	0.115	18	1.58
BGlul E386A	3	-	22	0.14	0.1	None	25.0	0.250	0.115	18	2.10
BGlul E386A with α -GlcF**	3	10	22	0.16	0.1	10	25.0	0.250	0.115	18	2.10
BGlul E386S	6	-	24	0.20	0.1	None	28.0	0.260	0.115	18	1.80

Table 3.1 Crystallization conditions and X-ray diffraction of protein crystals (continued).

Crystals	Crystallization condition					Cryo solution					Resolution* (Å)
	Protein (mg/ml)	Ligand (mM)	PEG MME 5000 (%)	(NH ₄) ₂ SO ₄ (M)	MES pH 6.7 (M)	Ligand (mM)	PEG MME 5000 (%)	(NH ₄) ₂ SO ₄ (M)	MES pH 6.7 (M)	Glycerol (%)	
BGlu1 E386S with α -GlcF**	6	10	20	0.22	0.1	10	28	0.26	0.115	18	1.85
BGlu1 E386G/S334A with cellotetraose**	2	2	20	0.22	0.1	75	24	0.26	0.115	18	2.10
BGlu1 E386G/Y341A with cellotetraose**	3	2	16	0.18	0.1	75	24	0.26	0.115	18	1.90
BGlu1 E386G/Y341L with cellotetraose	3	2	22	0.22	0.1	75	24	0.26	0.115	18	2.60
BGlu1 E386G/N245V with cellotetraose	4	2	20	0.12	0.1	75	24	0.26	0.115	18	2.00
BGlu1 E386G/S334A with cellopentaose	2	2	16	0.18	0.1	25	24	0.26	0.115	18	1.75

Table 3.1 Crystallization conditions and X-ray diffraction of protein crystals (continued).

Crystals	Crystallization condition					Cryo solution					Resolution* (Å)
	Protein (mg/ml)	Ligand (mM)	PEG MME 5000 (%)	(NH ₄) ₂ SO ₄ (M)	MES pH 6.7 (M)	Ligand (mM)	PEG MME 5000 (%)	(NH ₄) ₂ SO ₄ (M)	MES pH 6.7 (M)	Glycerol (%)	
BGlu1 E386G/Y341A with cellopentaose	2	2	20	0.18	0.1	25	24	0.26	0.115	18	1.70
BGlu1 E386G/Y341L with cellopentaose	2	2	22	0.16	0.1	25	24	0.26	0.115	18	1.90
BGlu1 E386G/N245V with cellopentaose	3	2	22	0.14	0.1	25	24	0.26	0.115	18	2.70

*Resolution of a whole dataset collected with acceptable statistics in the outer shell.

**Ligand electron density was seen in the active site.

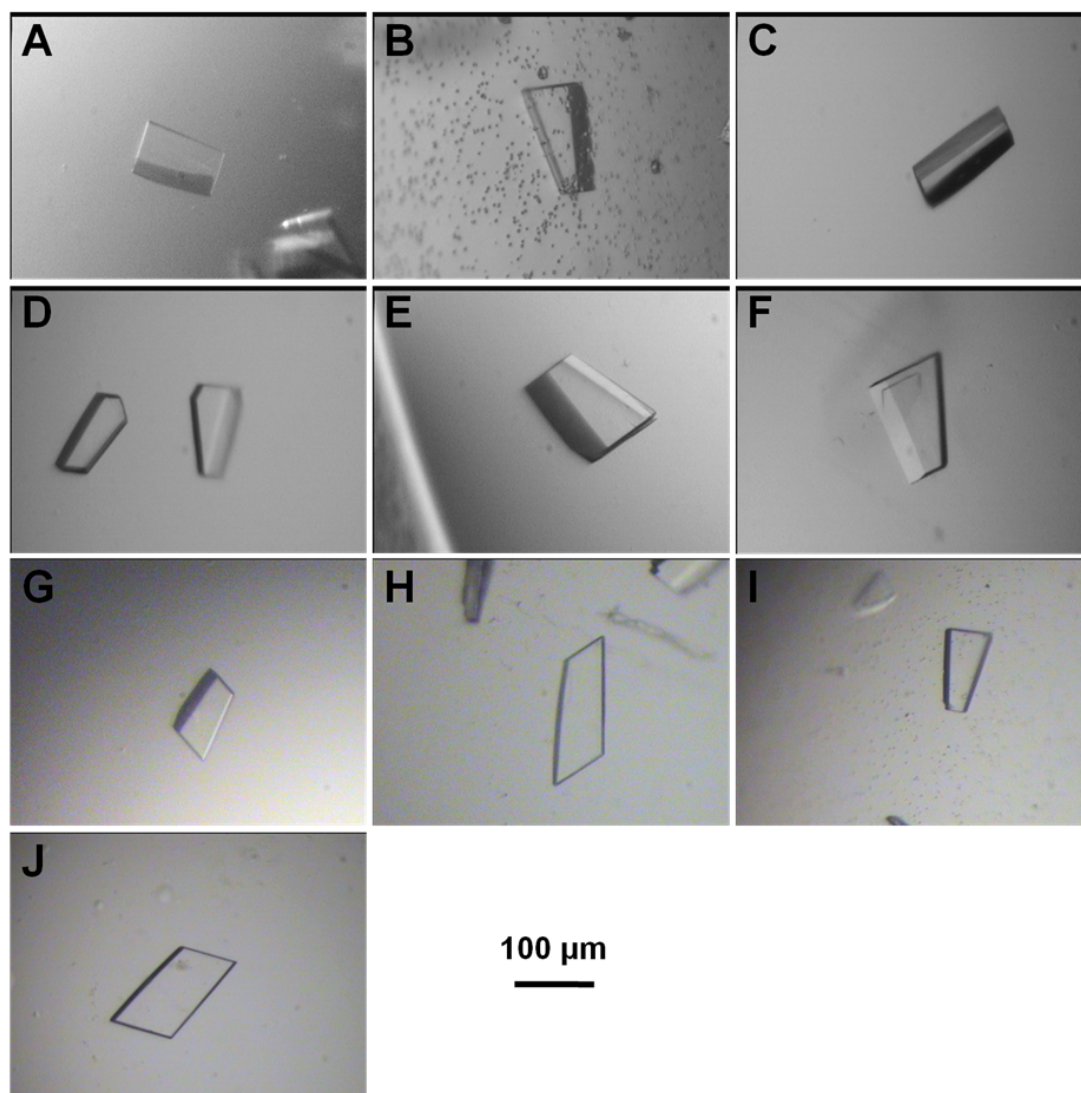


Figure 3.5 Crystals of BGlu1 glycosynthase enzymes with and without ligands. A, crystals of free BGlu1 E386G; B, crystal of BGlu1 E386G with 10 mM α -GlcF; C, crystal of BGlu1 E386G with 10 mM *p*NPC2; D, crystals of BGlu1 E386G with 10 mM α -GlcF and 10 mM *p*NPC2; E, crystals of BGlu1 E386G with 2 mM cellotetraose; F, crystal of BGlu1 E386G with 2 mM cellopentaose; G, crystal of free BGlu1 E386A; H, crystals of BGlu1 E386A with 10 mM α -GlcF; I, crystals of free BGlu1 E386S and J, crystal of BGlu1 E386S with 10 mM α -GlcF. The maximum size crystals had the approximate dimensions of up to 150 x 70 x 20 μ m.

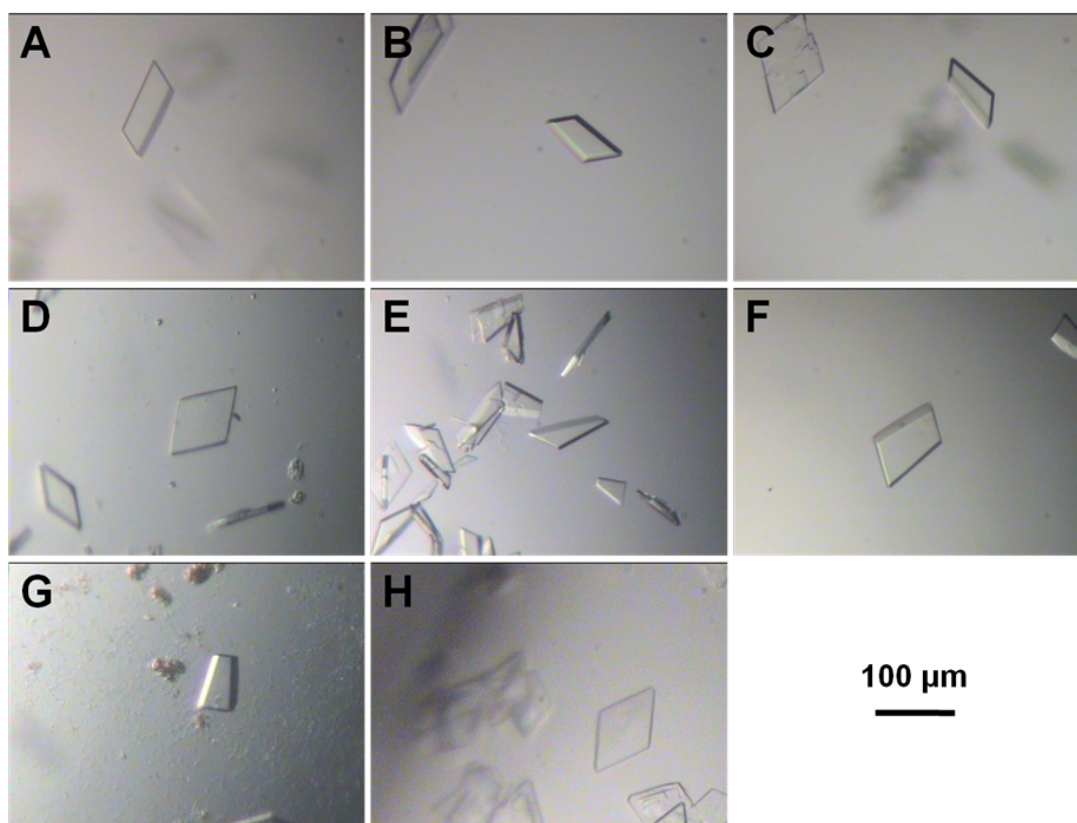


Figure 3.6 Crystals of BGlu1 glycosynthase mutants with cellooligosaccharides. A, crystals of BGlu1 E386G/S334A with 2 mM cellotetraose; B, crystals of BGlu1 E386G/Y341A with 2 mM cellotetraose; C, crystals of BGlu1 E386G/Y341L with 2 mM cellotetraose; D, crystals of BGlu1 E386G/N245V with 2 mM cellotetraose; E, crystals of BGlu1 E386G/S334A with 2 mM cellopentaose; F, crystals of BGlu1 E386G/Y341A with 2 mM cellopentaose; G, crystals of BGlu1 E386G/Y341L with 2 mM cellopentaose and H, crystals of BGlu1 E386G/N245V with 2 mM cellopentaose. The maximum size crystals had approximate dimensions of up to 110 x 70 x 10 μm.

3.3 3D structures of three glycosynthases in complexes with substrates

To assess the structural basis for the differing glycosynthase efficiencies of BGlu1 E386G, E386S and E386A, the structures of these glycosynthases and those of their complexes with α -GlcF were determined by X-ray crystallography (see Tables 3.2 and 3.3 for diffraction and structure statistics). Structures of the E386G glycosynthase, both co-crystallized and soaked with 10 mM *p*NPC2, as well as with both 10 mM α -GlcF and 10 mM *p*NPC2, were determined, but *p*NPC2 was not observed in the active site. Nonetheless, α -GlcF was observed in the active site of the ternary complex crystals, and if the crystals were soaked for longer periods (30 min, 1 hr and 3 hr), the crystal mosaicities generally increased and the crystals broke down after soaking for approx. 3 hr, suggesting that they may have produced long oligosaccharides that pushed the crystal matrix apart.

The structures of BGlu1 E386A and BGlu1 E386S apo enzymes and their complexes with α -GlcF were compared with those of BGlu1 E386G. Crystals of the apo glycosynthase enzymes and of their complexes were found to belong to space group $P2_12_12_1$ and were isomorphous with wild type BGlu1 crystals (Chuenchor *et al.*, 2006; 2008). Diffraction data and model parameters for the structures of the glycosynthases are summarized in Tables 3.2 and 3.3. The α -GlcF binds to the glycosynthases in a relaxed 4C_1 chair conformation stacked onto the indole ring of W433 at the -1 subsite, in the same position as the 2-deoxy-2-fluoro- α -D-glucosyl moiety (G2F) in its covalent complex with BGlu1 (PDB: 2RGM, Chuenchor *et al.*, 2008), and makes all the hydrogen bonds previously observed for that complex. In all

three mutants (Figures 3.7, 3.8 and 3.9), the active site residues R86, N175 and N313, as well as the fluorine and O2 of α -GlcF, interact with a single ordered water molecule that is also found in the structure of the covalent intermediate of BGlu1 with G2F, at the same position as the nucleophile carbonyl oxygen of apo wild type BGlu1 (PDB: 2RGL, Chuenchor *et al.*, 2008). As seen in Figure 3.8, the water is closer to the fluorine in the E386S structure, while it is generally closer to the hydrogen-bonding side chains in the BGlu1 E386G structure and is in an intermediate position in the BGlu1 E386A structure.

Since no density for *p*NPC2 could be seen in the active site, the longer acceptors cellotetraose and cellopentaose were soaked into the BGlu1 E386G crystals and the structures determined, with the statistics shown in Tables 3.2 and 3.3. However, the observed electron densities shown in Figures 3.10 and 3.11 indicated that these oligosaccharides bound in the -1 subsite as glycosynthase products or hydrolase substrates, as previously seen for the BGlu1 E176Q acid/base mutant, rather than in the positions of acceptor substrates. In order to obtain sufficient ligand occupancies in the active site, the crystals were soaked in cryoprotectant saturated with the cellotetraose or cellopentaose, rather than the 2 mM cellotetraose and 1 mM cellopentaose used for the BGlu1 E176Q mutant. This resulted in the binding of an extra cellotetraose on the surface of the protein between molecule A of one asymmetric unit and molecule B of another asymmetric unit. This had little effect on the crystal packing and is not likely of any biological significance.

The comparison of the structures of BGlu1 E386G in complex with cellotetraose and cellopentaose with those of the BGlu1 E176Q mutant in complex with cellotetraose and cellopentaose (PDB: 3F5J and 3F5K, Chuenchor *et al.*, 2011)

in Figure 3.12 reveals very similar positions of the active site amino acid residues, except the E176 (the acid/base, which is mutated to glutamine in the previous complex structures) and N245 sidechain positions were shifted slightly. Likewise the Glc1, Glc2, Glc3 and Glc4 glucosyl residues from the nonreducing ends of cellotetraose and cellopentaose at subsites -1, +1, +2 and +3 in the active site of BGlul E386G adopt very similar positions in the two complexes, although they were shifted slightly, and Glc5 in the active site of BGlul E386G at subsite +4 had lower electron density than that in the cellopentaose complex with BGlul E176Q and a slightly different position (Figure 3.12).

Hydrogen bonding interactions between the glucosyl residues of cellotetraose or cellopentaose, ordered water molecules and amino acid residues in the active site of BGlul E386G are shown in Figure 3.13. The hydrogen bonds and aromatic-sugar stacking interactions of the Glc3, Glc4 and Glc5 residues at subsites +2, +3 and +4 are similar to those in the BGlul E176Q complex with cellopentaose. The slight shifts in oligosaccharide sugar moiety positions and the position of the N245 sidechain allowed the N245 δ N to form hydrogen bonds with Glc2 O6 and Glc3 O2, rather than the bonds to Glc3 O2 and O3 observed in the E176Q complexes (Chuenchor *et al.*, 2011). Other residues that make obvious interactions with the oligosaccharides include Y341, which interacts via water-mediated hydrogen bonds and stacking interactions at subsites +2 to +4, and S334, which forms water-mediated hydrogen bonds at subsite +3.

Table 3.2a Data collection statistics.

	E386G	E386G α-GlcF	E386A	E386A α-GlcF	E386S	E386S α-GlcF
PDB code	3SCN	3SCO	3SCP	3SCQ	3SCR	3SCS
Space group	$P2_12_12_1$	$P2_12_12_1$	$P2_12_12_1$	$P2_12_12_1$	$P2_12_12_1$	$P2_12_12_1$
Unit cell parameters (Å, °)	a = 79.4 b = 100.8 c = 127.4 $\alpha = \beta = \gamma = 90^\circ$	a = 79.9 b = 100.8 c = 127.1 $\alpha = \beta = \gamma = 90^\circ$	a = 79.6 b = 100.9 c = 127.6 $\alpha = \beta = \gamma = 90^\circ$	a = 80.1 b = 100.9 c = 126.8 $\alpha = \beta = \gamma = 90^\circ$	a = 79.7 b = 101.0 c = 127.5 $\alpha = \beta = \gamma = 90^\circ$	a = 80.1 b = 100.7 c = 127.0 $\alpha = \beta = \gamma = 90^\circ$
No. of molecules per ASU	2	2	2	2	2	2
Resolution range (Å)	30-2.20 (2.28-2.20)	30-1.95 (2.02-1.95)	30-2.10 (2.18-2.10)	30-2.10 (2.18-2.10)	30-1.80 (1.86-1.80)	30-1.85 (1.92-1.85)
No. of unique observations	51498	73721	60736	60561	95127	87779
Redundancy	5.6 (5.4)	6.8 (4.8)	5.4 (5.4)	6.0 (5.8)	7.2 (7.2)	7.2 (7.2)
Completeness (%)	97.5 (92.6)	97.8 (92.9)	99.9 (100)	99.5 (97.8)	99.9 (99.9)	99.9 (99.9)
$I/\sigma(I)$	13.9 (4.4)	21.4 (3.9)	11.7 (3.6)	16.0 (4.9)	15.7 (3.8)	16.2 (4.6)
R_{sym} (%) ^a	11.4 (46.3)	7.9 (39.5)	13.8 (45.4)	12.3 (43.9)	11.2 (46.2)	12.2 (43.7)

Numbers in parentheses are outer shell parameters.

$$^a R_{\text{sym}} = \frac{\sum_{\text{hkl}} \sum_i |I_i(\text{hkl}) - \langle I(\text{hkl}) \rangle|}{\sum_{\text{hkl}} \sum_i I(\text{hkl})}$$

Table 3.2b Data collection statistics.

	E386G_C4	E386G_C5	S334A_C4	Y341A_C4
PDB code	3SCT	3SCU	3SCV	3SCW
Space group	<i>P</i> 2 ₁ 2 ₁ 2 ₁	<i>P</i> 2 ₁ 2 ₁ 2 ₁	<i>P</i> 2 ₁ 2 ₁ 2 ₁	<i>P</i> 2 ₁ 2 ₁ 2 ₁
Unit cell parameters (Å, °)	a = 79.3 b = 101.0 c = 127.2 α = β = γ = 90°	a = 79.5 b = 100.8 c = 127.2 α = β = γ = 90°	a = 79.4 b = 101.5 c = 127.3 α = β = γ = 90°	a = 79.3 b = 101.3 c = 127.4 α = β = γ = 90°
No. of molecules per ASU	2	2	2	2
Resolution range (Å)	30-1.60 (1.66-1.60)	30-1.58 (1.64-1.58)	30-2.10 (2.18-2.10)	30-1.90 (1.97-1.90)
No. of unique observations	134069	139830	60078	80727
Redundancy	4.7 (4.6)	6.0 (6.0)	7.3 (7.2)	7.3 (7.3)
Completeness (%)	99.1 (97.3)	100 (100)	99.9 (100)	99.3 (98.9)
<i>I</i> /σ(<i>I</i>)	19.0 (3.5)	23.7 (3.9)	13.0 (4.3)	16.7 (4.6)
<i>R</i> _{sym} (%) ^a	6.8 (45.8)	7.1 (45.5)	15.0 (46.9)	10.8 (44.3)

Numbers in parentheses are outer shell parameters.

$$^a R_{\text{sym}} = \frac{\sum_{\text{hkl}} \sum_i |I_i(\text{hkl}) - \langle I(\text{hkl}) \rangle|}{\sum_{\text{hkl}} \sum_i I(\text{hkl})}$$

Table 3.3a Refinement statistics.

	E386G	E386G α-GlcF	E386A	E386A α-GlcF	E386S	E386S α-GlcF
PDB code	3SCN	3SCO	3SCP	3SCQ	3SCR	3SCS
Resolution range (Å)	25-2.20	26-1.95	30-2.10	25-2.10	23-1.80	25.1.85
No. of amino-acid residues	944	944	944	944	944	944
No. of protein atoms	7608	7608	7610	7610	7612	7612
No. of water molecules	651	833	760	782	865	870
Refined carbohydrate	None	α -GlcF	None	α -GlcF	None	α -GlcF
No. of carbohydrate atoms	None	24 ^f	None	24 ^f	None	24 ^f
No. of other hetero atoms	35	47	47	35	47	47
R_{factor} (%) ^b	19.8	17.2	17.8	17.7	17.8	17.5
R_{free} (%) ^c	24.0	20.7	20.8	20.6	20.8	20.5
Ramachandran statistics ^d						
Most favored regions (%)	88.7	89.8	89.2	89.9	89.2	90.0
Additionally allowed regions (%)	11.3	10.2	10.8	9.9	10.8	9.9
Outlier regions (%)	0.0	0.0	0.0	0.2	0.0	0.1
R.m.s.d. from ideality						
Bond distances (Å)	0.011	0.013	0.013	0.010	0.013	0.013
Bond angle (°)	1.35	1.39	1.40	1.30	1.40	1.38
Estimated coordinate error (Å) ^e	0.22	0.14	0.17	0.17	0.12	0.12
Mean B factors (Å ²)						
All protein atoms	16.0	16.6	12.6	10.8	11.5	9.5
Waters	25.1	28.5	24.7	20.9	24.5	20.6
Hetero atoms	35.5	33.0	33.9	24.9	24.6	21.8
Carbohydrate atoms	None	14.0	None	8.2	None	5.7
Subsite -1 (A/B)	None	14.0/13.9	None	7.3/9.1	None	5.8/5.6
Subsite +1 (A/B)	None	None	None	None	None	None
Subsite +2 (A/B)	None	None	None	None	None	None
Subsite +3 (A/B)	None	None	None	None	None	None
Subsite +4 (A/B)	None	None	None	None	None	None

$$^b R_{\text{factor}} = (\sum |F_o| - |F_c|) / \sum |F_o|$$

^cBased on 5% of the unique observations not included in the refinement.

^dRamachandran values were determined from PROCHECK (Laskowski *et al.*, 1993).

^eBased on R_{free} values, as calculated by Refmac 5.5.0110.

^fTwelve per protein molecule in the asymmetric unit.

Table 3.3b Refinement statistics.

	E386G_C4	E386G_C5	E386G/S334A_C4	E386G/Y341A_C4
PDB code	3SCT	3SCU	3SCV	3SCW
Resolution range (Å)	26-1.60	28-1.58	23-2.10	24-1.90
No. of amino-acid residues	944	944	944	944
No. of protein atoms	7608	7608	7606	7594
No. of water molecules	912	922	781	902
Refined carbohydrate	Cellotetraose	Cellopentaose	Cellotetraose	Cellotetraose
No. of carbohydrate atoms	135	112	135	135
No. of other hetero atoms	35	35	35	35
R_{factor} (%) ^b	19.1	17.4	17.4	17.0
R_{free} (%) ^c	20.8	19.2	20.6	19.8
Ramachandran statistics ^d				
Most favored regions (%)	89.1	89.4	90.0	89.3
Additionally allowed regions (%)	10.9	10.6	10.0	10.7
Outlier regions (%)	0.0	0.0	0.0	0.0
R.m.s.d. from ideality				
Bond distances (Å)	0.008	0.010	0.010	0.010
Bond angle (°)	1.36	1.38	1.33	1.32
Estimated coordinate error (Å) ^e	0.089	0.079	0.17	0.13
Mean B factors (Å ²)				
All protein atoms	13.5	11.3	10.6	11.1
Waters	27.6	24.9	21.3	25.5
Hetero atoms	24.3	19.9	27.5	26.1
Carbohydrate atoms	42.9	37.6	36.1	30.3
Subsite -1 (A/B)	30.5/31.2	21.8/21.9	28.5/33.0	18.6/19.5
Subsite +1 (A/B)	39.9/39.6	33.0/34.8	35.4/37.6	21.8/23.9
Subsite +2 (A/B)	42.5/42.1	38.8/41.1	40.1/40.7	27.0/27.4
Subsite +3 (A/B)	45.7/46.1	42.5/44.0	43.5/44.3	40.3/40.9
Subsite +4 (A/B)	None	46.9/48.2	None	None

See footnotes from Table 3.3a.

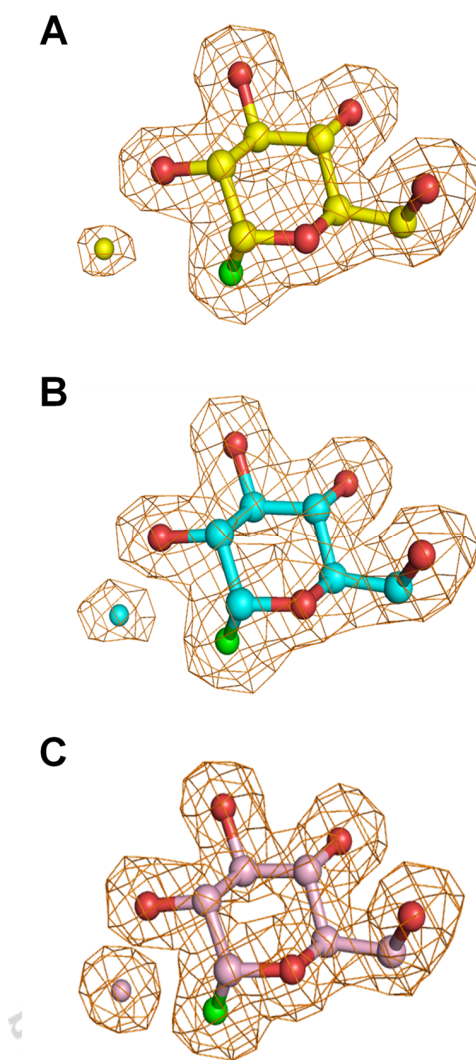


Figure 3.7 The electron densities of α -GlcF and water in the -1 subsite of BGlu1 E386G (yellow carbons, A), BGlu1 E386A (cyan carbons, B) and BGlu1 E386S (pink carbons, C). The electron density (F_o-F_c) maps were calculated for each structure with all heteroatoms omitted from the active site, and are shown in brown mesh at an electron density equivalent to $+3\sigma$. The α -GlcF is shown in ball and stick representation, while the water is shown as an isolated sphere. Oxygen is shown in red and fluorine in green.

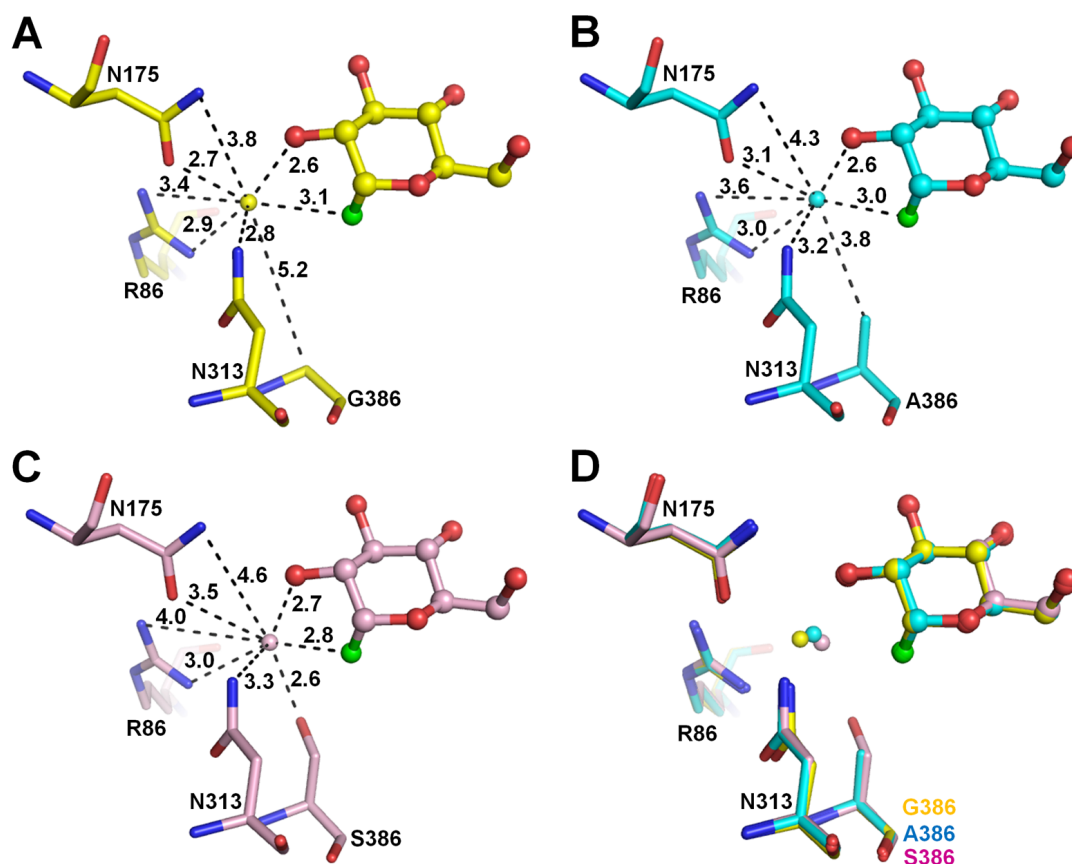


Figure 3.8 Comparison of the active sites of rice BGlucanase E386G, E386A and E386S glycosynthases. An active site water molecule is seen in the wild type covalent intermediate as well as in all three glycosynthase mutant complexes with α -GlcF. This water occupies a very similar position in BGlucanase E386G (A), BGlucanase E386A (B) and BGlucanase E386S (C), with the superimposition of all three of these rice BGlucanase glycosynthases being shown in (D). The α -GlcF is represented as balls and sticks, the surrounding amino acid residues are shown as sticks, and the water molecule is represented as a ball. Oxygen is shown in red, nitrogen in blue, and fluorine in green. Distances (in Ångstroms) are shown from the one water molecule to the surrounding polar groups and the mutated sidechains. No other water molecules were observed in this part of the active site in any of the structures.

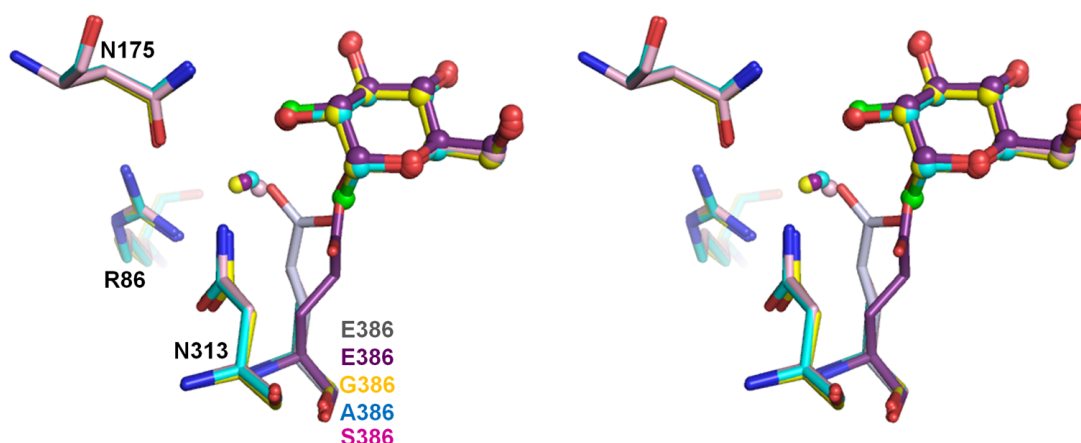


Figure 3.9 Comparison of active sites of rice BGlu1 E386G, E386A and E386S glycosynthases and free BGlu1 and its 2-fluoroglucosyl enzyme intermediate. An active site water molecule is seen in the wild type covalent intermediate as well as in all three glycosynthase mutant complexes with α -GlcF. This water is bound at the same location as the catalytic nucleophile in the free wild type enzyme. The superimposition of these rice BGlu1 glycosynthases, BGlu1 E386G (yellow carbons), BGlu1 E386A (cyan carbons) and BGlu1 E386S (magenta carbons), and apo BGlu1 (gray carbons) with the structure of the 2-fluoroglucosyl enzyme intermediate (purple carbons) is shown in wall-eyed stereo. The α -GlcF is represented as balls and sticks and the water molecule is represented as a ball. Oxygen is shown in red, nitrogen in blue, and fluorine in green.

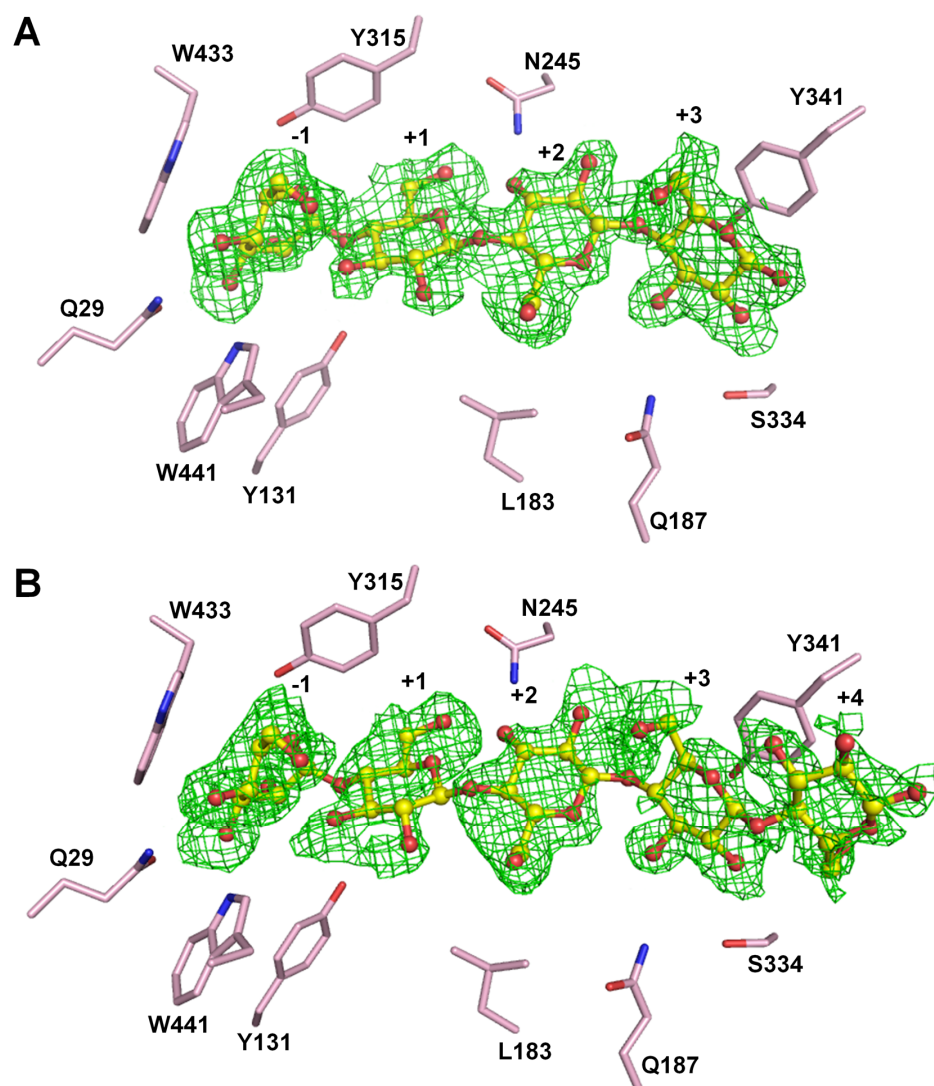


Figure 3.10 The Fo-Fc electron density maps of oligosaccharides in the active sites of BGlu1 E386G. The Fo-Fc maps were calculated for each structure with all heteroatoms omitted from the active site, and are shown in green mesh at an electron density equivalent to $+1\sigma$. The ligands from the final structures are shown in ball and stick representation. The carbons are colored in yellow and oxygen is shown in red. (A) BGlu1 E386G complexed with cellotetraose and (B) BGlu1 E386G complexed with cellopentaose. The sidechains of amino acid residues in the active site are shown in stick representation with pink carbons, red oxygens and blue nitrogens.

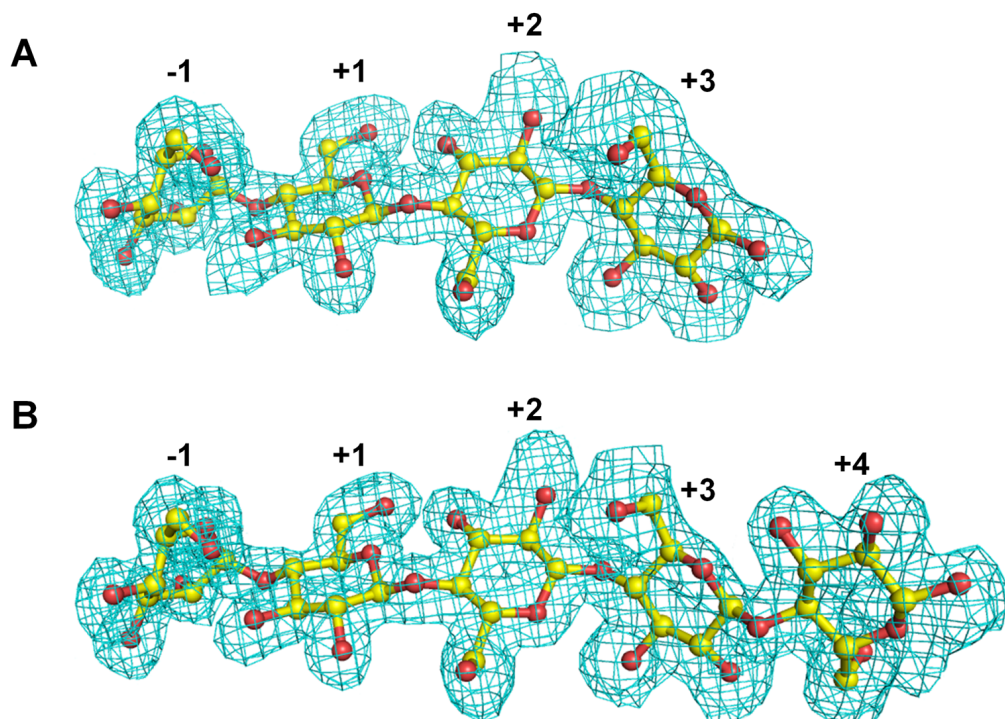


Figure 3.11 The 2Fo-Fc electron densities of oligosaccharides in the active site of the BGlucanase 1 E386G. The 2Fo-Fc maps were calculated for each structure with all heteroatoms in the active site, and are shown in blue mesh at $+1\sigma$. The ligands from the final structures are shown in ball and stick representation. The carbons are colored in yellow and oxygens in red. (A) The BGlucanase 1 E386G complex with cellotetraose and (B) the BGlucanase 1 E386G complex with cellopentaose.

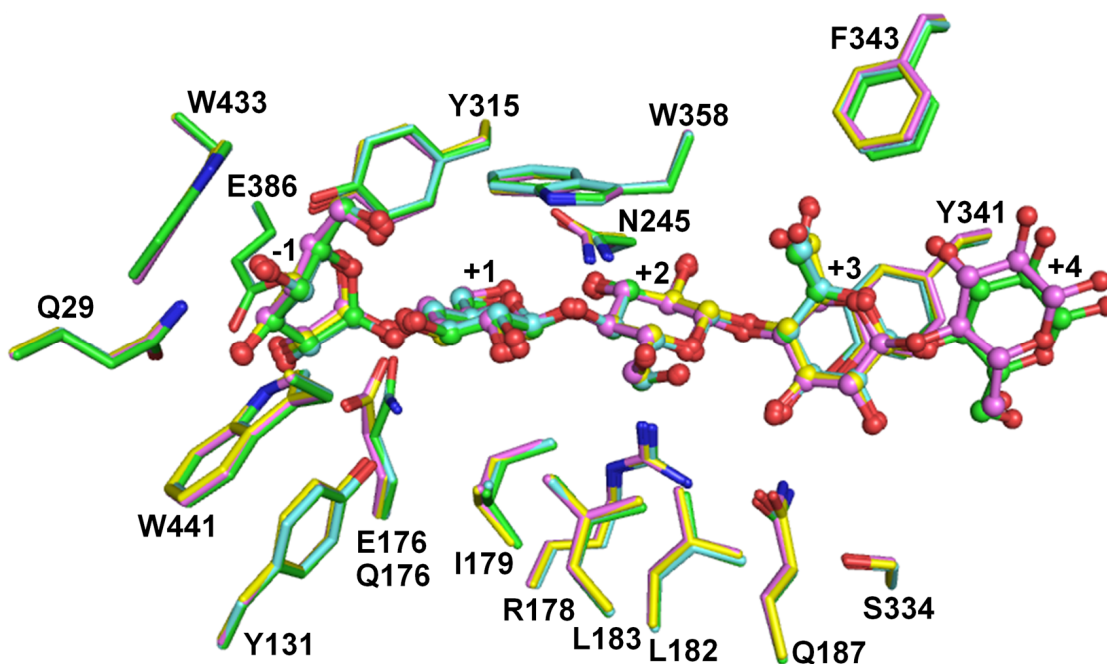


Figure 3.12 Comparison of cellotetraose and cellopentaose binding in the active site of BGLu1 E386G and BGLu1 E176Q. Superimposition of BGLu1 E386G glycosynthase in complexes with cellotetraose (yellow carbons) and cellopentaose (pink carbons) with the structures of the BGLu1 E176Q acid/base mutant complexes with cellotetraose (cyan carbons) and cellopentaose (green carbons). The ligands are shown in ball and stick representation. Nitrogens are shown in blue and oxygens in red.

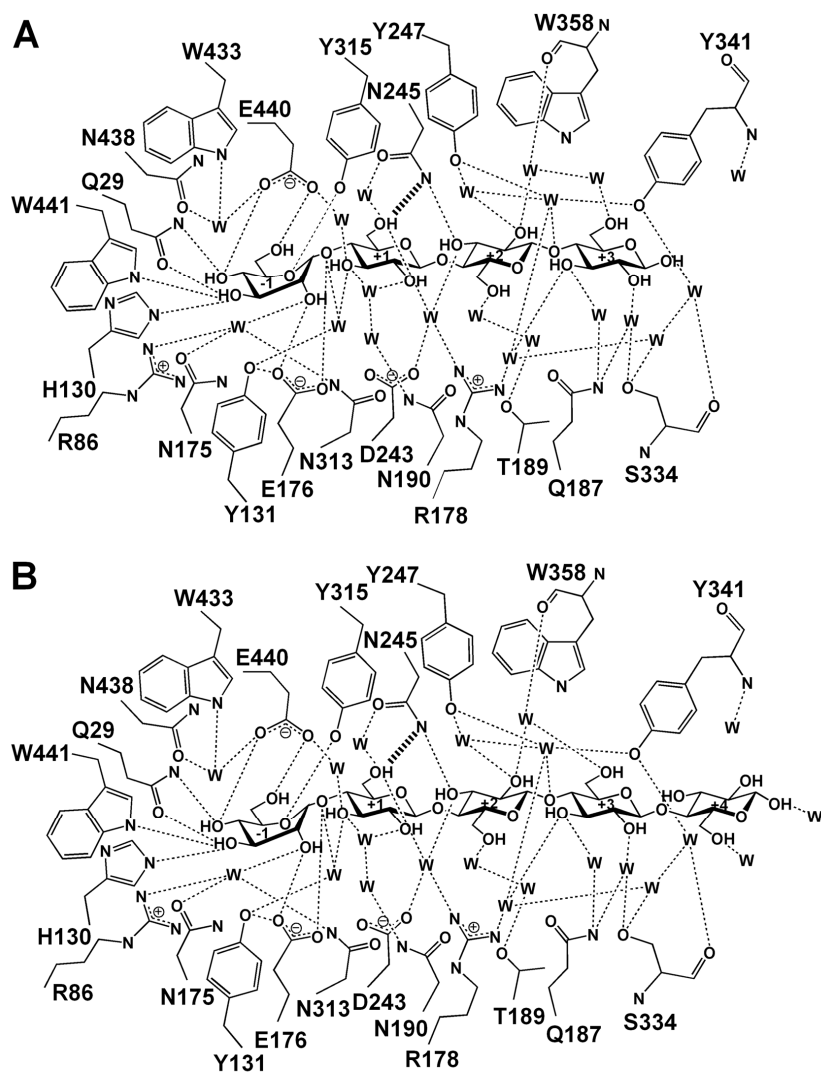


Figure 3.13 Diagrams of the strong hydrogen bonds between oligosaccharides, surrounding amino acid residues and the network of water molecules in the active site of BGLu1 E386G. Hydrogen bonds with measured distances of 3.2 Å or less are shown as dashed lines to indicate the hydrophilic interactions. (A) Active site of BGLu386G complexed with cellotetraose. (B) Active site of BGLu386G complexed with cellopentaose. The direct hydrogen bond between N245 and Glc2, which is not seen in the complexes of cellotetraose and cellopentaose with BGLu1 E176Q, is shown as a darker dashed line. Water molecules are represented as W.

3.4 Oligosaccharide-binding residue mutants

We hypothesized that mutation of residues that interact with cellooligosaccharides might yield weaker binding variants, and that the corresponding glycosynthases might produce shorter oligosaccharides (i.e. they would be less efficient at synthesizing long oligosaccharides). Based on the observed interactions between S334 and Y341 and the cellooligosaccharides, the BGlu1 mutants S334A, Y341A and Y341L were generated. The affinity of the BGlu1 N245V mutant, which was previously shown to have higher K_m values for *p*NPGlc, cellobiose and cellotriose than does BGlu1 wild type (Chuenchor *et al.*, 2008), was also investigated with longer oligosaccharides. Only slightly higher values of K_m and slightly lower catalytic efficiency values (k_{cat}/K_m) for cellotriose, cellotetraose and cellopentaose were seen for the BGlu1 S334A, Y341A, and Y341L mutants compared to wild type BGlu1 (Table 3.4). The BGlu1 N245V mutant had a 10-fold lower k_{cat}/K_m value than wild type for cellotriose, but only 3-fold lower for cellotetraose and cellopentaose. Kinetic subsite analysis by the method of Hiromi *et al.* (1973) (with the assumption of an intrinsic k_{cat}) verified that the BGlu1 S334A, Y341A and Y341L mutations had little effect on the apparent affinity at the +3 and +4 subsites. Even the very low efficiency of the BGlu1 N245V mutant hydrolysis of cellotriose appeared to be compensated by binding subsequent glucosyl residues in cellotetraose and cellopentaose, giving the mutant a high apparent subsite +3 affinity.

Table 3.4 Kinetic parameters of BGlu1 wild type and mutants for hydrolysis of celotriose, cellotetraose and cellopentaose.

Substrate	Kinetic parameters	BGlu1	S334A	Y341A	Y341L	N245V
Celotriose	K_m (mM)	0.50±0.05	0.62±0.05	0.97±0.07	0.97±0.05	11.2±0.8
	k_{cat} (s ⁻¹)	15.6±0.6	20.3±0.7	26.5±0.7	23.3±0.5	36.1±0.9
	k_{cat}/K_m (M ⁻¹ s ⁻¹)	31,000	33,000	27,000	24,000	3,230
Cellotetraose	K_m (mM)	0.37±0.04	0.52±0.04	0.70±0.05	0.54±0.03	5.3±0.2
	k_{cat} (s ⁻¹)	23.7±1.1	29.1±1.2	35.5±1.0	26.5±0.4	103.5±1.6
	k_{cat}/K_m (M ⁻¹ s ⁻¹)	64,000	56,000	58,000	49,000	20,000
	Subsite affinity (subsite +3, kJ mol ⁻¹)	1.8	1.4	1.6	1.8	4.5
Cellopentaose	K_m (mM)	0.28±0.02	0.36±0.03	0.44±0.02	0.36±0.02	3.83±0.18
	k_{cat} (s ⁻¹)	27.5±1.2	31.8±1.5	32.3±0.6	25.6±0.4	139±3
	k_{cat}/K_m (M ⁻¹ s ⁻¹)	98,000	88,000	73,000	71,000	36,300
	Subsite affinity (subsite +4, kJ mol ⁻¹)	1.1	1.1	0.93	0.93	1.6

Subsite affinities were calculated by the method of Hiromi *et al.*, 1973:

$-\Delta G = RT \ln[(k_{cat}/K_m)_n / (k_{cat}/K_m)_{n-1}]$ as a means of estimating the effect of each successive sugar residue.

3.5 Transglycosylation

To compare transglycosylation activities, the BGlu1 E386G enzyme and the four BGlu1 E386G glycosynthase mutants, S334A, Y341A, Y341L and N245V, were incubated with α -GlcF donor and *p*NPC2 acceptor at molar ratios of 1:2, 1:1, 2:1 or 5:1. The reactions at 1:2, 1:1, 2:1 and 5:1 ratios resulted in clear product solutions for Y341A, Y341L and N245V, but the reaction of 2:1 donor:acceptor with BGlu1 E386G and 5:1 donor to acceptor with BGlu1 E386G and BGlu1 E386G/S334A resulted in precipitated products (Figure 3.14), which were previously shown to comprise cellooligosaccharides of up to 11 glucosyl residues for the BGlu1 E386G glycosynthase (Hommalai *et al.*, 2007). The soluble products were monitored by TLC (Figure 3.15) and HPLC (Figure 3.16) and quantified by HPLC (Table 3.5). The E386G/S334A mutant has similar glycosynthase activity to BGlu1 E386G and synthesized soluble *p*NP-oligosaccharide products with lengths up to *p*NP- β -cellonanaoside (*p*NPC9), as judged by LC-MS analysis (Figure 3.16). In TLC, the longer products appeared as a dark spot at the origin. The E386G/N245V mutant synthesizes small but significant amounts of *p*NP- β -cellopentaoside (*p*NPC5) for all reactions and longer *p*NP-cellooligosaccharides for the reaction at the 5:1 donor:acceptor ratio. However, the E386G/Y341A and Y341L mutants synthesized only very small amounts of longer products (*p*NPC5), unless the donor to acceptor ratio was increased to 5:1. The hydrolysis product, glucose, was also more evident in these mutants.

When the soluble products of the reactions at the 1:1 donor to acceptor substrate ratio were analyzed by HPLC, the longest products detected were degree of polymerization (DP) 9 (*p*NPC9) for the BGlu1 E386G glycosynthase and its S334A

mutant, DP 7 for the BGlu1 E386G/N245V mutant and DP 6 for the BGlu1 E386G/Y341A and BGlu1 E386G/Y341L mutants (Figure 3.16 and Table 3.5). Although the BGlu1 E386G glycosynthase and its mutants gave similar relative amounts of *p*NP- β -cellotrioside (*p*NPC3) products, the E386G/Y441A mutant gave half the amount of *p*NP- β -cellotetraoside (*p*NPC4) products, and 1/13 the relative amount of *p*NPC5, and 1/90 the amount of *p*NP- β -cellohexaoside (*p*NPC6), while the Y441L and N245V mutants showed similar, but less extreme, drops in relative amounts of products with DP increasing from 3 to 6 compared to their parent glycosynthase.



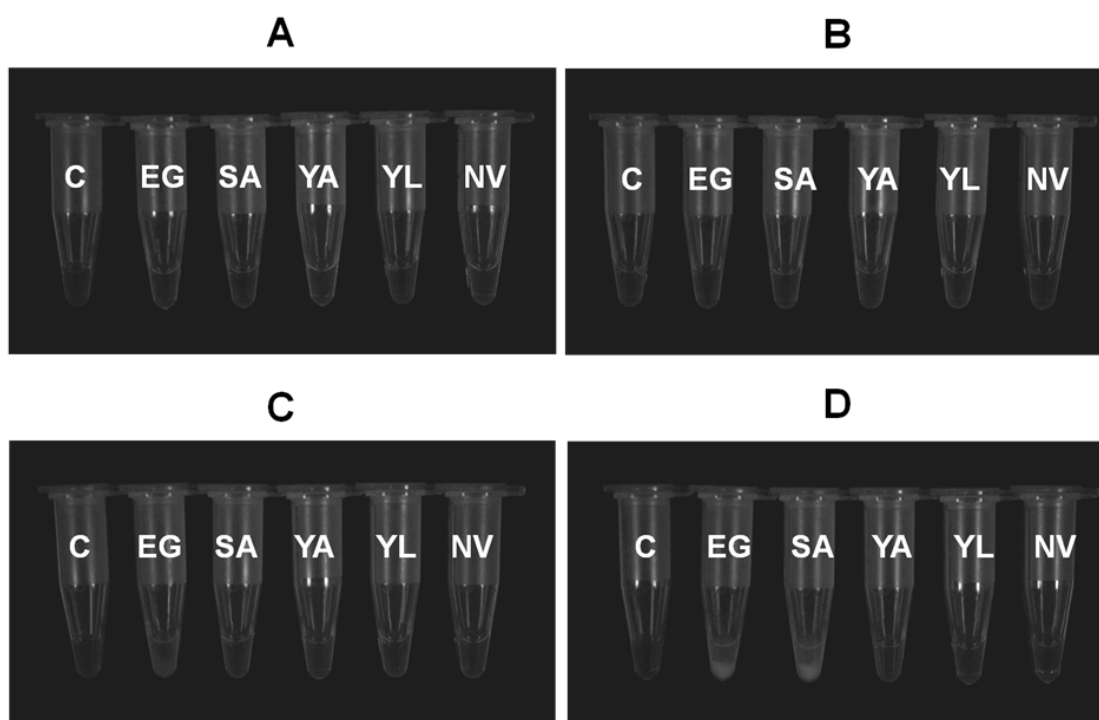


Figure 3.14 Transglucosylation reactions between α -GlcF donor and *pNPC2* acceptor at various molar ratios. The reactions between α -GlcF donor and *pNPC2* acceptor at ratios of 1:2 (A), 1:1 (B), 2:1 (C) and 5:1 (D) were incubated with BGlu1 E386G and BGlu1 E386G mutants in NH_4HCO_3 (pH 7.0) at 30°C for 16 hr. Tube C, control reaction without enzyme; tube EG, BGlu1 E386G; tube SA, BGlu1 E386G/S334A; tube YA, BGlu1 E386G/Y341A; tube YL, BGlu1 E386G/Y341L and tube NV, BGlu1 E386G/N245V. Precipitated products were only seen in the EG tubes at 2:1 and 5:1 donor to acceptor ratios and SA tube at 5:1.

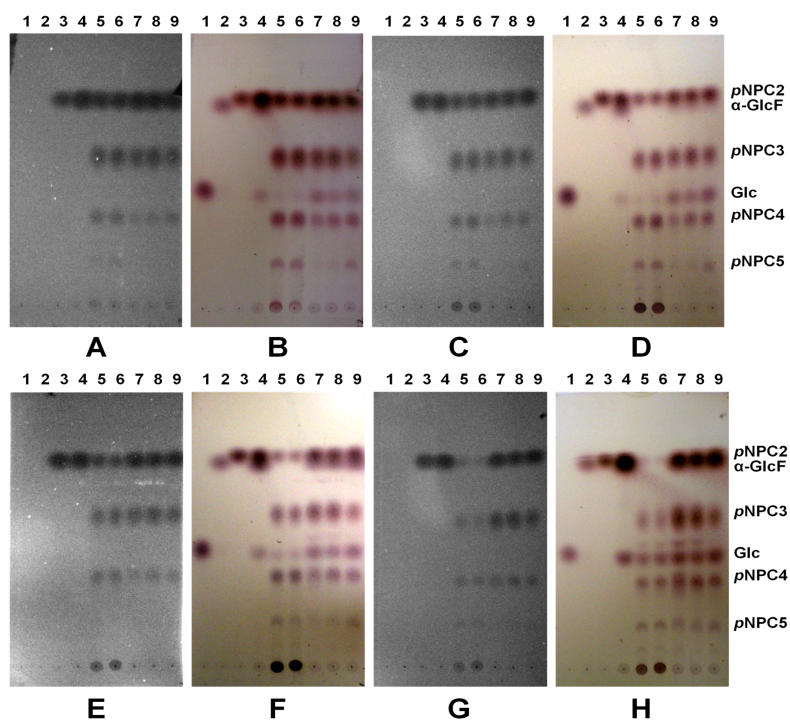


Figure 3.15 TLC detection of products of transglucosylation reactions between α -GlcF donor and *pNPC2* acceptor at various molar ratios. The reactions between α -GlcF donor and *pNPC2* acceptor at ratios of 1:2 (A and B), 1:1 (C and D), 2:1 (E and F) and 5:1 (G and H) were incubated with BGlu1 E386G and BGlu1 E386G mutants in NH_4HCO_3 (pH 7.0) at 30°C for 16 hr. The soluble products were separated by silica TLC, using EtOAc-MeOH-water (7:2.5:1, v/v/v) as a developing solvent and detected under UV light (A, C, E and G) or by exposure to 10% sulfuric acid in ethanol followed by charring to detect carbohydrates (B, D, F and H). Lane 1, glucose; Lane 2, α -GlcF; Lane 3, *pNPC2*; Lanes 4-9, reactions without enzyme (4); with BGlu1 E386G (5); with BGlu1 E386G/S334A (6); with BGlu1 E386G/Y341A (7); with BGlu1 E386G/Y341L (8) and with BGlu1 E386G/N245V (9). Based on the LC-MS analysis (Figure 3.16 and Table 3.5) and Hommalai *et al.*, 2007, the products were identified as *pNPC3*, *pNPC4*, *pNPC5* and longer *pNP*-cellooligosaccharides.

Table 3.5 Glycosynthase reaction products of BGlu1 E386G glycosynthase and its mutants with equal amounts of α -glucosyl fluoride donor and *p*NPC2 acceptor.

Glycosynthase	Percent of <i>p</i> NP-glucoside product (%yield) ^a								
	DP 1	DP 2	DP 3	DP 4	DP 5	DP 6	DP 7	DP 8	DP 9
E386G	0.22±0.01	51.0±0.1	25.6±0.01	13.1±0.02	6.7±0.03	2.7±0.008	0.57±0.009	0.06±0.004	0.008±0.0002
E386G/S334A	0.16±0.01	48.7±0.1	27.6±0.07	14.5±0.05	6.5±0.03	2.1±0.003	0.39±0.014	0.03±0.003	0.004±0.0001
E386G/Y341A	0.63±0.03	68.5±0.1	24.6±0.06	5.7±0.1	0.50±0.02	0.03±0.002	0.00	0.00	0.00
E386G/Y341L	0.15±0.01	60.1±0.04	30.1±0.02	8.7±0.01	0.86±0.01	0.07±0.002	0.00	0.00	0.00
E386G/N245V	0.28±0.02	66.4±0.1	22.8±0.05	8.2±0.05	2.1±0.03	0.30±0.013	0.02±0.002	0.00	0.00

^aPreparative reactions in 150 mM NH₄HCO₃ buffer, pH 7.0, 30°C, at a 1:1 molar ratio of α -GlcF donor: *p*NPC2 acceptor (10 mM each), and 40 μ M enzyme concentration. The relative percents are in terms of peak area per total 300 nm absorbance in *p*NP-glycoside products and substrate peaks separated by HPLC on a ZORBAX carbohydrate column. The molecular mass [Mass + ³⁵Cl]⁻ of each eluted compound was confirmed by mass spectrometry: *p*NPGlc (336 *m/z*), *p*NPC2 (498 *m/z*), *p*NPC3 (660 *m/z*), *p*NPC4 (822 *m/z*), *p*NPC5 (984 *m/z*), *p*NPC6 (1146 *m/z*), *p*NP- β -D-celloheptaoside (*p*NPC7, 1308 *m/z*), *p*NP- β -D-cellooctaoside (*p*NPC8, 1471 *m/z*), and *p*NPC9 (1633 *m/z*) (Appendix A). DP, degree of polymerization, DP 1 is *p*NPGlc generated by hydrolysis, DP 2 is the starting substrate, *p*NPC2, and the remaining peaks are transglucosylation products.

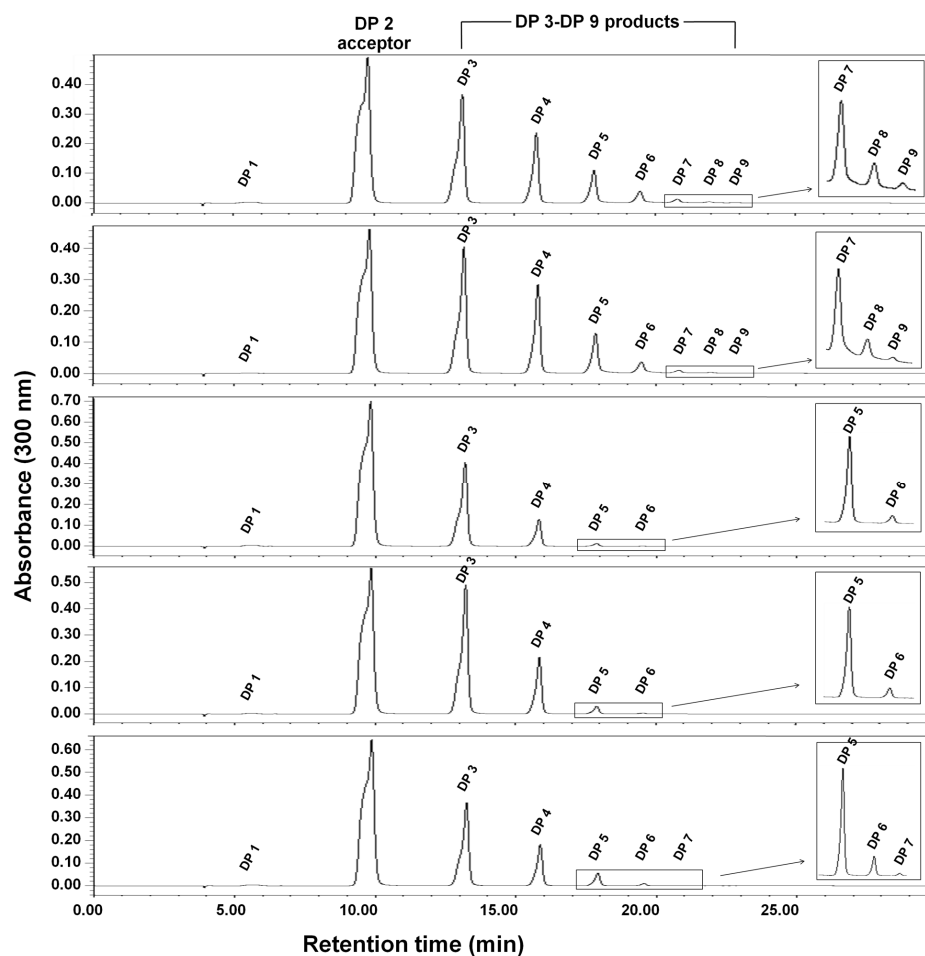


Figure 3.16 HPLC elution profiles of the transglucosylation products for reaction of α -GlcF donor and *p*NPC2 acceptor. The transglucosylation reactions catalyzed by the rice BGlul E386G glycosynthase (A) and its mutants: BGlul E386G/S334A (B), BGlul E386G/Y341A (C), BGlul E386G/Y341L (D) and BGlul E386G/N245V (E) at a 1:1 molar ratio of α -GlcF donor: *p*NPC2 acceptor, and 40 μ M enzyme concentration. The molecular mass [Mass + ^{35}Cl] $^{-}$ of each eluted compound was confirmed by mass spectrometry (Appendix A): pG (*p*NPGlc, 336 *m/z*), DP 2 (*p*NPC2, 498 *m/z*), DP 3 (*p*NPC3, 661 *m/z*), DP4 (*p*NPC4, 823 *m/z*), DP 5 (*p*NPC5, 985 *m/z*), DP 6 (*p*NPC6, 1147 *m/z*), DP 7 (*p*NPC7, 1309 *m/z*), DP 8 (*p*NPC8, 1471 *m/z*), and DP 9 (*p*NPC9, 1633 *m/z*). The insets show the later peaks at an enlarged scale.

3.6 Structures of oligosaccharide-binding site mutants

To explain the effects of these mutations, the structures of BGlu1 E386G glycosynthase mutants complexed with cellotetraose and cellopentaose were investigated by X-ray crystallography. The crystals of BGlu1 E386G/Y341L and BGlu1 E386G/N245V with cellotetraose, and BGlu1 E386G/S334A, BGlu1 E386G/Y341A, BGlu1 E386G/Y341L and BGlu1 E386G/N245V with cellopentaose gave poor X-ray diffraction and no electron densities for cellotetraose and cellopentaose were observed in the active sites of these glycosynthase mutants. However, cellotetraose was observed in the active site of the BGlu1 E386G/S334A and BGlu1 E386G/Y341A mutants, as shown in Figures 3.17 and 3.18. The structures of the S334A and Y341A mutants of the BGlu1 E386G glycosynthase with cellotetraose were solved to compare them to that of the BGlu1 E386G complex with cellotetraose. The glucosyl residues of cellotetraose and amino acid residues in the active site of the structure of the BGlu1 E386G/S334A glycosynthase mutant are similar to those in the cellotetraose complex of BGlu1 E386G, while the Glc2, Glc3 and Glc4 at subsites +1, +2 and +3 in the structure of the Y341A glycosynthase mutant are flipped nearly 180° compared to the structure of BGlu1 E386G with cellotetraose (Figure 3.19). The Glc3 and Glc4 in the active site of the BGlu1 E386G/Y341A mutant moved from their positions in the active site of BGlu1 E386G, so that O6 of Glc4 directly hydrogen bonds to Q187 Nε, while N245 may now form only a weak interaction with Glc2 O2 (3.3 Å) (Figure 3.20), rather than the hydrogen bonds with Glc2 and Glc3 observed in the BGlu1 E386G complex described earlier.

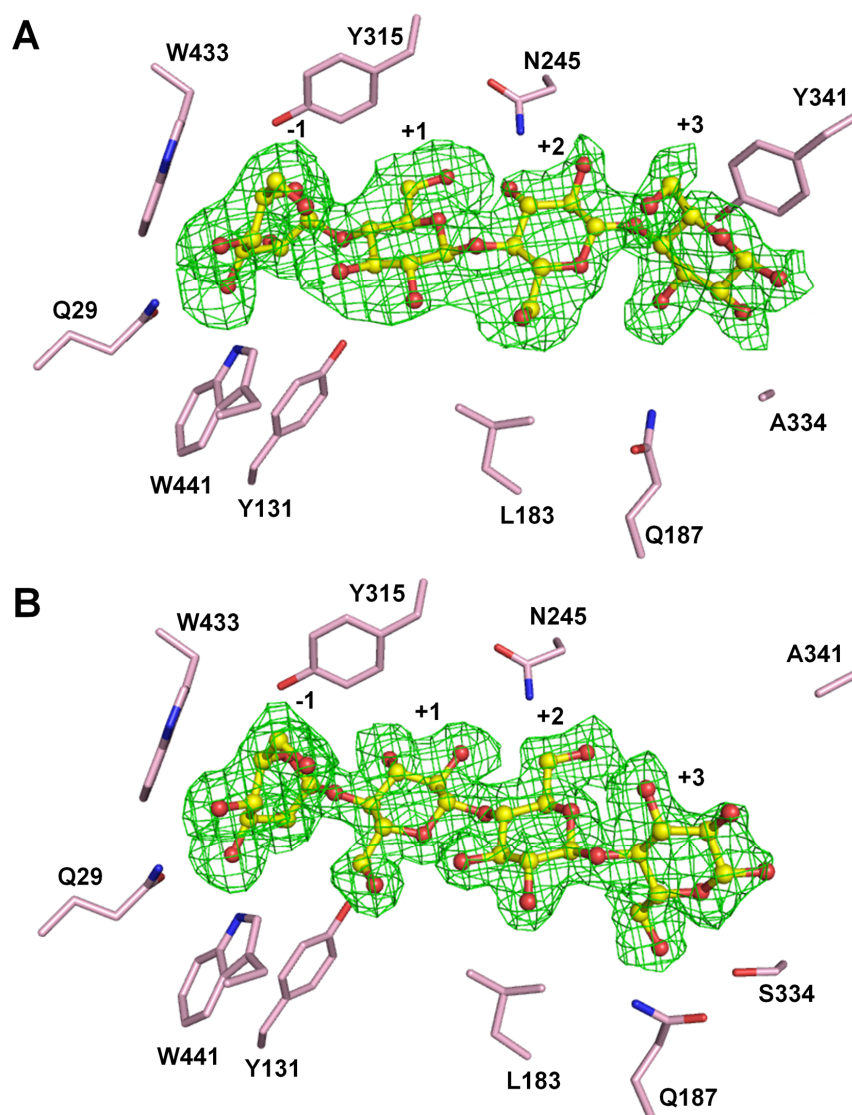


Figure 3.17 The Fo-Fc electron density maps of cellotetraose in the active sites of the BGluc E386G/S334A and BGluc E386G/S334A mutants. The Fo-Fc maps were calculated for each structure with all heteroatoms omitted from the active site, and are shown in green mesh at $+1\sigma$. The ligands from the final structures are shown in ball and stick representation. The carbons are colored in yellow and oxygen is shown in red. (A) BGluc E386G/S334A complexed with cellotetraose and (B) BGluc E386G/Y341A complexed with cellotetraose. The sidechains of amino acid residues in the active site are shown with pink carbons.

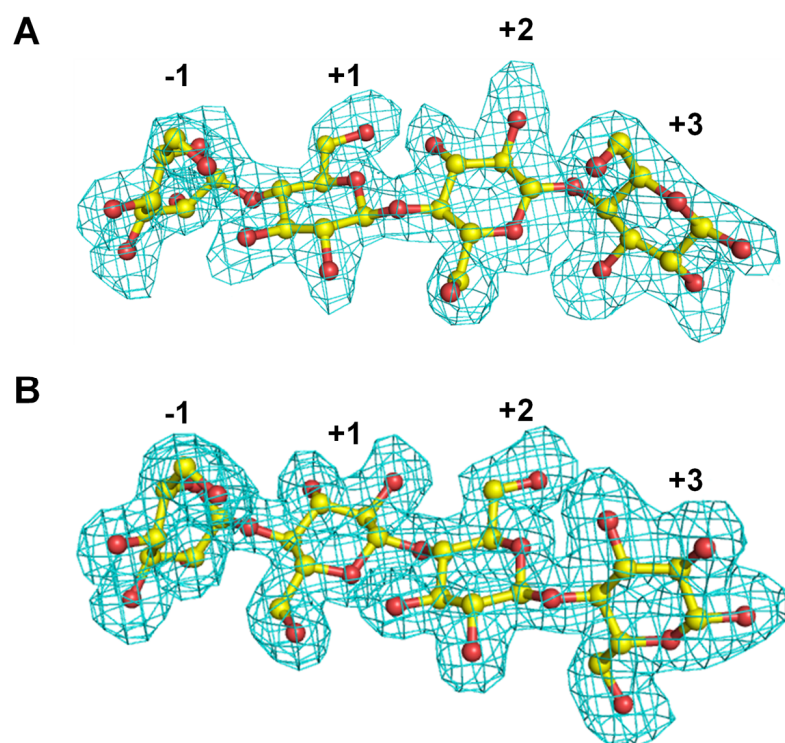


Figure 3.18 The 2Fo-Fc electron densities of cellotetraose in the active sites of the BGlucanase E386G/S334A (A) and BGlucanase E386G/S334A (B) mutants. The 2Fo-Fc maps were calculated for each structure with all heteroatoms in the active site, and are shown in blue mesh at $+1\sigma$. The ligands from the final structures are shown in ball and stick representation. The carbons are colored in yellow and oxygens in red.

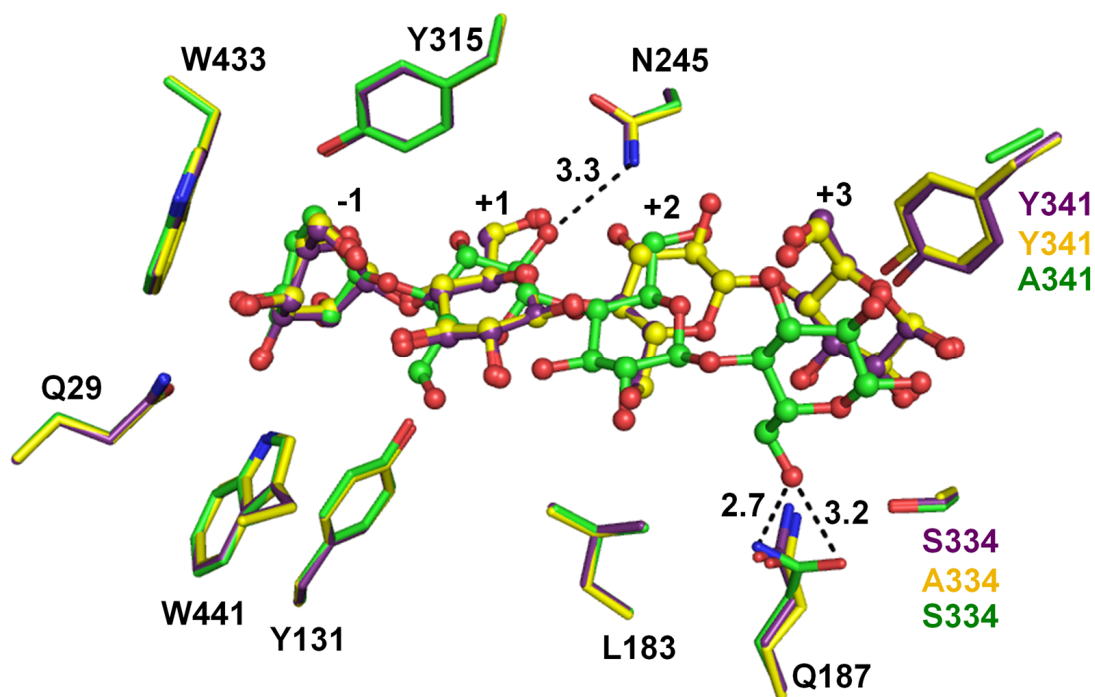


Figure 3.19 Comparison of cellotetraose binding in the active site of BGluc1 E386G, BGluc1 E386G/S334A and BGluc1 E386G/Y341A. Superimposition of the active sites of BGluc1 E386G (violet carbons), BGluc1 E386G/S334A (yellow carbons) and BGluc1 E386G/Y341A (green carbons) in complexes with cellotetraose. The direct hydrogen bonds between the glucosyl moieties in the +1 to +3 subsites of the active site of BGluc1 E386G/Y341A were identified as O6 of Glc4 with Gln187 N ϵ and O ϵ and a weak interaction of O2 of Glc2 with Asn245 N δ , which are shown as dashed lines labeled with their measured distances in Åströms. The ligands are represented as balls and sticks.

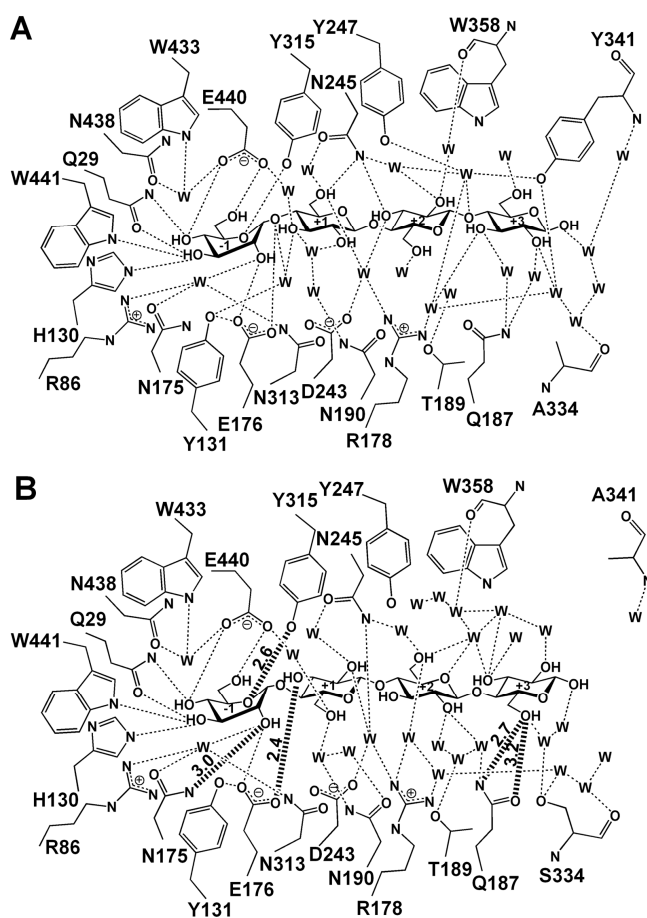


Figure 3.20 Diagrams of the strong hydrogen bonds between cellotetraose, surrounding amino acid residues and the network of water molecules in the active sites of BGluc1 E386G/S334A and BGluc1 E386G/Y341A. (A) Active site of the BGluc1 E386G/S334A mutant complex with cellotetraose, which is nearly identical to that of BGluc1 E386G, except for the loss of hydrogen bonds between the S334 sidechain and two water molecules. (B) Active site of the complex of the BGluc1 E386G/Y341A mutant with cellotetraose, showing the flip of the glucosyl residues in subsites +1 to +3 that results in a completely different network. The direct hydrogen bonds with Q187 and shortened hydrogen bonds from N175 and Y315 are shown in darkened dashed lines with their distances in Å marked on the lines. Water molecules are represented by W (without a residue number).

3.7 Donor specificity: transglycosylation activity of E386G using various donors

As is the case with many GH1 glycosidases (Day and Withers 1986), the wild type BGlu1 β -D-glucosidase has relatively broad substrate specificity, since it can hydrolyze *p*NPGlc, *p*NPFuc, *p*NPGal, *p*NPMan, *p*NPXyl and *p*NPAra, as well as β -(1 \rightarrow 2), β -(1 \rightarrow 3), β -(1 \rightarrow 4) and β -(1 \rightarrow 6) glycosidic linkages (Opassiri *et al.*, 2003; 2004). This suggests that BGlu1 glycosynthase might also utilize other glycosyl fluoride donors and thus make mixed products. The donor specificity of rice BGlu1 E386G glycosynthase was tested with a range of glycosyl fluorides using *p*NPC2 as acceptor. Incubation of 40 μ M enzyme with an equimolar ratio of α -glycosyl fluoride donor and *p*NPC2 (10 mM each) established that the glycosynthase can transfer monosaccharides from α -AraF, α -FucF, α -GalF, α -ManF and α -XylF donors (Figure 3.21). The BGlu1 E386G synthesized trisaccharides, using α -AraF (lane AF), α -FucF (lane FF), α -GalF (lane GaF), α -ManF (lane MF) and α -XylF (lane XF) as donors, and tetrasaccharides using α -FucF and α -ManF as donors, while α -GlcF resulted in products containing up to at least 6 glucosyl residues (lane GF), as previously reported (Hommalai *et al.*, 2007).

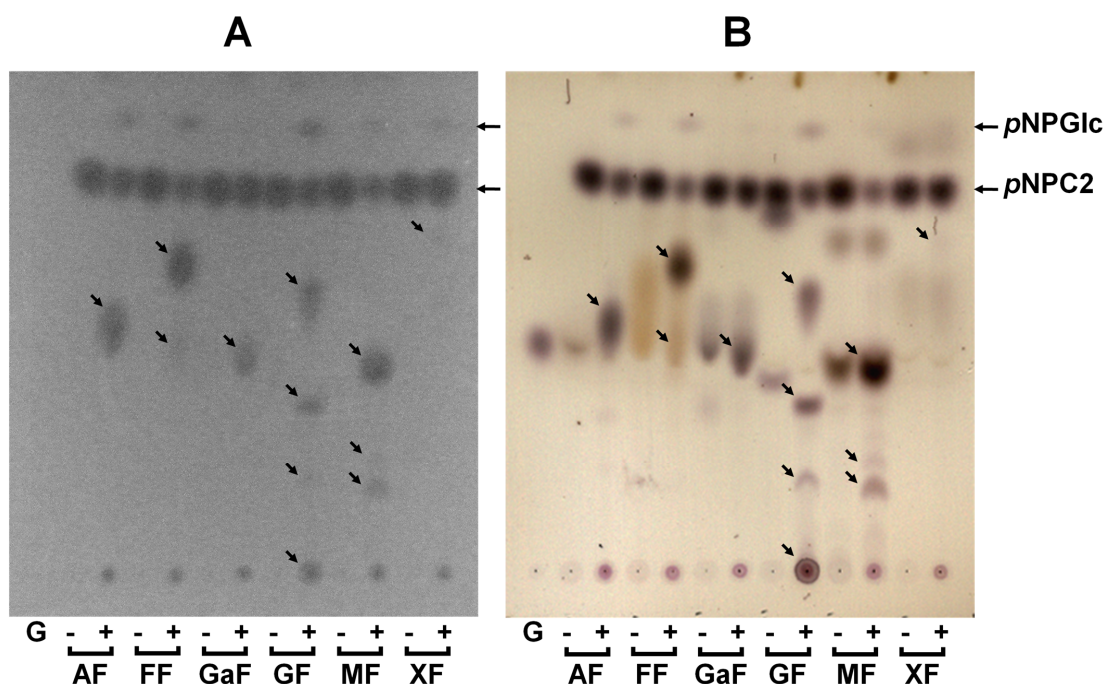


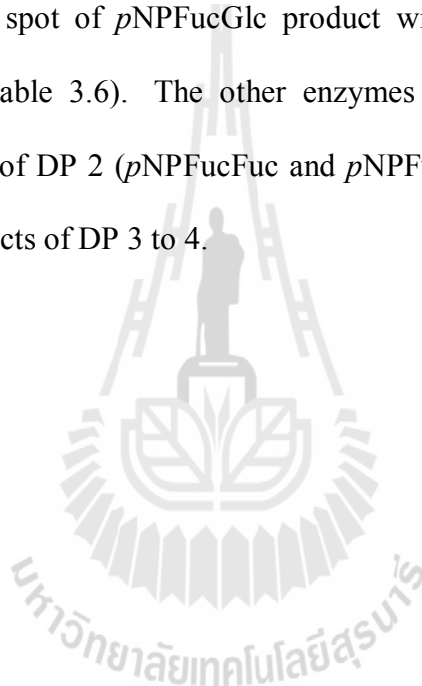
Figure 3.21. Products of transglycosylation catalyzed by BGluc1 E386G with various donors detected by thin layer chromatography. BGluc1 E386G was incubated with 10 mM *pNPC2* and 10 mM donors in 150 mM NH_4HCO_3 buffer, pH 7.0, at 30°C for 16 hr. The reactions were performed without (-) or with (+) enzyme. Silica gel TLC analysis was performed with EtOAc-MeOH-water (7:2.5:1, v/v/v) as a developing solvent, and products detected under UV light (A) or by dipping in 10% sulfuric acid in ethanol followed by charring (B). The samples loaded were G: glucose standard; and reactions with the following donors: AF, α -AraF; FF, α -FucF; GaF, α -GalF; GF, α -GlcF; MF, α -ManF and XF, α -XylF. Arrows highlight the positions of products containing *pNPC2* acceptor. The hydrolysis product *pNPGlc* was observed at the top of the TLC.

3.8 Acceptor specificity: transglycosylation activity of BGlu1 E386G and its mutants from α -glucosyl fluoride to various *p*NP-glycoside acceptors

The wild type BGlu1 β -glucosidase has high transglycosylation activity from *p*NPGlc donor to pyridoxine acceptor, producing pyridoxine 5'-O- β -D-glucoside, as well as several uncharacterized *p*NP-oligosaccharides in the same reaction (Opassiri *et al.*, 2004). To define the acceptor specificity of the rice BGlu1 E386G and whether active site entry cleft mutations affect this specificity, BGlu1 E386G glycosynthase and its 4 mutants: BGlu1 E386G/S334A, BGlu1 E386G/Y341A, BGlu1 E386G/Y341L and BGlu1 E386G/N245V were incubated with α -GlcF donor and, independently, equimolar amounts of glucose, cellobiose, *p*NPGlc, *p*NPFuc, *p*NPGal, *p*NPMan and *p*NPXyl acceptors. As seen in Figures 3.22, 3.23 and 3.24, glucose, cellobiose, *p*NPGlc, *p*NPFuc, *p*NPGal and *p*NPXyl all served as acceptors, but no transfer to *p*NPMan was observed (data not shown). The S334A mutant had similar glycosynthase activity to the original BGlu1 E386G glycosynthase using cellobiose and *p*NPGlc as acceptors (Figures 3.23 and 3.24), whereas the Y341A, Y341L and N245V mutants synthesized shorter oligosaccharides, as had been anticipated. The E386G glycosynthase and its mutants synthesize single products when using *p*NPXyl and *p*NPGal as acceptors, and more than two products when glucose, cellobiose, *p*NPGlc and *p*NPFuc are employed in that role (Figures 3.22, 3.23 and 3.24, and Tables 3.6 and 3.7).

The glycosynthases appeared to use glucose, cellobiose, *p*NPFuc, *p*NPGal, *p*NPGlc and *p*NPXyl as acceptors, but not *p*NPMan. To try to improve the synthesis

of longer products, the reactions with *p*NPFuc, *p*NPGal and *p*NPXyl acceptors were performed with twice the amount of the enzymes. The E386G glycosynthase could synthesize longer products with *p*NPFuc, but not with the other acceptors, when the amount of enzyme was increased to 80 μ M (Figure 3.25). The α -GlcF and *p*NPFuc were hydrolyzed more than in the reaction with 40 μ M of enzymes. The BGlu1 E386G/N245V mutant had higher α -GlcF hydrolysis, but lower *p*NPFuc hydrolysis, and had a very dark spot of *p*NPFucGlc product with *p*NPFuc acceptor (Figures 3.25A and D, and Table 3.6). The other enzymes had similar amounts of two products in the range of DP 2 (*p*NPFucFuc and *p*NPFucGlc) and Y341 mutants had quite a few long products of DP 3 to 4.



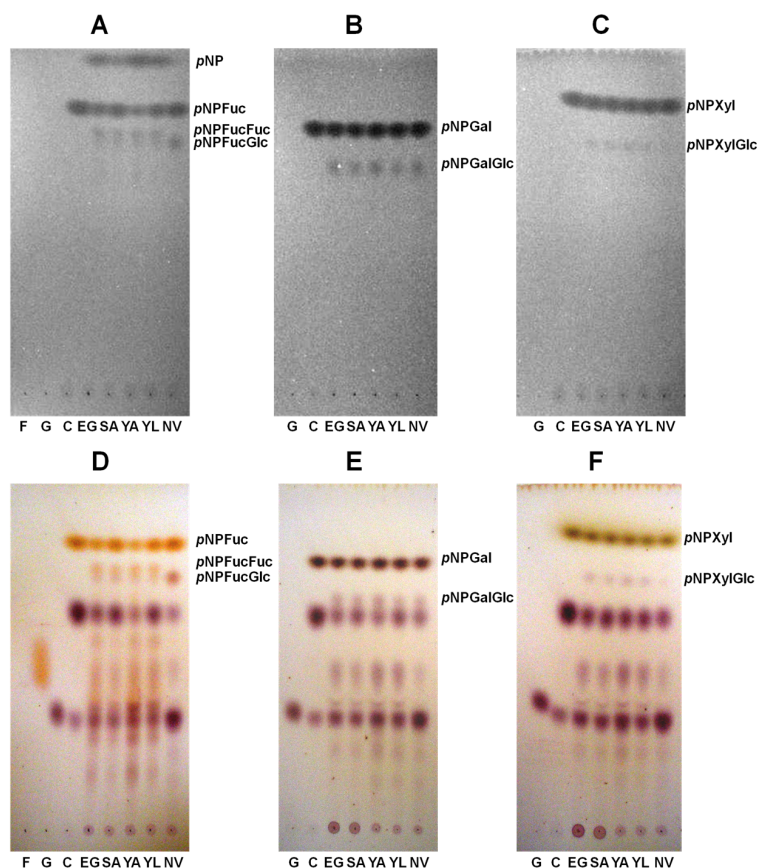


Figure 3.22 TLC detection of transglycosylation catalyzed by BGlu1 E386G glycosynthase and its mutants using α -GlcF donor and *pNPFuc*, *pNPGal* or *pNPXyl* acceptors. Enzymes (40 μ M) were incubated with 10 mM α -GlcF and 10 mM acceptors in 150 mM NH_4HCO_3 , pH 7.0, at 30°C for 16 hr. The reactions were performed without enzyme (control, C marked) or with the enzymes: EG, BGlu1 E386G; SA, BGlu1 E386G/S334A; YA, BGlu1 E386G/Y341A; YL, BGlu1 E386G/Y341L; and NV, BGlu1 E386G/N245V. The products were separated by silica gel TLC, with EtOAc-MeOH-water (7:2.5:1, v/v/v) as a developing solvent and detected under UV light (A, B and C) or spreading with 10% sulfuric acid in ethanol followed by charring (D, E and F). Acceptors were A and D, *pNPFuc*; B and E, *pNPGal*; C and F, *pNPXyl*. Standard sugars are shown in lanes F, fucose, and G, glucose.

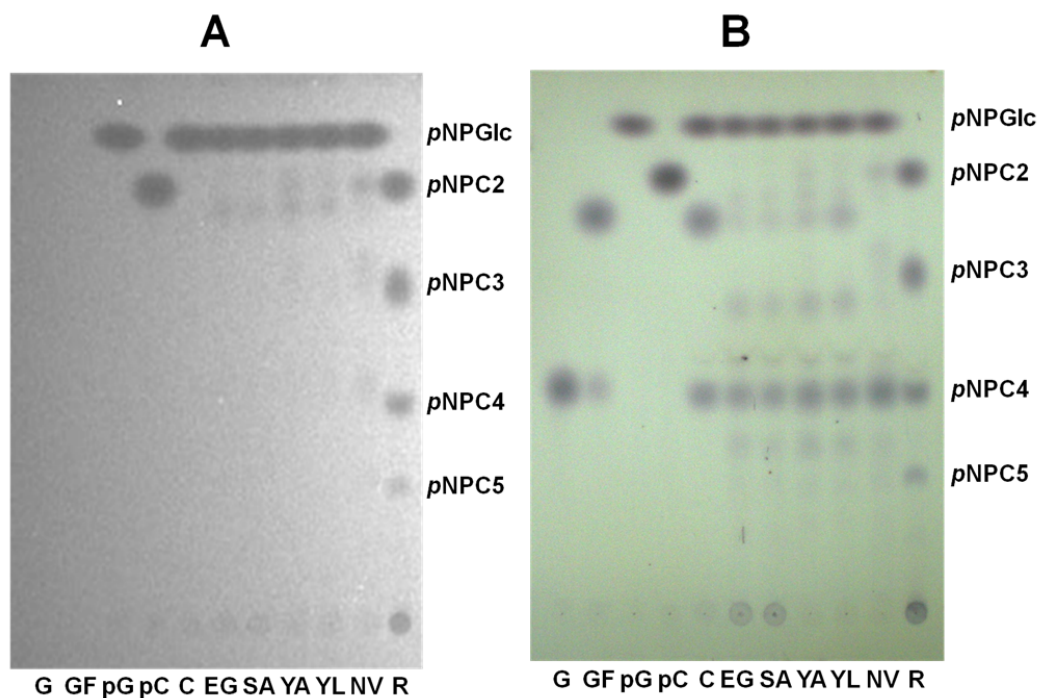


Figure 3.23 TLC detection of transglycosylation catalyzed by BGlu1 E386G glycosynthase and its mutants using α -GlcF donor and *p*NPGlc acceptor. Enzymes (40 μ M) were incubated with 10 mM α -GlcF and 10 mM *p*NPGlc in 150 mM NH_4HCO_3 , pH 7.0, at 30°C for 16 hr. The reactions were performed without enzyme (control, C marked) or with the enzymes: EG, BGlu1 E386G; SA, BGlu1 E386G/S334A; YA, BGlu1 E386G/Y341A; YL, BGlu1 E386G/Y341L; and NV, BGlu1 E386G/N245V. The products were separated by silica gel TLC, with EtOAc-MeOH-water (7:2.5:1, v/v/v) as a developing solvent and detected under UV light (A) or spreading with 10% sulfuric acid in ethanol followed by charring (B). Other lanes include G, glucose; GF, α -GlcF; pG, *p*NPGlc; pC, *p*NPC2; R, reaction of α -GlcF and *p*NPC2 catalyzed by E386G.

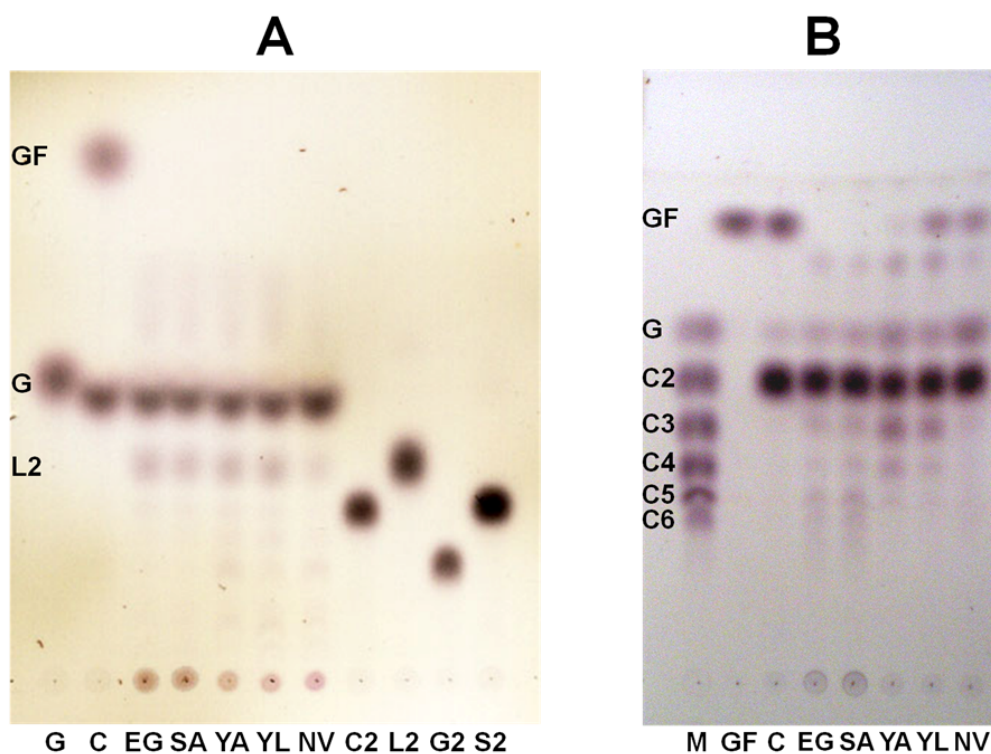


Figure 3.24 TLC detection of transglycosylation catalyzed by BGlu1 E386G glycosynthase and its mutants using α -GlcF donor and glucose or cellobiose acceptors. Enzymes (40 μ M) were incubated with 10 mM α -GlcF and 10 mM glucose (A) or 10 mM cellobiose (B) in 150 mM NH_4HCO_3 , pH 7.0, at 30°C for 16 hr. The reactions were performed without enzyme (control, C marked) or with the enzymes: EG, BGlu1 E386G; SA, BGlu1 E386G/S334A; YA, BGlu1 E386G/Y341A; YL, BGlu1 E386G/Y341L; and NV, BGlu1 E386G/N245V. The products were separated by silica gel TLC, with EtOAc-MeOH-water (7:2.5:1 (v/v/v) for glucose or 2:1:1 (v/v/v) for cellobiose) as a developing solvent, and products detected by spreading with 10% sulfuric acid in ethanol followed by charring (B). Standards are G, glucose; GF, α -GlcF; C2, cellobiose; L2, laminaribiose; G2, gentiobiose; S2, sophorose; M, standards: G, glucose; C2, cellobiose; C3, cellotriose; C4, cellotetraose; C5, cellopentaose and C6, cellohexaose.

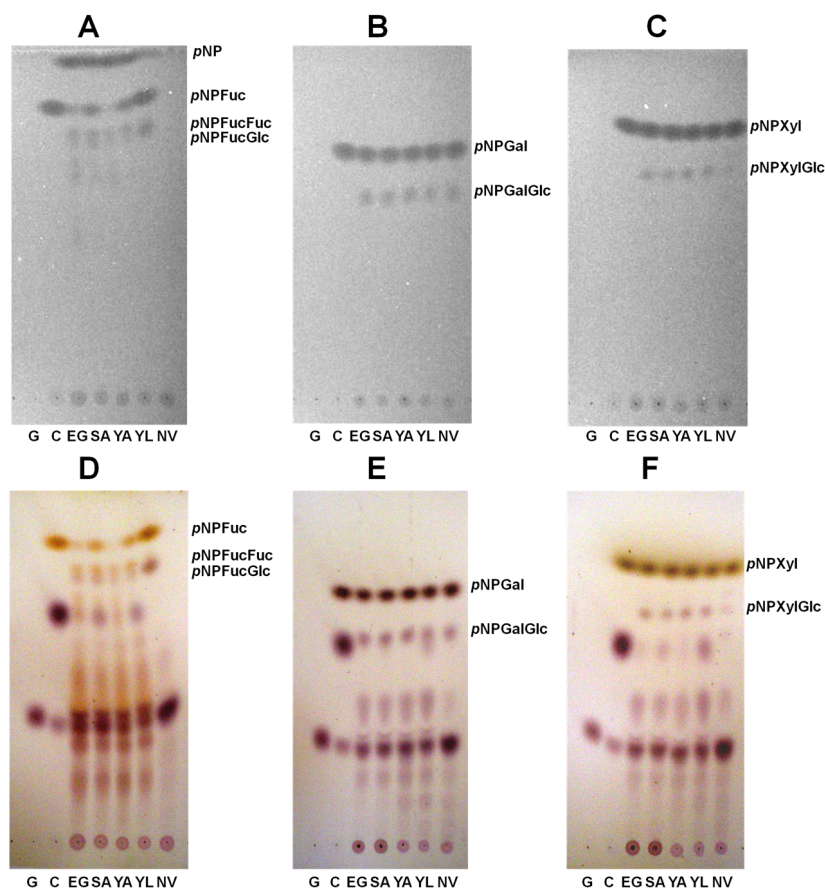


Figure 3.25 TLC detection of transglycosylation catalyzed by 80 μM BGlu1 E386G glycosynthase and its mutants with $\alpha\text{-GlcF}$ donor and *pNPFuc*, *pNPGal* or *pNPXyl* acceptors. The 80 μM enzymes were incubated with 10 mM $\alpha\text{-GlcF}$ and 10 mM acceptors in 150 mM NH_4HCO_3 , pH 7.0, at 30°C for 16 hr. The reactions were performed without enzyme (control, C marked) or with the enzymes: EG, BGlu1 E386G; SA, BGlu1 E386G/S334A; YA, BGlu1 E386G/Y341A; YL, BGlu1 E386G/Y341L; and NV, BGlu1 E386G/N245V. The products were separated by silica gel TLC, with EtOAc-MeOH-water (7:2.5:1, v/v/v) as a developing solvent and detected under UV light (A, B and C) or spreading with 10% sulfuric acid in ethanol followed by charring (D, E and F). Acceptors were A and D, *pNPFuc*; B and E, *pNPGal*; and C and F, *pNPXyl*. Lane G is glucose standard.

Table 3.6 Products of glycosynthase reactions of BGlu1 E386G glycosynthase and its 4 glycosynthase mutants using α -glucosyl fluoride donor and *p*NPFuc acceptor.

	Percent of <i>p</i> NP-glycoside products (% yield) ^a						
	DP 0	DP 1	DP 2	DP 2	DP 3	DP 4	DP 4
Mass	138 ^b	320 ^b	466 ^b	482 ^b	628 ^b	774 ^b	790 ^b
<u>Glycosynthase</u>							
E386G	45.70	47.49	2.55	3.89	0.15	0.17	0.00
E386G/S334A	28.24	65.05	2.22	4.35	0.04	0.05	0.00
E386G/Y341A	73.38	19.91	2.64	3.60	0.12	0.29	0.00
E386G/Y341L	30.89	63.74	2.41	2.91	0.00	0.00	0.00
E386G/N245V	3.77	84.67	0.48	10.93	0.07	0.03	0.00
2xE386G	79.75	11.77	2.25	4.59	0.88	0.53	0.15
2xE386G/S334A	54.35	35.88	3.08	6.26	0.10	0.22	0.04
2xE386G/Y341A	91.80	1.69	2.29	3.28	0.49	0.35	0.00
2xE386G/Y341L	59.99	32.63	3.66	3.59	0.06	0.08	0.00
2xE386G/N245V	8.18	79.12	1.23	11.29	0.08	0.04	0.00

^aPreparative reactions in 150 mM NH₄HCO₃ buffer, pH 7.0, 30°C, at a 1:1 molar ratio of α -GlcF donor:*p*NPFuc acceptor, and 40 μ M or 80 μ M (2x) enzyme concentrations for 16 hr. The relative percents are in terms of peak area per total 300 nm absorbance in *p*NP-glycoside products and substrates peaks separated by HPLC on a ZORBAX carbohydrate column.

^bThe molecular mass [Mass+³⁵Cl]⁻ of each eluted compound was confirmed by mass spectrometry. *p*NPFuc (320 *m/z*); *p*NPFucFuc (466 *m/z*); *p*NPFucGlc (482 *m/z*); *p*NPFucGlcFuc or *p*NPFucFucGlc (628 *m/z*); *p*NPFucGlcFucFuc, *p*NPFucFucGlcFuc or *p*NPFucFucFucGlc (774 *m/z*) and *p*NPFucGlcFucGlc, *p*NPFucFucGlcGlc, or *p*NPFucGlcGlcFuc (790 *m/z*). DP, degree of polymerization, DP 0 is the hydrolytic product *p*NP, DP 1 is the starting substrate, *p*NPFuc, and the rest are transglucosylation products.

Table 3.7 Products of glycosynthase reactions of BGlu1 E386G glycosynthase and its 4 mutants using α -glucosyl fluoride donor and *p*NPGlc acceptor.

	Percent of <i>p</i> NP-glycoside product % yield) ^a					
	DP 0	DP 1	DP 2	DP 3	DP 4	DP 5
Mass	138 ^b	336 ^b	498 ^b	661 ^b	823 ^b	985 ^b
Glycosynthase						
E386G	3.45	93.25	2.67	0.22	0.28	0.08
E386G/S334A	1.76	94.52	2.99	0.22	0.34	0.08
E386G/Y341A	4.80	87.33	5.28	1.10	0.44	0.03
E386G/Y341L	1.85	92.86	4.21	0.57	0.41	0.04
E386G/N245V	0.29	89.10	5.68	2.82	1.87	0.21

^aPreparative reactions in 150 mM NH₄HCO₃ buffer, pH 7.0, 30°C, at a 1:1 molar ratio of α -GlcF donor:*p*NPGlc acceptor (10 mM each), and 40 μ M enzyme concentration for 16 hr. The relative percents are in terms of peak area per total 300 nm absorbance in *p*NP-glycoside products and substrates peaks separated by HPLC on a ZORBAX carbohydrate column.

^bThe molecular mass [Mass+³⁵C] of each eluted compound was confirmed by mass spectrometry. *p*NPGlc (336 *m/z*); *p*NP-disaccharide (498 *m/z*); *p*NP-trisaccharide (661 *m/z*); *p*NP-tetrasaccharide (823 *m/z*) and *p*NP-pentasaccharide (985 *m/z*).

DP, degree of polymerization, DP 0 is the hydrolytic product *p*NP, DP 1 is the starting substrate, *p*NPGlc, and the rest are transglucosylation products.

3.9 NMR characterization of reaction product linkages

To determine the regioselectivity of the glycosidic bonds formed in glycosynthase reactions, the products from reactions of α -FucF with *p*NPC2, and α -ManF with *p*NPC2 were synthesized with E386G and products from reaction of α -GlcF and *p*NPFuc were synthesized with both BGlu1 E386G and BGlu1 E386G/N245V for analysis by NMR spectroscopy. Reaction mixtures were separated by reverse-phase chromatography and TLC. The masses of the purified products were determined by ESI-MS, followed by determination of their linkages by NMR.

Both BGlu1 E386G and BGlu1 E386G/N245V glycosynthases were found to synthesize the same product linkages of Fuc- β -(1 \rightarrow 3)-Fuc-*p*NP (No. 3, reaction of BGlu1 E386G and No. 6, reaction of BGlu1 E386G/N245V in Table 3.8 and the following sections), Glc- β -(1 \rightarrow 3)-Fuc-*p*NP (Table 3.8), No. 4, reaction of BGlu1 E386G and No. 7, reaction of BGlu1 E386G/N245V) and Fuc- β -(1 \rightarrow 4)-Glc- β -(1 \rightarrow 3)-Fuc-*p*NP (No. 5, reaction of BGlu1 E386G and No. 8, reaction of BGlu1 E386G/N245V) in the reactions containing *p*NPFuc and α -GlcF. In the reaction products with *p*NPC2 as acceptor, the linkages were Man- β -(1 \rightarrow 4)-Glc- β -(1 \rightarrow 4)-Glc-*p*NP (Table 3.8, No. 2, reaction of BGlu1 E386G) and Fuc- β -(1 \rightarrow 4)-Glc- β -(1 \rightarrow 4)-Glc-*p*NP (Table 3.8, No. 1, reaction of BGlu1 E386G). The NMR spectral peaks and MS ion peaks are listed in the following sections, and the conclusions summarized in Table 3.8.

3.9.1 NMR and MS Spectra:

3.9.1.1 4-Nitrophenyl [(2,3,4-tri-*O*-acetyl- β -D-fucopyranosyl)-(1 \rightarrow 4)-*O*-2,3,6-tri-*O*-acetyl- β -D-glucopyranosyl]-(1 \rightarrow 4)-*O*-2,3,6-tri-*O*-acetyl- β -D-glucopyranoside (1)

$^1\text{H-NMR}$ (400 MHz, CDCl_3): δ 8.21 (m, 2 H, Ar), 7.05 (m, 2 H, Ar), 5.29 (dd, 1 H, $J_{2,3}$ 8.5, $J_{3,4}$ 8.2 Hz, H-3), 5.23-5.15 (m, 4H, H-2, H-3', H4'', H-1) 5.08 (dd, 1H, $J_{1''2''}$ 8.0 $J_{2''3''}$ 10.3 Hz, H-2''), 4.94 (dd, 1H, $J_{2''3''}$ 10.3, $J_{3''4''}$ 3.4 Hz, H-3''), 4.87 (dd, 1H, $J_{1'2'}$ 8.1, $J_{2'3'}$ 9.5 Hz, H-2'), 4.55 (m, 1H, H-6a), 4.53 (d, 1H, $J_{1'2'}$ 8.1 Hz, H-1'), 4.43 (d, 1H, $J_{1''2''}$ 8.0 Hz, H-1''), 4.41 (m, 1H, H-6'a), 4.16-4.14 (m, 2H, H-6b, H-6'b), 3.88 (dd, 1H, $J_{3,4}$ 8.2, $J_{4,5}$ 10.1 Hz, H-4), 3.81 (dd, 1H, $J_{3'4'}$ 9.5, $J_{4'5'}$ 9.4 Hz, H-4'), 3.91-3.78 (m, 1H, H-5), 3.76-3.71 (m, 1H, H-5''), 3.65-3.59 (m, 1H, H-5'), 2.20-1.90 (9s, 27H, 9xCH₃CO), 1.20 (d, 3H, Me). ESI-MS: m/z 632 [M+Na]⁺.

3.9.1.2 4-Nitrophenyl [(2,3,4,6-tetra-*O*-acetyl- β -D-mannopyranosyl)-(1 \rightarrow 4)-*O*-2,3,6-tri-*O*-acetyl- β -D-glucopyranosyl]-(1 \rightarrow 4)-*O*-2,3, 6-tri-*O*-acetyl- β -D-glucopyranoside (2)

$^1\text{H-NMR}$ (400 MHz, CDCl_3): δ 8.21 (m, 2 H, Ar), 7.06 (m, 2 H, Ar), 5.40 (brd, 1 H, $J_{2''3''}$ 3.0, H-2''), 5.29 (dd, 1H, $J_{2,3}$ 8.5, $J_{3,4}$ 8.5 Hz, H-3), 5.21 (dd, 1H, $J_{1,2}$ 7.3, $J_{2,3}$ 8.5 Hz, H-2), 5.20 (dd, 1H, $J_{3''4''}$ 10.0, $J_{4''5''}$ 8.5 Hz, H-4''), 5.17 (d, 1H, $J_{1,2}$ 7.3 Hz, H-1), 5.15 (dd, 1H, $J_{2',3'}$ 9.4, $J_{3',4'}$ 9.7 Hz, H-3'), 5.01 (dd, 1H, $J_{2''3''}$ 3.0, $J_{3''4''}$ 10.0 Hz, H-3''), 4.88 (dd, 1H, $J_{1'2'}$ 7.9, $J_{2',3'}$ 9.4 Hz, H-2'), 4.64 (brs, 1H, H-1''), 4.55 (dd, 1H, $J_{5,6a}$ 1.8, $J_{6a,6b}$ 11.8 Hz, H-6a), 4.52 (d, 1H, $J_{1'2'}$ 7.9 Hz, H-1'), 4.34 (dd, 1H, $J_{6'a,6'b}$ 12.45, $J_{5',6'a}$ 5.2 Hz, H-6'a), 4.31-4.28 (m, 2H, H-6''a, H-6''b), 4.12 (dd, 1H, $J_{6'a,6'b}$ 12.5, $J_{5',6'b}$ 2.1 Hz, H-6'b), 4.11 (dd, 1H, $J_{6a,6b}$ 11.8, $J_{5,6b}$ 4.9 Hz, H-6b), 3.91-3.81

(m, 3H, H-4, H-4', H-5), 3.64-3.58 (m, 2H, H-5', H-5''), 2.16-1.99 (10s, 30H, 10xCH₃CO). ESI-MS: m/z 648 [M+Na]⁺.

3.9.1.3 4-Nitrophenyl (2,3,4-tri-*O*-acetyl- α -D-fucopyranosyl)-(1 \rightarrow 3)-2,4-di-*O*-acetyl- β -D-fucopyranoside (3 and 6)

¹H-NMR (400 MHz, CDCl₃): δ 8.21 (m, 2 H, Ar), 7.05 (m, 2 H, Ar), 5.50 (dd, 1 H, $J_{1,2}$ 8.1, $J_{2,3}$ 9.9 Hz, H-2), 5.35 (brd, 1H, $J_{3,4}$ 3.4 Hz, H-4), 5.20 (brd, 1H, $J_{3',4'}$ 3.3 Hz, H-4'), 5.11 (dd, 1H, $J_{1',2'}$ 7.9, $J_{2',3'}$ 10.7 Hz, H-2'), 5.07 (d, 1H, $J_{1,2}$ 8.1 Hz, H-1), 4.95 (dd, 1H, $J_{2',3'}$ 10.7, $J_{3',4'}$ 3.4 Hz, H-3'), 4.55 (d, 1H, $J_{1',2'}$ 7.9 Hz, H-1'), 3.98 (dd, 1H, $J_{2,3}$ 9.9, $J_{3,4}$ 3.4 Hz, H-3), 3.94 (m, 1H, H-5'), 3.76 (m, 1H, H-5), 2.20-1.98 (5s, 15H, 5xCH₃CO), 1.30 (d, 3H, H6'a, H6'b, H6'c), 1.20 (d, 3H, H6a, H6b, H6c). ESI-MS: m/z 454 [M+Na]⁺.

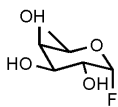
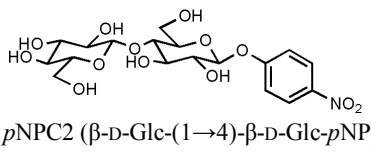
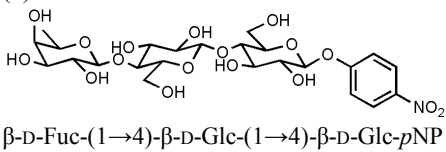
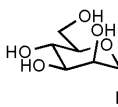
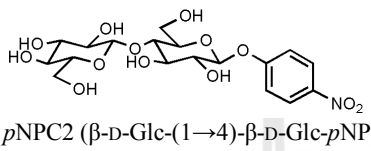
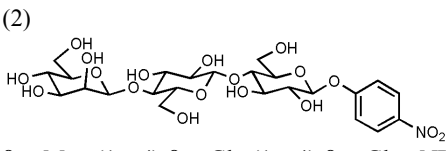
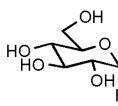
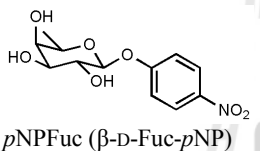
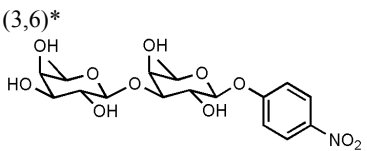
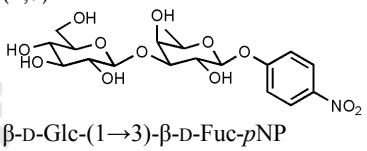
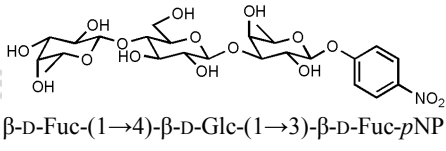
3.9.1.4 4-Nitrophenyl (2,3,4,6-tetra-*O*-acetyl- α -D-glucopyranosyl)-(1 \rightarrow 3)-2,4-di-*O*-acetyl- β -D-fucopyranoside (4 and 7)

¹H-NMR (400 MHz, CDCl₃): δ 8.21 (m, 2 H, Ar), 7.06 (m, 2 H, Ar), 5.46 (dd, 1 H, $J_{1,2}$ 8.0, $J_{2,3}$ 10.0 Hz, H-2), 5.34 (brd, 1H, $J_{3,4}$ 3.4 Hz, H-4), 5.17 (dd, 1H, $J_{3',4'}$ 9.3, $J_{4',5'}$ 9.0 Hz, H-4'), 5.12 (dd, 1H, $J_{2',3'}$ 9.0, $J_{3',4'}$ 9.3 Hz, H-3'), 5.08 (d, 1H, $J_{1,2}$ 8.0 Hz, H-1), 4.93 (dd, 1H, $J_{1',2'}$ 7.8, $J_{2',3'}$ 9.0 Hz, H-2') 4.65 (d, 1H, $J_{1',2'}$ 7.8 Hz, H-1'), 4.33 (dd, 1H, $J_{5',6'a}$ 2.6, $J_{6'a,6'b}$ 12.3 Hz, H-6'a), 4.15 (dd, 1H, $J_{5',6'b}$ 3.8, $J_{6'a,6'b}$ 12.3 Hz, H-6'b), 3.97-3.92 (m, 2H, H-3, H-5), 3.69-3.65 (m, 2H, H-5'), 2.18-2.00 (6s, 18H, 6xCH₃CO), 1.25 (d, 3H, H6a, H6b, H6c). ESI-MS: m/z 470 [M+Na]⁺.

3.9.1.5 4-Nitrophenyl [(2,3,4-tri-*O*-acetyl- β -D-fucopyranosyl)-(1 \rightarrow 4)-*O*-2,3,6-tri-*O*-acetyl- β -D-glucopyranosyl)-(1 \rightarrow 3)-*O*-2,4-di-*O*-acetyl- β -D-fucopyranoside (5 and 8)

$^1\text{H-NMR}$ (400 MHz, CDCl_3): δ 8.21 (m, 2 H, Ar), 7.06 (m, 2 H, Ar), 5.48 (dd, 1 H, $J_{1,2}$ 8.0, $J_{2,3}$ 10.0 Hz, H-2), 5.33 (brd, 1H, $J_{3,4}$ 3.0 Hz, H-4), 5.20 (brd, 1H, $J_{3'',4''}$ 3.3 Hz, H-4''), 5.17-5.03 (m, 4H, H-1, H-3', H-2'', H-3''), 4.89 (dd, 1H, $J_{1',2'}$ 7.9, $J_{2',3'}$ 8.8 Hz, H-2'), 4.58 (d, 1H, $J_{1',2'}$ 7.9 Hz, H-1'), 4.45 (d, 1H, $J_{1'',2''}$ 8.2 Hz, H-1''), 4.30 (dd, 1H, $J_{5,6'a}$ 3.0, $J_{6'a,6'b}$ 12.1 Hz, H-6'a), 4.14 (dd, 1H, $J_{5',6'b}$ 3.9, $J_{6'a,6'b}$ 12.1 Hz, H-6'b), 3.98-3.91 (m, 2H, H-3, H-5), 3.73-3.63 (m, 3H, H-4', H-5', H-5''), 2.19-2.00 (8s, 24H, 8x CH_3CO), 1.35 (d, 3H, H6a, H6b, H6c), 1.25 (d, 3H, H6''a, H6''b, H6''c). ESI-MS: m/z 616 $[\text{M}+\text{Na}]^+$.

Table 3.8 Structures of products of glycosynthase reactions of BGlu1 E386G and BGlu1 E386G/N245V.

Rxn	Donor	Acceptor	Product
1	 α -FucF	 p NPC2 (β -D-Glc-(1 \rightarrow 4)- β -D-Glc- p NP)	(1)  β -D-Fuc-(1 \rightarrow 4)- β -D-Glc-(1 \rightarrow 4)- β -D-Glc- p NP
2	 α -ManF	 p NPC2 (β -D-Glc-(1 \rightarrow 4)- β -D-Glc- p NP)	(2)  β -D-Man-(1 \rightarrow 4)- β -D-Glc-(1 \rightarrow 4)- β -D-Glc- p NP
3	 α -GlcF	 p NPFuc (β -D-Fuc- p NP)	(3,6)*  β -D-Fuc-(1 \rightarrow 3)- β -D-Fuc- p NP
			(4,7)  β -D-Glc-(1 \rightarrow 3)- β -D-Fuc- p NP
			(5,8)**  β -D-Fuc-(1 \rightarrow 4)- β -D-Glc-(1 \rightarrow 3)- β -D-Fuc- p NP

* Formed by wild type BGlu1 β -glucosidase contaminant.

** Formed by successive action of glycosynthase and wild type BGlu1 contaminant.

No. 1-5: products from glycosynthase reactions of BGlu1 E386G.

No. 6-8: products from glycosynthase reactions of BGlu1 E386G/N245V.

3.10 Cyclophellitol inhibition

The presence of *p*NP-glycoside hydrolysis products and products where *p*NPFuc acted as a glycosyl donor suggested contamination of the BGlu1 E386G glycosynthase with wild type BGlu1 β -D-glucosidase, which can hydrolyze and transglycosylate from β -linked substrates, unlike its glycosynthase. To confirm the wild type BGlu1 contamination of the BGlu1 E386G, two approaches were used, production of a less revertible glycosynthase and inhibition of wild type enzyme with the covalent inhibitor cyclophellitol. A new mutation of BGlu1 E386G was made by changing GAA (Glu) to GGC instead of GGG to encode the Gly, in order to decrease the probability of misread as Glu (GAG) by the ribosome or of a reversion mutation in the expression culture. The protein expressed from this mutation (BGlu1 E386G2) exhibited 33-fold lower *p*NPGlc hydrolysis activity compared to the original BGlu1 E386G glycosynthase (the *p*NPGlc hydrolysis activities of BGlu1, BGlu1 E386G and BGlu1 E386G2 were 1900, 1.1 and 0.033 $\mu\text{mol min}^{-1} \text{mg}^{-1}$ protein, respectively).

Cyclophellitol inactivates retaining β -D-glucosidases by forming a covalent adduct with the catalytic nucleophile, which is recalcitrant to rescue by transglycosylation (Gloster *et al.*, 2007). As shown in Figure 3.27, inactivation of rice BGlu1 by cyclophellitol followed pseudo-first order kinetics of inactivation (based on the linear curves for $-\ln V/V_0$ versus time), similar to previous reports for other β -D-glucosidases (Withers and Umezawa, 1991; Gloster *et al.*, 2007). Cyclophellitol acted as an irreversible inactivator of the rice BGlu1 β -D-glucosidase with an equilibrium constant for initial binding, K_i of 5.7 μM and an inactivation rate constant, k_i of 0.35 min^{-1} (Figure 3.27B).

To prove which transglycosylation products of the E386G and E386G2 glycosynthases were due to the true activities of the glycosynthases, they were pre-incubated with 2 mM cyclophellitol for 2 hr, which completely inhibited wild type BGlu1 activity (Figure 3.26), before testing the transglycosylation of *p*NP-Fuc with α -GlcF. The E386G glycosynthase synthesized two products in the range of *p*NP-disaccharides and a few trisaccharides in the reaction without cyclophellitol and a single product, corresponding to *p*NP-FucGlc, after pre-incubation with 2 mM cyclophellitol, while the E386G2 synthesized only a single product, corresponding to *p*NP-FucGlc, after pre-incubation without or with 2 mM cyclophellitol (Figure 3.28). The wild type BGlu1 synthesized transglycosylation products after pre-incubation without cyclophellitol, but could not synthesize any product after pre-incubation with 2 mM cyclophellitol. Moreover, uninhibited wild type BGlu1 synthesized only one product in the *p*NP-disaccharide range, corresponding to *p*NP-FucFuc, which was seen with BGlu1 E386G, but not BGlu1 E386G2, confirming that the original BGlu1 E386G glycosynthase was contaminated with wild type BGlu1. This result also confirms that the wild type BGlu1 could not transfer from α -GlcF, suggesting it is unlikely to have contributed to the production of hetero-disaccharide products in the analysis of glycosynthase donor specificity.

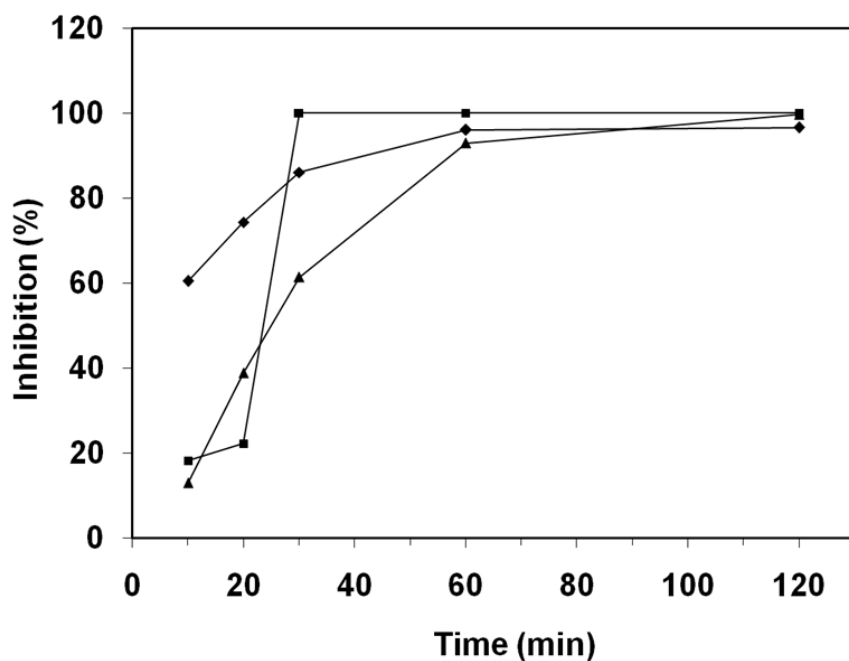
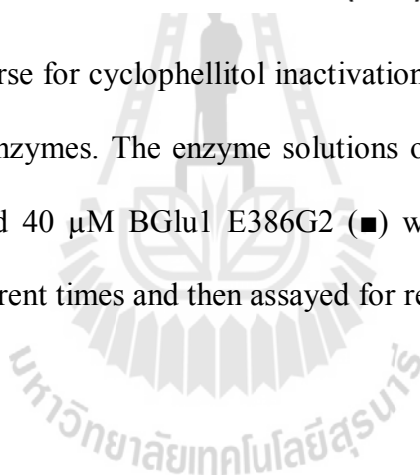


Figure 3.26 Time course for cyclophellitol inactivation of rice BGlul, BGlul E386G and BGlul E386G2 enzymes. The enzyme solutions of 0.2 μM BGlul (▲), 40 μM BGlul E386G (◆) and 40 μM BGlul E386G2 (■) were pre-incubated with 1 μM cyclophellitol for different times and then assayed for release of *p*NP from *p*NPGlc.



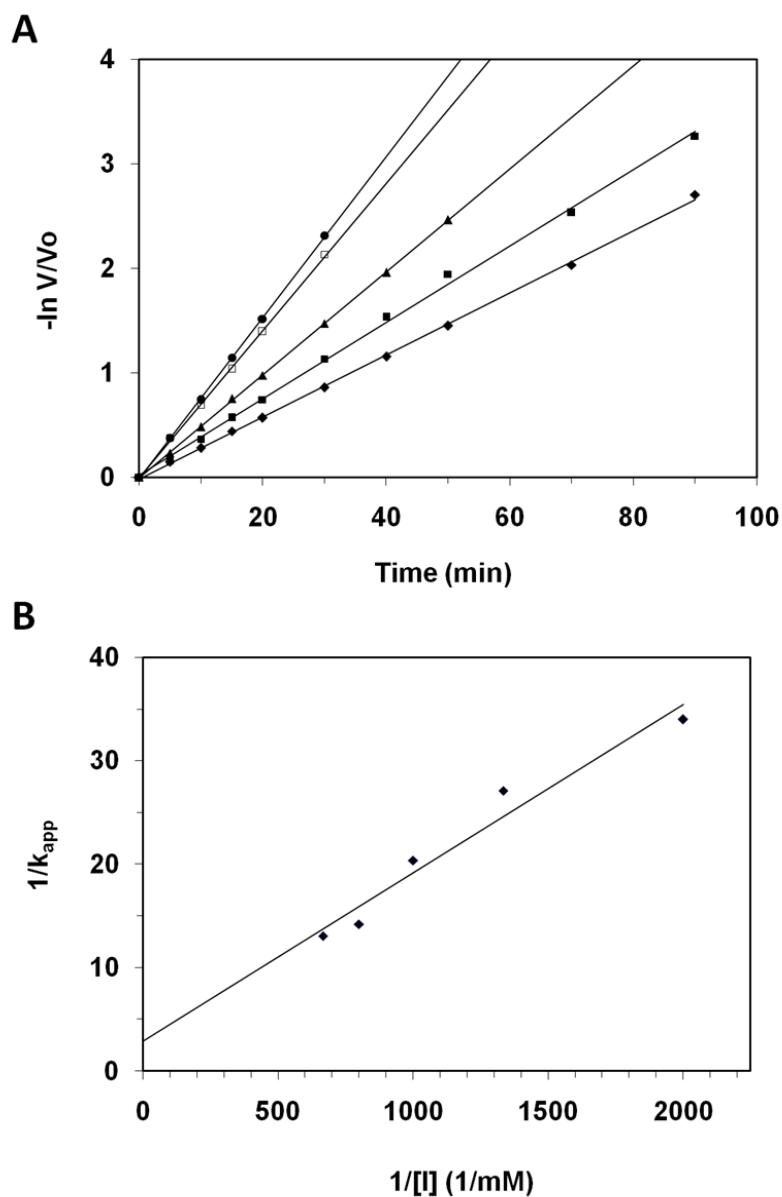


Figure 3.27 Cyclophellitol inhibition of rice BGlu1. A: Semi-logarithmic plot of the remaining wild type BGlu1 β -glucosidase activity (reflecting the remaining free enzyme, E/E_0) versus time at various concentrations of cyclophellitol, (\bullet), 0.5 μM ; (\square), 0.75 μM ; (\blacktriangle), 1 μM ; (\blacksquare), 1.25 μM ; (\blacklozenge), 1.5 μM . B: Replot of the inverse of the apparent first order rate constants (k_{app} , the slopes of the $-\ln V/V_0$ versus time curves) from A versus the inverse of the inhibitor concentration, $1/[I]$. Slope = 0.0163, x-intercept = -176.96 mM^{-1} and y-intercept = 2.88 min.

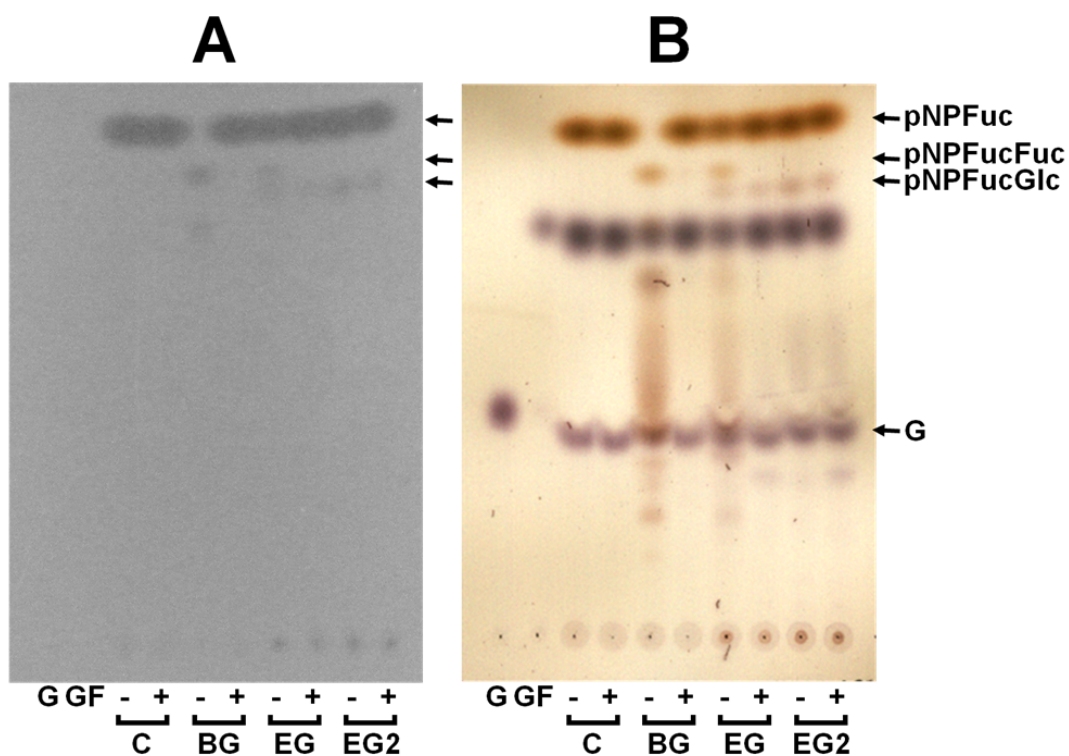


Figure 3.28 Effect of cyclophellitol inhibition on transglycosylation products of rice BGl1, BGl1 E386G and BGl1 E386G2 with *p*NPFuc and α -GlcF. The 0.2 μ M BGl1, 40 μ M BGl1 E386G and 40 μ M BGl1 E386G2 were pre-incubated without (-) or with (+) 2 mM cyclophellitol for 2 hr, then transglycosylation reactions with 10 mM *p*NPFuc and 10 mM α -GlcF in 150 mM NH_4HCO_3 , pH 7.0, were incubated at 30°C for 16 hr. Silica gel TLC analysis was performed with EtOAc-MeOH-water (7:2.5:1, v/v/v) as a developing solvent, and products detected under UV light (A) or by spreading with 10% sulfuric acid in ethanol followed by charring (B). Lane G, glucose standard; GF, α -GlcF; C, control of 10 mM *p*NPFuc and 10 mM α -GlcF without enzyme; BG, reaction with wild type BGl1; EG, reaction with BGl1 E386G; EG2, reaction with BGl1 E386G2.

3.11 Transglycosylation activity of BGlu1 E386G2

Since no wild type hydrolysis and transglycosylation activities were detected in the BGlu1 E386G2 preparation under the conditions of the standard reaction, its glycosynthase activity with various donors and acceptors was tested as previously described for BGlu1 E386G. The BGlu1 E386G2 could transglycosylate *pNPC2* with α -AraF, α -FucF, α -GalF, α -ManF and α -XylF as donors to produce trisaccharides, but Figure 3.29 shows that only a faint spot of tetrasaccharide was seen with α -FucF donor, in contrast to the large amounts seen with the original BGlu1 E386G glycosynthase preparation. However, tiny amounts of tetrasaccharides were observed with all α -glycosyl fluoride donors by LC-MS (Table 3.9). The BGlu1 E386G2 glycosynthase could also use glucose, cellobiose, *pNPFuc*, *pNPGal*, *pNPGlc*, *pNPXyl* and *pNPC2* as acceptors to synthesize oligosaccharides similar to the E386G (Figure 3.30), but *pNP*-glycosides resulting from addition of more than one Glc could only be detected with *pNPC2* as acceptor on TLC. The BGlu1 E386G2 synthesized only a single TLC-detectable product with *pNPFuc* as acceptor and showed no hydrolytic activity toward acceptors, indicating the products *pNPFuc* oligosaccharides seen with the original BGlu1 E386G preparation resulted from the wild type BGlu1 transglycosylation activity. When *pNPGlc* was used as an acceptor, only a faint *pNP*-disaccharide product spot could be seen (Figure 3.30, lane pG), explaining why it was not detected in previous work (Hommalai *et al.*, 2007). This spot had a mobility slightly lower than *pNPC2*, suggesting it might be *pNP*-gentiobioside, but this identity was not confirmed. Similarly, the products with cellobiose as acceptor were very faint, though at least two products could be detected by sulfuric acid charring (Figure 3.30B, lane C2). However, small amounts of longer *pNP*-oligosaccharide products

from reactions with each of the *p*NP-glycoside acceptors, which could not be detected by TLC, could be detected by LC-MS, including triosides of all, tetraosides from *p*NPGlc, *p*NPXyl and *p*NPMan, and pentaoside from *p*NPGlc acceptor (Table 3.10).

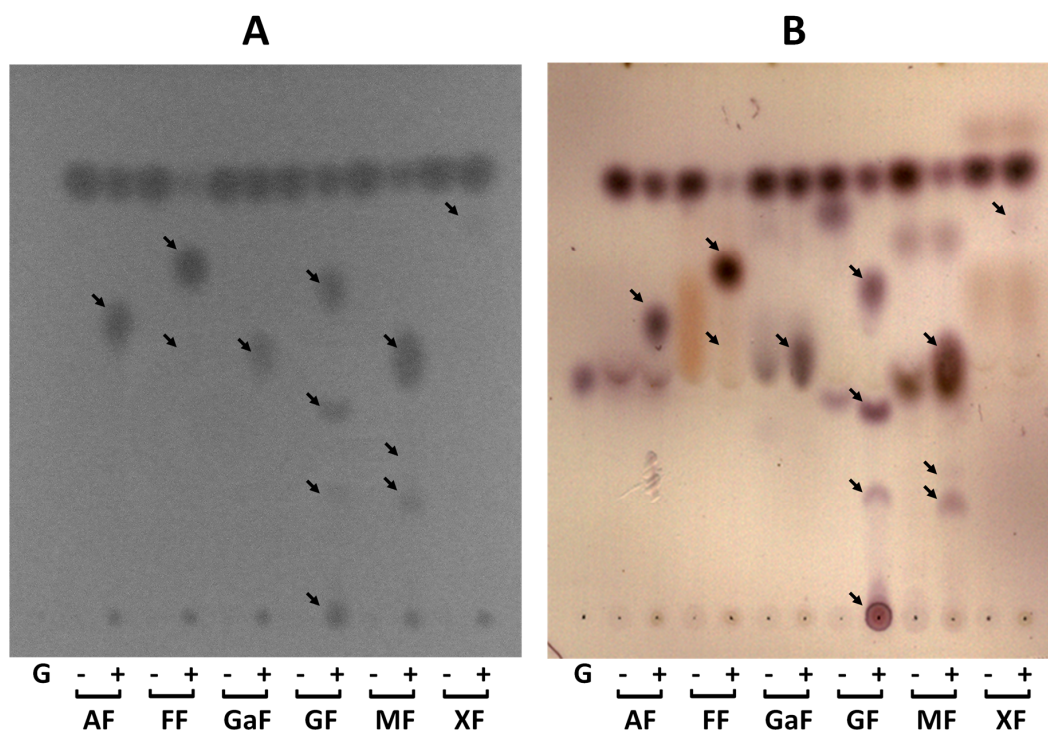


Figure 3.29 TLC detection of transglycosylation catalyzed by BGlu1 E386G2 with various donors. The BGlu1 E386G2 was incubated with 10 mM *p*NPC2 and 10 mM donors in 150 mM NH_4HCO_3 , pH 7.0, at 30°C for 16 hr. The reactions were performed without (-) or with (+) enzyme. The products were separated by silica gel TLC with EtOAc-MeOH-water (7:2.5:1, v/v/v) as a developing solvent and *p*NP-containing products were detected under UV light (A), then carbohydrates were detected by exposure to 10% sulfuric acid in ethanol, followed by charring (B). G is glucose. A and B show reactions with the donors: AF, α -AraF; FF, α -FucF; GaF, α -GalF; GF, α -GlcF; MF, α -ManF; and XF, α -XylF.

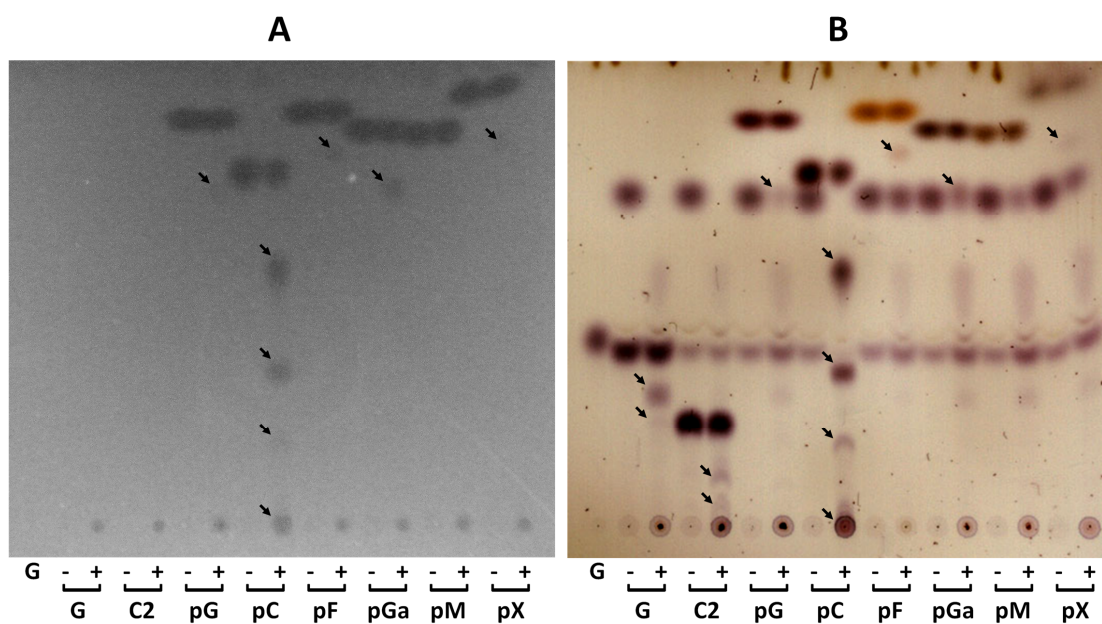
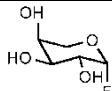
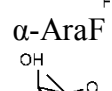
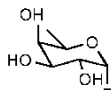
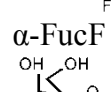
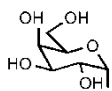
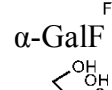
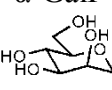
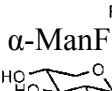
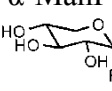
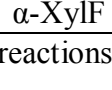


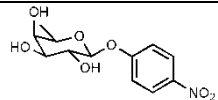
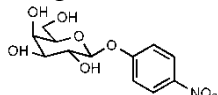
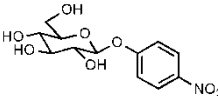
Figure 3.30 TLC detection of transglycosylation catalyzed by BGlu1 E386G2 with various acceptors. The BGlu1 E386G2 was incubated with 10 mM α -GlcF and 10 mM acceptors in 150 mM NH_4HCO_3 , pH 7.0, at 30°C for 16 hr. The reactions were performed without (-) or with (+) enzyme. The products were separated by silica gel TLC with EtOAc-MeOH-water (7:2.5:1, v/v/v) as a developing solvent and detected under UV light (A) or by exposure to 10% sulfuric acid in ethanol, followed by charring (B). The first lane is glucose standard. The acceptor substrates given for the different lanes are: G, glucose; C2, cellobiose; pG, *p*NPGlc; pC, *p*NPC2; pF, *p*NPFuc; pGa, *p*NPGal; pM, *p*NPMan; and pX, *p*NPXyl.

Table 3.9 Products of glycosynthase reactions of BGlu1 E386G2 glycosynthase using different donors and *p*NPC2 acceptor^a.

Rxn	Donor	<i>p</i> NP-oligosaccharide product (% yield)		
		Tri	Tetra	Total Yield
9b		25	0.051	25.1
c		59	0.072	59.1
	α -AraF	(630)	(762)	
10b		49	0.011	49.0
c		98	1.4	99.4
	α -FucF	(644)	(790)	
11b		15	0.013	15.0
c		42	0.018	42.0
	α -GalF	(660)	(822)	
12b		19	0.21	19.2
c		71	7.9	78.9
	α -ManF	(660)	(822)	
13b		1.2	0.0091	1.21
c		3.1	0.013	3.11
	α -XylF	(630)	(762)	

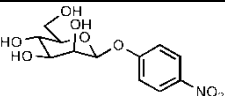
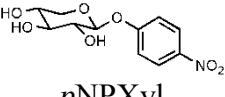
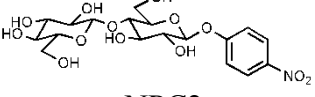
^aPreparative reactions in 150 mM NH₄HCO₃ buffer, pH 7.0, 30°C, at a 1:1^b and 3:1^c molar ratios of glycosyl fluoride donor:*p*NPC2 acceptor, and 40 μ M E386G2 concentration for 24 hr. The relative percents are in terms of peak area per total 300 nm absorbance in *p*NP-glycoside products separated by HPLC on a ZORBAX carbohydrate column. The molecular mass [Mass+³⁵Cl]⁻ of each eluted compound was confirmed by mass spectrometry, as shown by the mass in parenthesis (in a.m.u).

Table 3.10a Products of glycosynthase reactions of BGlu1 E386G2 glycosynthase using α -glucosyl fluoride donor and different acceptors^a.

Rx n	Acceptor	<i>p</i> NP-oligosaccharide product (% yield)								
		Di	Tri	Tetra	Penta	Hexa	Hepta	Octa	Nana	Total Yield
14b	 <i>p</i> NPFuc	4.2	0.040							4.24
c		7.3 (482)	0.074 (644)	-	-	-	-	-	-	7.37
15b	 <i>p</i> NPGal	9.1	0.15							9.25
c		11 (498)	0.21 (660)	-	-	-	-	-	-	11.2
16b	 <i>p</i> NPGlc	3.0	0.49	0.15	0.12					3.76
c		3.4	0.55	0.14	0.13	-	-	-	-	4.22
		(498)	(660)	(822)	(984)					

^aPreparative reactions in 150 mM NH₄HCO₃ buffer, pH 7.0, 30°C, at a 1:1^b and 3:1^c molar ratios of α -GlcF donor:*p*NP-glycoside acceptor, and 40 μ M E386G2 concentration for 24 hr. The relative percents are in terms of peak area per total 300 nm absorbance in *p*NP-glycoside products separated by HPLC on a ZORBAX carbohydrate column. The molecular mass [Mass+³⁵Cl]⁻ of each eluted compound was confirmed by mass spectrometry as shown in parenthesis (in a.m.u).

Table 3.10b Products of glycosynthase reactions of BGlu1 E386G2 glycosynthase using α -glucosyl fluoride donor and different acceptors^a.

Rx n	Acceptor	<i>p</i> NP-oligosaccharide product (% yield)								
		Di	Tri	Tetra	Penta	Hexa	Hepta	Octa	Nana	Total Yield
17b		0.062	0.035	0.046	-	-	-	-	-	0.143
c	<i>p</i> NPMan	0.068 (498)	0.032 (660)	0.039 (822)	-	-	-	-	-	0.139
18b		3.1	0.1	0.052	-	-	-	-	-	3.25
c	<i>p</i> NPXyl	4.0 (468)	0.17 (630)	0.051 (792)	-	-	-	-	-	4.22
19b			26 (660)	16 (822)	11 (984)	3.5 (1146)	0.47 (1308)	0.03 (1471)	0.002 (1633)	57.0
	<i>p</i> NPC2									

See footnotes from Table 3.10a.

CHAPTER IV

DISCUSSION

4.1 Protein expression and purification

Rice BGlu1 proteins: β -glucosidase enzymes, glycosynthase enzymes, glycosynthase mutant enzymes and new construct glycosynthase enzyme, were expressed in the *E. coli* strain Origami(DE3) as N-terminal thioredoxin and hexahistidine tag fusion proteins. Thioredoxin fusion protein was purified by 3 to 4 purification steps, depending on the desired purity. All enzymes were purified by 1st IMAC, enterokinase cleavage and 2nd IMAC for characterization, while the glycosynthase and its mutant enzymes were further purified by Superdex 200 gel filtration chromatography for crystallization. In each case, separate IMAC resin columns were used for each type of enzyme to avoid cross-contamination. Although, the purity of the proteins after the 2nd IMAC and S200 gel filtration steps appeared similar, based on SDS-PAGE (Figures 3.1-3.4), the glycosynthase and its mutant enzymes were still passed through Superdex 200 gel filtration to eliminate any trace amount of impurity that was not obvious on SDS-PAGE. Finally, >95% pure proteins were used for crystallization.

4.2 Protein crystallization

In order to determine three-dimensional structures by X-ray crystallography, high concentrations of pure, fresh proteins are required for protein crystallization. The glycosynthase and its mutant enzymes derived from rice BGlu1 could be crystallized by the hanging drop vapor diffusion method with microseeding and varied around the conditions used for crystallization of BGlu1 (Chuenchor *et al.*, 2006; 2008). Highly pure and homogeneous, freshly prepared proteins yielded reproducible, good quality crystals, whereas mixed or old proteins produced only poor crystals. Moreover, when the protein preparation, precipitant or another reagent was changed, the crystallization conditions were optimized around the previous successful condition to reproduce good quality crystals.

4.3 3D structures of three glycosynthases in complexes with substrates

The structures of BGlu1 E386G, E386A and E386S glycosynthases without and with α -GlcF donor substrate and *p*NPC2 acceptor substrate were determined to investigate the binding of the substrates in their active sites. The E386G glycosynthase was both co-crystallized and soaked with *p*NPC2, as well as with both α -GlcF and *p*NPC2, but *p*NPC2 was not observed in the active site. Nonetheless, α -GlcF was observed in the active sites of structures from crystals soaked with α -GlcF alone or both α -GlcF and *p*NPC2. During crystallization of the BGlu1 E386G with *p*NPC2, *p*NP was observed in the crystallization drops, suggesting the *p*NP may have come from autolysis of the substrate or the hydrolysis of the substrate by wild type

BGlu1 (E386) β -glucosidase contamination, as describe in Section 3.10, or the β -glucosidase activity of the BGlu1 E386G could be rescued by MES in the crystallization drops (Chuenchor *et al.*, 2011). When the crystals were soaked for longer periods, the crystal mosaicities generally increased and the crystals broke down after soaking for approx. 3 hr, suggesting they may have produced long oligosaccharides that pushed the crystal matrix apart.

The determination of the structures of the BGlu1 E386G, E386A and E386S glycosynthases in apo and α -GlcF-bound forms is the most thorough structural investigation of one enzyme's glycosynthase mutants to date and the first description of an α -GlcF complex for a glycosynthase (Figure 3.8). It was anticipated that the structures of the rice BGlu1 glycosynthases, E386G, E386A and E386S could help explain why the glycosynthase activity of BGlu1 E386G was 3-fold higher than that of E386S and 19-fold higher than E386A (Hommalai *et al.*, 2007). It was previously speculated that an additional water molecule might bind in the glycine glycosynthase in the position of the serine hydroxyl of the serine glycosynthase and form a similar interaction as the Ser hydroxyl, but with more optimal geometry (Mayer *et al.*, 2000). However, the structures were indeed very similar and there was no evidence for an extra water in the glycine glycosynthase. One water was found in a position that was conserved with that observed to stabilize the covalent complex of the BGlu1 with G2F (Figure 3.9) (Chuenchor *et al.*, 2008), and which also corresponds to the position of the nucleophile O ϵ of apo wild type BGlu1. This water molecule position is similar to that of the water in the structure of Man26A β -mannanase E320G glycosynthase complexed with mannobiose (Jahn *et al.*, 2003b). The E386G mutant is likely the most efficient glycosynthase due to the flexible positioning of this water

molecule and surrounding protein atoms, as well as other dynamic issues that cannot be fully understood from the static X-ray crystallographic structural model. Indeed, the current initial Michaelis complex structures do not account for changes in the ternary complex with the acceptor and at the transition state, which may be more critical for determining the relative activities (Ducros *et al.*, 2003).

The higher glycosynthase activity of E386S relative to E386A may be because the water of E386S is closer to the fluorine of α -GlcF than in E386A. The strong hydrogen bond between the S386 O γ and the water that hydrogen bonds to the fluorine atom may aid fluoride ion departure better than the weaker hydrogen bond between water and fluoride in the E386A mutant. Jahn *et al.* (2003) suggested that the serine can directly hydrogen bond to the fluoride to aid its departure, but the S386 residue in BGlu1 E386S is pointed to the water molecule noted above, suggesting its coordination of the water is more important than direct interaction with the fluorine atom in the BGlu1 E386G glycosynthase. As noted by Ducros *et al.* (2003) for *Humicola insolens* Cel7B Ser glycosynthase complexes with lactose or cellobiose, the Ser hydroxyl may be closer to the fluoride in the transition state, thereby contributing more to its departure. Paradoxical as it may seem, both the strong hydrogen bond from the hydroxyl of the Ser glycosynthase (E386S) and the greater flexibility of the Gly glycosynthase (E386G) appear to increase the glycosynthase activity compared to the Ala glycosynthase (E386A).

4.4 Structures of BGlu1 E386G glycosynthase complexed with cellooligosaccharides

The oligosaccharides cellotetraose and cellopentaose, which could serve as glycosynthase acceptors or products, were soaked into the E386G crystals and the structures were determined. When the crystals were cocrystallized with 2 mM cellotetraose or cellopentaose and soaked in cryoprotectant with the same concentrations of cellooligosaccharides, no cellotetraose or cellopentaose was observed in the active site. Although the oligosaccharides added for cocrystallization may be hydrolyzed by BGlu1 contamination (Section 3.10), the results also suggested the concentration used for soaking the crystals was too low to yield high occupancy binding. Therefore, the crystals from cocrystallization with 2 mM cellotetraose or cellopentaose were soaked in cryoprotectant saturated with the cellotetraose or cellopentaose, rather than the 2 mM cellotetraose and 1 mM cellopentaose concentrations previously used for the BGlu1 E176Q mutant.

The structures of rice BGlu1 E386G in complex with cellotetraose and cellopentaose confirmed that the interactions between the amino acids and glucose moieties in the active site seen in the E176Q acid/base mutant (Chuenchor *et al.*, 2011) are also found in the glycosynthase, except the slight shift in N245 to straddle Glc2 O6 and Glc3 O2 (Figure 3.13), rather than Glc3 O2 and O3 in the E176Q cellooligosaccharide complexes. This shift may reflect an inherent plasticity in oligosaccharide binding by this enzyme. Other residues that make obvious interactions with the oligosaccharides include S334 and Y341, residues that interact primarily with Glc4 and Glc5 at the +3 and +4 subsites. The Y341 residue interacts via a water-mediated hydrogen bond to the glycosidic oxygen between subsites +2

and +3 and aromatic-sugar stacking interactions at subsites +3 and +4, while the sidechain and α -carbonyl of S334 form water-mediated hydrogen bonds at subsite +3.

4.5 Oligosaccharide-binding residue mutants

Based on the observed interactions between S334 and Y341 and the oligosaccharides (Figures 3.19 and 3.20), the BGlu1 mutants S334A, Y341A and Y341L were generated to investigate how they would affect hydrolysis and synthesis of cellooligosaccharides. The BGlu1 N245V mutant was previously shown to hydrolyse *p*NPGLc, cellobiose and cellotriose more slowly than does the wild type β -glucosidase (Chuenchor *et al.*, 2008), which reflects the flexibility of N245 to hydrogen bond to sugars in either the +1 subsite (in E176Q with laminaribiose) or the +2 subsite (in E176Q with cellopentaose and cellotetraose) (Chuenchor *et al.*, 2011), or both (in the E386G structures determined in this work). The BGlu1 S334A, Y341A and Y341L mutants had slightly lower catalytic activities for cellotriose, cellotetraose and cellopentaose than the wild type BGlu1. Moreover, the BGlu1 N245V mutant had considerably lower activity than the wild type, in line with its formation of hydrogen bonds at the +2 subsite. Although the S334 and Y341 residues interact primarily with Glc4 and Glc5 at the +3 and +4 subsites, thereby contributing to the hydrolysis of cellooligosaccharides, the effects were small, likely due to the presence of an alternative binding mode for cellooligosaccharide hydrolysis, as discussed below.

4.6 Transglycosylation

The hypothesis that the long cellooligosaccharide-binding cleft of rice BGlu1 allowed its glycosynthase to synthesize longer oligosaccharides than do other

exoglycosidase-based glycosynthases has been proposed (Hommalai *et al.*, 2007). Since the BGlu1 mutants S334A, Y341A, Y341L and N245V were in the oligosaccharide binding site and had small effects on cellooligosaccharide hydrolysis, the same mutations of E386G glycosynthase were tested to see whether they affected the production of long oligosaccharides in transglycosylation reactions with α -GlcF donor and *p*NPC2 acceptor. The BGlu1 E386G/Y341A, E386G/Y341L and E386G/N245V glycosynthases synthesize shorter *p*NP-cellooligosaccharides than do the unmodified E386G glycosynthase and the E386G/S334A mutant glycosynthase under the same conditions. Small and similar amounts of the hydrolysis product *p*NPGlc were also seen in the HPLC of E386G glycosynthase and its mutants, due to approx. 0.1% BGlu1 E386 β -glucosidase contamination in the expression system (Table 3.5, Figure 3.28). Another hydrolysis product, glucose, which is produced from both α -GlcF and *p*NP-oligosaccharides, was more evident in the aglycone binding cleft mutants (Figure 3.15). Since only a small amount of *p*NPGlc was produced from *p*NPC2 hydrolysis in each case (<1% of the total *p*NP-oligosaccharides, Table 3.5), and the binding site mutants of the hydrolase are slightly less efficient at release of Glc from *p*NP-oligosaccharides, this is unlikely to result from hydrolysis of *p*NP-oligosaccharides. Therefore, the extra glucose in the mutants is likely a result of the less efficient acceptor binding, resulting in an increased partitioning of the reaction to hydrolysis of α -GlcF relative to transglycosylation.

4.7 Structures of oligosaccharide-binding site mutants

The structures of BGlu1 E386G glycosynthase mutants complexed with cellobetraose and cellopentaose were investigated to explain the effect of these

mutants. Cellotetraose was observed only in the active site of the BGlu1 E386G/S334A and BGlu1 E386G/Y341A mutants, while no electron densities for cellotetraose and cellopentaose were observed in the active sites of the other glycosynthase mutants. These results may be because the crystal sizes for other complexes were too small, thus gave poor X-ray diffraction (Figure 3.6). The cellotetraose and amino acid residues in the active site of the BGlu1 E386G/S334A glycosynthase mutant are similar to those in the cellotetraose complex of BGlu1 E386G. In contrast, the Glc2, Glc3 and Glc4 at subsites +1, +2 and +3 in the structure of the Y341A glycosynthase mutant are flipped nearly 180°, and moved from their positions in the active site of BGlu1 E386G (Figures 3.19 and 3.20), thus O6 of Glc4 directly hydrogen bonds to Q187 Nε. The relatively small effects of mutation of Y341 on the hydrolysis of oligosaccharides was initially surprising, particularly those with glucose residues that would stack on its aromatic ring. However, the structure of the Y341A mutant of the E386G glycosynthase could explain this as being due to the change in position of the oligosaccharide in the active site.

The alternative binding mode observed for cellotetraose in the structures of the Y341A glycosynthase mutant appears to still allow the hydrolytic reaction to occur, as long as the -1 subsite is filled correctly and the target glycosidic bond is in a similar position as in the complexes with the BGlu1 E176Q and E386G mutants. However, the synthesis of oligosaccharides by the glycosynthase requires the oligosaccharide acceptor to bind with the nonreducing residue in the weakly binding +1 subsite, where the shift in position may be more destabilizing. The fact that only the initial binding mode is observed in BGlu1 E176Q and E386G crystals without additional mutations suggests that it is the most stable binding mode. However, the small effects of the

Y341 mutants on hydrolysis suggest that the energy of binding in the second mode observed in the BGlu1 E386G/Y341A mutant complex with cellotetraose may be only slightly less favorable than that in the previously observed mode. This suggests that the wild type BGlu1 can bind celooligosaccharides in more than one position, which may allow efficient funneling of these substrates into the active site. The lower production of long oligosaccharides in the glycosynthase with this mutation suggests that the glycosynthase activity requires the originally observed binding mode or both binding modes for efficient production of long celooligosaccharides.

4.8 Donor and acceptor specificities

The rice BGlu1 E386G glycosynthase was capable of synthesizing longer oligosaccharides using α -AraF, α -FucF, α -GalF, α -ManF and α -XylF donors and *p*NPC2 acceptor (Figure 3.21). Moreover, the BGlu1 E386G and its glycosynthase mutants could use glucose, cellobiose, *p*NPGlc, *p*NPFuc, *p*NPGal and *p*NPXyl as acceptors (Figures 3.22, 3.23 and 3.24, and Tables 3.6 and 3.7), but no transglucosylation product was observed for *p*NPMan by TLC, although very low amounts were detectable by LC-MS. The S334A mutant had similar glycosynthase activity to the original BGlu1 E386G glycosynthase (Figures 3.23 and 3.24), whereas the Y341A, Y341L and N245V mutants synthesized shorter oligosaccharides. The E386G glycosynthase could synthesize longer products with *p*NPFuc, but not with the other acceptors, when the amount of enzyme was increased to 80 μ M (Figure 3.25 and Table 3.6). The results suggested that the E386G glycosynthase and its mutants have relatively broad substrate specificity to synthesize mixed oligosaccharide

products, which is similar to hydrolysis of a broad range of substrates by the wild type BGlu1 β -D-glucosidase (Opassiri *et al.*, 2004).

In their previous study, Hommalai *et al.* (2007) never observed the formation of products with glucose, cellobiose and *p*NPGlc as acceptors, but glycosyl transfer products of *p*NPGlc have been observed with wild type BGlu1 β -glucosidase (Opassiri *et al.*, 2004). In addition, the *p*NPGlc and *p*NPFuc were cleaved to *p*NP, glucose and fucose (Figures 3.22 and 3.25, Tables 3.6 and 3.7), while *p*NPGlc was produced from *p*NPC2 (top of Figure 3.21), which suggested wild type contamination of the BGlu1 E386G glycosynthase preparation (Section 3.10). In every case, new IMAC resins were used for purification of the glycosynthases, so it is unlikely contamination could have occurred during purification. Comparison of purification of wild type BGlu1 and BGlu1 E386G by the method of Hommalai *et al.* (2007) indicated that these enzymes could not have been separated by purification (data not shown). Therefore, it appeared that a mutation in the Origami(DE3) *E. coli* strain being used for expression may have led to a higher than normal reversion rate, possibly by misreading on the ribosome or reversion mutations in a few cells in the expression culture (Parker, 1989; Kramer and Farabaugh, 2007). This suggested that some of the products formed may have been generated by a combination of glycosynthase and wild type transglycosylation activities.

4.9 NMR characterization of reaction product linkages

Characterization of purified products provided evidence for the combined action of BGlu1 wild type and E386G glycosynthase. Mass spectrometric and NMR characterization identified the purified products of reaction of α -GlcF and *p*NPFuc

catalyzed by the BGlu1 E386G preparation as Fuc- β -(1 \rightarrow 3)-Fuc-*p*NP, Glc- β -(1 \rightarrow 3)-Fuc-*p*NP and Fuc- β -(1 \rightarrow 4)-Glc- β -(1 \rightarrow 3)-Fuc-*p*NP (Table 3.8). Since glycosynthase mutants of BGlu1 show very little *p*NP-glycoside hydrolysis (Hommalai *et al.*, 2007), the nonreducing end fucosyl moieties in products of Fuc- β -(1 \rightarrow 3)-Fuc-*p*NP and Fuc- β -(1 \rightarrow 4)-Glc- β -(1 \rightarrow 3)-Fuc-*p*NP from reaction of α -GlcF and *p*NPFuc most likely came from transfucosylation from *p*NPFuc by wild type BGlu1 contamination, as diagrammed in Figure 4.1A. Nonetheless, those products resulting from the transfer of glucosyl residues represent actual glycosynthase products, since the wild type BGlu1 enzyme cannot hydrolyze or transfer from α -glycosyl-fluorides.

Streptomyces β -glucosidase glycosynthase is regiospecific for production of β -(1 \rightarrow 3)-linkages to *p*NP-monosaccharide acceptors and can use *p*NPFuc and *p*NPGal acceptors (Faijes *et al.*, 2006), while *Agrobacterium* β -glucosidase, which is regiospecific to produce β -(1 \rightarrow 4)-linkages does not use these acceptor substrates effectively (Prade *et al.*, 1998; Mackenzie *et al.*, 1998; Mayer *et al.*, 2000; Kim *et al.*, 2004). As such, rice BGlu1 appears to be more similar to *Streptomyces* β -glucosidase glycosynthase in its activity toward these acceptors.

4.10 Cyclophellitol inhibition

The wild type BGlu1 contamination of the E386G preparation was confirmed by inhibition of the wild type enzyme with the covalent inhibitor cyclophellitol. As shown in Figure 4.1B, cyclophellitol inactivates retaining β -D-glucosidases by forming a covalent adduct with the catalytic nucleophile, which is recalcitrant to rescue by transglycosylation (Gloster *et al.*, 2007). The cyclophellitol inhibition

results show that the combination of wild type BGlu1 and E386G glycosynthase seen in the contaminated preparation was likely responsible for synthesis of the novel *p*NP-oligosaccharide Fuc- β -(1 \rightarrow 4)-Glc- β -(1 \rightarrow 3)-Fuc-*p*NP, which could not be produced by either enzyme alone (Figure 3.28). This points to the importance of testing for wild type hydrolase activity when assessing glycosynthase products, since the transglycosylation products of small amounts of contaminating hydrolase can be significant, given the large amount of glycosynthase needed for the transfer reactions.



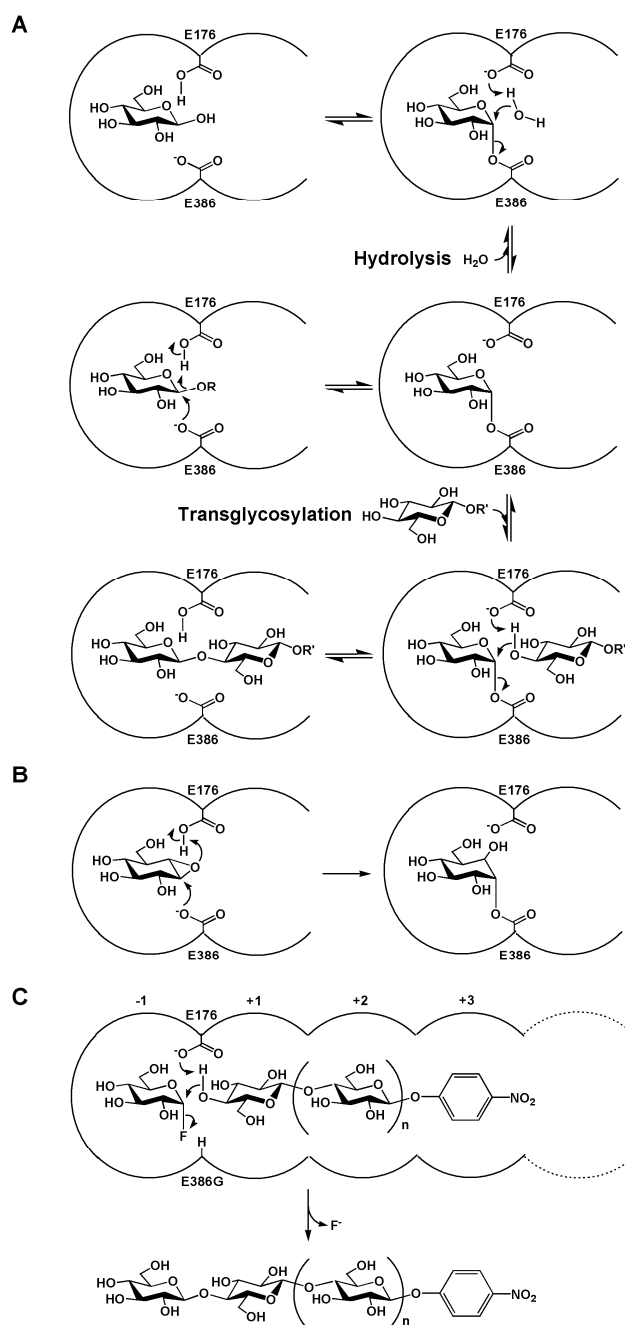


Figure 4.1 Reaction mechanisms of hydrolysis and transglycosylation catalyzed by rice BGlu1 β -glucosidase (A); covalent intermediate trapping of rice BGlu1 by cyclophellitol (B), and rice BGlu1 E386G glycosynthase (C). Note that cyclophellitol cannot react with BGlu1 E386 due to its lack of a catalytic nucleophile (Pengthaisong *et al.*, 2012).

4.11 Transglycosylation activity of BGlu1 E386G2

A new mutation of BGlu1 E386G was made by changing GAA (Glu) to GGC instead of GGG to give the Gly, in order to decrease the probability of misread as Glu (GAG) by the ribosome or of a reversion mutation in the expression culture. The BGlu1 E386G2 glycosynthase could transglycosylate a broad range of substrates similar to the original BGlu1 E386G glycosynthase (Figures 3.29 and 3.30), while no hydrolytic activity was detected in the standard assay. The E386G2 glycosynthase synthesized longer oligosaccharides using α -GlcF donor and *p*NPGlc, *p*NPMan, *p*NPXyl or *p*NPC2 acceptors (Table 3.10), similar to the glycosynthases from *Agrobacterium* β -glucosidase (Mackenzie *et al.*, 1998; Mayer *et al.*, 2000), while the *Streptomyces* E383A glycosynthase synthesized only disaccharide using α -GlcF and *p*NP-monosaccharide acceptors (Faijes *et al.*, 2006).

Surprisingly, there was a clear spot of laminaribiose when glucose was used as an acceptor (Figures 3.24 and 3.30), and this spot was seen in the other reactions, likely due to the presence of glucose from hydrolysis of α -GlcF. A similar product was also seen in each lane of the E386G2 reaction with *p*NPFuc and α -GlcF and in E386G prep reactions with 2 mM cyclophellitol, but not in the reaction with wild type BGlu1 (Figure 3.28). The production of laminaribiose is in line with the fact that laminaribiose is a much better substrate than cellobiose and other disaccharides for hydrolysis by the wild type BGlu1 β -glucosidase (Opassiri *et al.*, 2004), and binding of an acceptor glucose in position to make a (1 \rightarrow 3)-linkage would allow hydrogen bonding of its C1 hydroxyl with N245, as seen in the crystal structure with laminaribiose (Chuenchor *et al.*, 2011). The enzyme also catalyzed autocondensation

of α -GlcF, as seen by the smear above glucose in the TLC and LC-MS peaks with masses of 379 m/z ($[M+^{35}Cl]^-$).

Transglycosylation yields of BGlu1 E386G2 with a variety of donors and *p*NPC2 acceptor are shown in Table 3.9, and those with α -GlcF and a variety of acceptors in Table 3.10. Relatively high yields were obtained with α -FucF and α -ManF donors, but only low yield with α -XylF. The absence of a 5-methyl group apparently affects binding at the -1 subsite, although the activity was higher than that of non-evolved glycosynthases derived from *Agrobacterium* β -glucosidase (Mackenzie *et al.*, 1998; Mayer *et al.*, 2000; Kim *et al.*, 2004) and *Streptomyces* E383A (Faijes *et al.*, 2006), for which α -XylF was not a donor substrate. Moreover, E386G2 could use α -AraF as a donor, which has not previously been reported for a GH1 glycosynthase. The E386G2 glycosynthase gave low yields with *p*NPFuc, *p*NPGal, *p*NPGlc and *p*NPXyl acceptors and α -GlcF donor, compared to the *Streptomyces* E383A glycosynthase (Faijes *et al.*, 2006).

Although *p*NPGal and *p*NPFuc, on which the glycosyl residue could be added either β -(1 \rightarrow 3) or β -(1 \rightarrow 6) due to their axial 4-OH, gave the highest yields for disaccharide production, only very small amounts of trisaccharides and no tetrasaccharides were detected on LC-MS. In contrast, *p*NPGlc, for which small amounts of 3 disaccharide peaks could be seen on LC-MS (data not shown), was a better starting substrate from production of trisaccharides and tetrasaccharides could only be detected for substrates with equatorial 4-OH groups (*p*NPGlc, *p*NPXyl and *p*NPMan). As noted previously (Hommalai *et al.*, 2007), the BGlu1 E386G glycosynthase appears to require a β -(1 \rightarrow 4)-linked primer, such as *p*NPC2, before it can transfer successive glucosyl residues onto a β -(1 \rightarrow 4)-linked chain with high

regioselectivity. This suggests the β -(1 \rightarrow 4)-linked disaccharides produced in the first transfer served as efficient acceptor substrates for further linkages, while glycosides with other linkages did not.

Comparison of *Streptomyces* E383A, which efficiently adds β -(1 \rightarrow 3)-linked glycosyl residues to *p*NP-monosaccharides to produce disaccharides but not trisaccharides, with *Agrobacterium* glycosynthases, which tend to add β -(1 \rightarrow 4)-residues and make trisaccharides and tetrasaccharides (Mackenzie *et al.*, 1998; Mayer *et al.*, 2000), indicates a similar pattern. Both *Streptomyces* E383A and rice BGlu1 E386G2 can extend β -(1 \rightarrow 3)-linked *p*NP-disaccharides, but with poor efficiency compared to β -(1 \rightarrow 4)-linked *p*NPC2. This likely reflects the relatively straight structural nature of β -(1 \rightarrow 4)-linked oligosaccharides.

For *p*NPC2 acceptor, the BGlu1 E386G2 glycosynthase gave lower yields of trisaccharide products (26% with α -GlcF), but higher yields of tetrasaccharide (16%) and longer products, compared to *Agrobacterium* E358A (79% trisaccharide and 13% tetrasaccharide under comparable conditions) and E358S (88% trisaccharide, 7% tetrasaccharide) and *Streptomyces* E383A glycosynthase (80% trisaccharide and 3% tetrasaccharide). As noted previously, the unique feature of rice BGlu1 glycosynthases is their ability to produce long oligosaccharides (Hommalai *et al.*, 2007), so that BGlu1 E386G also produced cellopentaose in 11% yield. At donor to acceptor ratios above 1:1, the yields could not be assessed by HPLC with α -GlcF donor and *p*NPC2 acceptor, since these reactions resulted in precipitated products. Thus, BGlu1 E386G is more useful for synthesis of longer oligosaccharides, while the bacterial enzymes are better for synthesis of di- and tri- saccharides.

CHAPTER V

CONCLUSION

In this work, structural, mutational and enzymatic studies were used to elucidate the roles of catalytic cleft substrate-binding residues in rice BGlu1 hydrolysis of oligosaccharides and BGlu1 E386G glycosynthase transglycosylation of oligosaccharides. Structures were successfully determined for rice BGlu1 E386G, E386S and E386A glycosynthases in apo and α -glucosyl fluoride-bound complexes. Structures were also determined for E386G in complex with cellotetraose and cellopentaose. Mutagenesis of the residues N245, S334 and Y341 in the active site cleft was used to elucidate the roles of these residues in cellooligosaccharide hydrolysis by the parent β -glucosidase and synthesis by the glycosynthase. Structures of the E386G/S334A and E386G/Y341A glycosynthases in complexes with cellotetraose showed that the S334A mutation has little effect on binding, while the Y341 mutant binds in an alternate mode. The ability of the rice BGlu1 E386G glycosynthase to utilize various acceptors and donors and the effects of the mutations on this ability was also assessed. In order to complete this assessment, cyclophellitol was shown to be effective in inhibition of the wild type enzyme to allow only glycosynthase activity to contribute to the product formation.

The crystal structures of the rice BGlu1 E386G, E386A and E386S glycosynthases with and without α -glucosyl fluoride showed similar positions of active site residues and the stabilizing water molecule at the position of the

nucleophile of free BGlu1, so flexibility is likely the key to high activity in the BGlu1 E386G. Plasticity of the active site also appears to be important for binding oligosaccharides, since alterations in the sugar position result in direct hydrogen bonds from N245 at either the +1 or +2 subsites, and cellotetraose glucosyl residues may bind with their faces in different orientations to compensate for the loss of interactions from Y341. The greater effect of loss of Y341 on glycosynthase activity suggests that the binding of acceptors is not as flexible, so the effects of mutation of aglycone-binding residues on hydrolysis and transfer reactions may not be strictly comparable.

Pure rice BGlu1 E386G glycosynthase transfers glycosyl residues from a variety of α -glycosyl fluoride donors, in the reactivity order Glc > Fuc > Ara > Man > Gal > Xyl. Likewise, it transfers glucosyl residues from α -GlcF to several different acceptors, with a preference for formation of (1→4) linkages when the acceptor includes a nonreducing terminal β -(1→4)-linked oligosaccharide. Only equatorial hydroxyls on the ring appear to be glycosylated, so if the C4 hydroxyl is axial, the monosaccharide is added to the C3 hydroxyl. However the products formed in this way do not appear to serve as effective acceptors for further transfer reactions. Care must be taken to avoid contamination by wild type enzyme arising either from laboratory procedures, mutations in the expression culture or translational misincorporation, since, otherwise, initially formed glycosynthase products can be hydrolyzed, and unexpected transglycosylation products formed. When the presence of enzyme with the native nucleophile residue is suspected, cyclophellitol is a useful inhibitor that can be used to differentiate glycosynthase from β -glucosidase transglycosylation activities.



REFERENCES

REFERENCES

- Addington, T., Calisto, B., Alfonso-Prieto, M., Rovira, C., Fita, I., and Planas, A. (2011). Re-engineering specificity in 1,3-1,4- β -glucanase to accept branched xyloglucan substrates. **Proteins**. 79: 365-375.
- Akinbi, H.T., Epaud, R., Bhatt, H., and Weaver, T.E. (2000). Bacterial killing is enhanced by expression of lysozyme in the lungs of transgenic mice. **J. Immunol**. 165: 5760-5766.
- Alais, J. and David, S. (1990). Preparation of disaccharides having a β -D-mannopyranosyl group from N-phthaloyllactosamine derivatives by double or triple SN2 substitution. **Carbohydr. Res**. 201: 69-77.
- Amaya, M.F., Watts, A.G., Damager, I., Wehenkel, A., Nguyen, T., Buschiazzi, A., Paris, G., Frasch, A.C., Withers, S.G., and Alzari, P.M. (2004). Structural insights into the catalytic mechanism of *Trypanosoma cruzi* trans-sialidase. **Structure**. 12: 775-784.
- Barleben, L., Panjikar, S., Ruppert, M., Koepke, J., and Stockigt, J. (2007). Molecular architecture of strictosidine glucosidase: The gateway to the biosynthesis of the monoterpenoid indole alkaloid family. **Plant Cell**. 19: 2886-2897.
- Bojarová, P. and Kren, V. (2009). Glycosidases: A key to tailored carbohydrates. **Trends Biotechnol**. 27: 199-209.

- Bradford, M.M. (1976). A rapid and sensitive method for the quantification of microgram quantities of protein utilizing the principle of protein-dye binding. **Anal. Biochem.** 72: 264-273.
- Bravman, T., Belakhov, V., Solomon, D., Shoham, G., Henrissat, B., Baasov, T., and Shoham, Y. (2003). Identification of the catalytic residues in family 52 glycoside hydrolase, a β -xylosidase from *Geobacillus stearothermophilus* T-6. **J. Biol. Chem.** 278: 26742-26749.
- Burmeister, W.P., Cottaz, S., Driguez, H., Iori, R., Palmieri, S., and Henrissat, B. (1997). The crystal structures of *Sinapis alba* myrosinase and a covalent glycosyl-enzyme intermediate provide insights into the substrate recognition and active-site machinery of an S-glycosidase. **Structure.** 5: 663-675.
- Carbohydrate Active Enzymes database, glycoside hydrolase classification; URL <http://www.cazy.org/Glycoside-Hydrolases.html>
- Chuenchor, W., Pengthaisong, S., Yuvaniyama, J., Opassiri, R., Svasti, J., and Ketudat Cairns, J.R. (2006). Purification, crystallization and preliminary X-ray analysis of rice BGlu1 β -glucosidase with and without 2-deoxy-2-fluoro- β -D-glucoside. **Acta Crystallogr. F.** 62: 798-801.
- Chuenchor, W., Pengthaisong, S., Robinson, R.C., Yuvaniyama, J., Oonant, W., Bevan, D.R., Esen, A., Chen, C.-J., Opassiri, R., Svasti, J., and Ketudat Cairns, J.R. (2008). Structural insights into rice BGlu1 β -glucosidase oligosaccharide hydrolysis and transglycosylation. **J. Mol. Biol.** 377: 1200-1215.

- Chuenchor, W., Pengthaisong, S., Robinson, R.C., Yuvaniyama, J., Svasti, J., and Ketudat Cairns, J.R. (2011). The structural basis of oligosaccharide binding by rice BGlu1 beta-glucosidase. **J. Struct. Biol.** 173: 169-179.
- Cicek, M., Blanchard, D., Bevan, D.R., and Esen, A. (2000). The aglycone specificity-determining sites are different in 2,4-dihydroxy-7-methoxy-1,4-benzoxazin-3-one (DIMBOA)-glucosidase (Maize β -glucosidase) and dhurrinase (sorghum β -glucosidase). **J. Biol. Chem.** 275: 20002-20011.
- Cobucci-Ponzano, B., Strazzulli, A., Rossi, M., and Moracci, M. (2011). Glycosynthases in biocatalysis. **Adv. Synth. Catal.** 353: 2284-2300.
- Cortés, M.L., de Felipe, P., Martín, V., Hughes, M.A., and Izquierdo, M. (1998). Successful use of a plant gene in the treatment of cancer *in vivo*. **Gene Therapy.** 5: 1499-507.
- Cremer, D. and Pople, J.A. (1975). A general definition of ring puckering coordinates. **J. Am. Chem. Soc.** 97: 1354-1358.
- Crout, D.H. and Vic, G. (1998). Glycosidases and glycosyl transferases in glycoside and oligosaccharide synthesis. **Curr. Opin. Chem. Biol.** 2: 98-111.
- Czjzek, M., Cicek, M., Zamboni, V., Bevan, D.R., Henrissat, B., and Esen, A. (2000). The mechanism of substrate (aglycone) specificity in β -glucosidases is revealed by crystal structures of mutant maize β -glucosidase-DIMBOA, -DIMBOAGlc, and -dhurrin complexes. **Proc. Natl. Acad. Sci.** 97: 13555-13560.
- Czjzek, M., Cicek, M., Zamboni, V., Burmeister, W.P., Bevan, D.R., Henrissat, B., and Esen, A. (2001). Crystal structure of a monocotyledon (maize ZMGlu1)

- beta-glucosidase and a model of its complex with *p*-nitrophenyl β -D-thioglucoside. **Biochem. J.** 354: 37-46.
- Dan, S., Marton, I., Dekel, M., Bravdo, B.A., He, S., Withers, S., and Shoseyov, O. (2000). Cloning, expression, characterization and nucleophile identification of family 3, *Aspergillus niger* β -glucosidase. **J. Biol. Chem.** 275: 4973-4980.
- Davies, G. and Henrissat, B. (1995). Structures and mechanisms of glycosyl hydrolases. **Structure.** 3: 853-859.
- Davies, G.J., Wilson, K.S., and Henrissat, B. (1997). Nomenclature for sugar-binding subsites in glycosyl hydrolases. **Biochem. J.** 321: 557-559.
- Davis, I.W., Leaver-Fay, A., Chen, V.B., Block, J.N., Kapral, G.J., Wang, X., Murray, L.W., Arendall, W.B. III, Snoeyink, J., Richardson, J.S., and Richardson, D.C. (2007). MolProbity, all-atom contacts and structure validation for proteins and nucleic acids. **Nucleic Acids Res.** 35: W375-W383.
- Day, A.G. and Withers, S.G. (1986). The purification and characterization of a β -glucosidase from *Alcaligenes faecalis*. **Biochem. Cell Biol.** 64: 914-922.
- Day, A.J., Canada, F.J., Diaz, J.C., Kroon, P.A., McLauchlan, R., Faulds, C.B., Plumb, G.W., Morgan, M.R., and Williamson, G. (2000). Dietary flavonoid and isoflavone glycosides are hydrolysed by the lactase site of lactase phlorizin hydrolase. **FEBS Lett.** 468: 166-170.
- Dharmawardhana, D.P., Ellis, B.E., and Carlson, J.E. (1995). A β -glucosidase from lodgepole pine specific for the lignin precursor coniferin. **Plant Physiol.** 107: 331-339.
- Driguez, H. (2001). Thiooligosaccharides as tools for structural biology. **Chem. Biochem.** 2: 311-318.

- Ducros, V.M., Tarling, C.A., Zechel, D.L., Brzozowski, A.M., Frandsen, T.P., von Ossowski, I., Schülein, M., Withers, S.G., and Davies, G.J. (2003). Anatomy of glycosynthesis, structure and kinetics of the *Humicola insolens* Cel7B E197A and E197S glycosynthase mutants. **Chem. Biol.** 10: 619-628.
- Duroux, L., Delmotte, F. M., Lancelin, J. M., Kéravis, G. & Jay-Alleand, C. (1998). Insight into naphthoquinone metabolism: beta-glucosidase-catalysed hydrolysis of hydrojuglone beta-D-glucopyranoside. **Biochem. J.** 333: 275-283.
- Duvic, B. and Soderhall, K. (1992). Purification and partial characterization of a β -1,3-glucan-binding-protein membrane receptor from blood cells of the crayfish *Pacifastacus leniusculus*. **Eur. J. Biochem.** 207: 223-228.
- Dwek, R.A. (1996). Glycobiology: toward understanding the function of sugars. **Chem. Rev.** 96: 683-720.
- Emsley, P. and Cowtan, K. (2004). Coot: model-building tools for molecular graphics, **Acta Crystallogr. D Biol. Crystallogr.** 60: 2126-2132.
- Estrada, A., Yun, C.H., Van Kessel, A., Li, B., Hauta, S., and Laarveld, B. (1997). Immunomodulatory activities of oat β -glucan *in vitro* and *in vivo*. **Microbiol. Immunol.** 41: 991-998.
- Euler, A.R., Mitchell, D.K., Kline, R., and Pickering, L.K. (2005). Prebiotic effect of fructo-oligosaccharide supplemented term infant formula at two concentrations compared with unsupplemented formula and human milk. **J. Pediatr. Gastroenterol. Nutr.** 40: 157-164.

- Faijes, M., Saura-Vall, M., Perez, X., Conti, M., and Planas, A. (2006). Acceptor dependent regioselectivity of glycosynthase reactions by *Streptomyces* E383A β -glucosidase. **Carbohydr. Res.** 341: 2055-2065.
- Fairweather, J.K., Faijes, M., Driguez, H., and Planas, A. (2002). Specificity studies of *Bacillus* 1,3-1,4- β -glucanases and application to glycosynthase-catalyzed transglycosylation. **Chem. Biochem.** 3: 866-873.
- Fort, S., Boyer, V., Greffe, L., Davies, G.J., Moroz, O., Christiansen, L., Schulein, M., Cottaz, S., and Driguez, H. (2000). Highly efficient synthesis of β -(1-4)-oligo- and -polysaccharides using a mutant cellulase. **J. Am. Chem. Soc.** 122: 5429-5437.
- Gamblin, D.P., Scanlan, E.M., and Davis, B.G. (2009). Glycoprotein synthesis: an update. **Chem. Rev.** 109: 131-163.
- Gill, S.C. and von Hippel, P.H. (1989). Calculation of protein extinction coefficients from amino acid sequence data. **Anal. Biochem.** 182: 319-326.
- Gloster, T.M., Madsen, R., and Davies, G.J. (2007). Structural basis for cyclophellitol inhibition of a beta-glucosidase. **Org. Biomol. Chem.** 5: 444-446.
- Gunther, W. and Kunz, H. (1992). Synthesis of β -D-mannosides from β -D-glucosides via an intramolecular SN2 reaction at C-2. **Carbohydr. Res.** 228: 217-241.
- Haberer, G. and Kieber, J.J. (2002). Cytokinins. New insights into a classic phytohormone. **Plant Physiol.** 128: 354-362.
- Hakulinen, N., Paavilainen, S., Korpela, T., and Rouvinen, J. (2000). The crystal structure of β -glucosidase from *Bacillus circulans* sp. *alkalophilus*: ability to form long polymeric assemblies. **J. Struct. Biol.** 129: 69-79.

- Hancock, S.M., Vaughan, M.D., and Withers, S.G. (2006). Engineering of glycosidases and glycosyltransferases. **Curr. Opin. Chem. Biol.** 10: 509-519.
- Henrissat, B. (1991). A classification of glycosyl hydrolases based on amino-acid sequence similarities. **Biochem. J.** 280: 309-316.
- Henrissat, B. and Bairoch, A. (1993). New families in the classification of glycosyl hydrolases based on amino acid sequence similarities. **Biochem. J.** 293: 781-788.
- Henrissat, B. and Bairoch, A. (1996). Updating the sequence-based classification of glycosyl hydrolases. **Biochem. J.** 316: 695-696.
- Henrissat, B. and Davies, G. (1997). Structural and sequence-based classification of glycoside hydrolases. **Curr. Opin. Struct. Biol.** 7: 637-44.
- Hiroimi, K., Nitta, Y., Namura, C., and Ono, S. (1973). Subsite affinities of glucoamylase, examination of the validity of the subsite theory. **Biochim. Biophys. Acta.** 302: 362-375.
- Hommalai, G., Withers, S.G., Chuenchor, W., Ketudat Cairns, J.R., and Svasti, J. (2007). Enzymatic synthesis of cello-oligosaccharides by mutated rice β -glucosidases. **Glycobiology.** 17: 744-753.
- Honda, Y.W. and Kitaoka, M. (2006). The first glycosynthase derived from an inverting glycoside hydrolase. **J. Biol. Chem.** 281: 1426-1431.
- Honda, Y., Fushinobu, S., Hidaka, M., Wakagi, T., Shoun, H., Taniguchi, H., and Kitaoka, M. (2008). Alternative strategy for converting an inverting glycoside hydrolase into a glycosynthase. **Glycobiology.** 18: 325-330.

- Hrmova, M., Harvey, A.J., Wang, J., Shirley, N.J., Jones, G.P., Stone, B.A., Høj, P.B., and Fincher, G.B. (1996). Barley beta-D-glucan exohydrolases with beta-D-glucosidase activity. Purification, characterization, and determination of primary structure from a cDNA clone. **J. Biol. Chem.** 271: 5277-5286.
- Hrmova, M., MacGregor, E.A., Biely, P., Stewart, R.J., and Fincher, G.B. (1998) Substrate binding and catalytic mechanism of a barley β -D-glucosidase/(1,4)- β -D-glucan exohydrolase. **J. Biol. Chem.** 273: 11134-11143.
- Hrmova, M., Imai, T., Rutten, S.J., Fairweathers, J.K., Pelosi, L., Bulone, V., Driguez, H., and Fincher, G.B. (2002). Mutants of a barley (1-3)-beta-D-glucan endohydrolase synthesize crystalline (1-3)-beta-D-glucans. **J. Biol. Chem.** 277: 30102-30111.
- Ishihara, K., Miyazaki, H., Kurosaki, T., and Nakabayashi, N. (1995). Improvement of blood compatibility on cellulose dialysis membrane. III. Synthesis and performance of water-soluble cellulose grafted with phospholipid polymer as coating material on cellulose dialysis membrane. **J. Biomed. Mater. Res.** 29: 181-188.
- Isorna, P., Polaina, J., Latorre-Garcia, L., Canada, F.J., Gonzalez, B., and Aparicio, S.J. (2007). Crystal structures of *Paenibacillus polymyxa* glucosidase B complexes reveal the molecular basis of substrate specificity and give new insights into the catalytic machinery of family I glycosidases. **J. Mol. Biol.** 371: 1204-1218.
- Jahn, M., Marles, J., Warren, R.A., and Withers, S.G. (2003). Thioglycoligases: mutant glycosidases for thioglycoside synthesis. **Angew. Chem. Int. Ed. Engl.** 42: 352-354.

- Jahn, M., Stoll, D., Warren, R.A.J., Szabó, L., Singh, P., Gilbert, H.J., Ducros, V.M., Davies, G.J., and Withers, S.G. (2003). Expansion of the glycosynthase repertoire to produce defined manno-oligosaccharides. **Chem. Commun.** 12: 1327-1329.
- Jahn, M., Chen, H.M., Müllegger, J., Marles, J., Warren, R.A.J., and Withers, S.G. (2004). Thioglycosynthases: Double mutant glycosidases that serve as scaffolds for thioglycoside synthesis. **Chem. Commun.** 3: 274-275.
- Jakeman, D.L. and Withers, S.G. (2002). On expanding the repertoire of glycosynthases: mutant β -galactosidases forming β -(1,6)-linkages. **Can. J. Chem.** 80: 866-870.
- Jakob, C.A., Bodmer, D., Spirig, U., Battig, P., Marcil, A., Dignard, D., Bergeron, J.J., Thomas, D.Y., and Aebi, M. (2001). Htm1p, a mannosidase-like protein, is involved in glycoprotein degradation in yeast. **EMBO Rep.** 2: 423-430.
- Jenkins, J., Leggio, L.L., Harris, G., and Pickersgill, R. (1995). β -glucosidase, β -galactosidase, family A cellulases, family F xylanases and two barley glucanases form a superfamily of enzymes with 8-fold β/α architecture and with two conserved glutamates near the carboxy-terminal ends of β strands four and seven. **FEBS Lett.** 362: 281-285.
- Jones, T.A., Zou, J.Y., Cowan, S.W., and Kjeldgaard, M. (1991). Improved methods for building protein models in electron density maps and the location of errors in these models. **Acta Crystallogr. A.** 47: 110-119.
- Kacc, T. (1995). A modification of the phenol-sulphuric acid method of total sugar determination. **Appl. Biochem. Biotechnol.** 53: 207-214.

- Kempton, J.B. and Withers, S.G. (1992). Mechanism of *Agrobacterium* β -glucosidase: kinetic studies. **Biochemistry**. 31: 9961-9969.
- Ketudat Cairns, J.R. and Esen, A. (2010). β -Glucosidases. **Cell Mol. Life Sci.** 67: 3389-3405.
- Kim, Y.W., Lee, S.S., Warren, R.A.J., and Withers, S.G. (2004). Directed evolution of a glycosynthase from *Agrobacterium* sp. increases its catalytic activity dramatically and expands its substrate repertoire. **J. Biol. Chem.** 279: 42787-42793.
- Kim, Y.W., Chen, H., and Withers, S.G. (2005). Enzymatic transglucosylation of xylose using a glycosynthase. **Carbohydr. Res.** 340: 2735-2741.
- Kim, Y.W., Fox, D.T., Hekmat, O., Kantner, T., McIntosh, L.P., and Withers, S.G. (2006). Glycosynthase-based synthesis of xylo-oligosaccharides using an engineered retaining xylanase from *Cellulomonas fimi*. **Org. Biomol. Chem.** 4: 2025-2032.
- Kim, Y.W., Lovering, A.L., Chen, H.M., Kantner, T., McIntosh, L.P., Strynadka, N.C.J., and Withers, S.G. (2006). Expanding the thioglycosylase strategy to the synthesis of α -linked thioglycosides allows structural investigation of the parent enzyme/substrate complex. **J. Am. Chem. Soc.** 128: 2202-2203.
- Klemm, D., Schumann, D., Udhardt, U., and Marsch, S. (2001). Bacterial synthesized cellulose-artificial blood vessels for microsurgery. **Prog. Polym. Sci.** 26: 1561-1603.
- Knapp, S., Vocadlo, D., Gao, Z., Kirk, B., Lou, J., and Withers, S.G. (1996). NAG-Thiazoline, an N-acetyl- β -hexosaminidase inhibitor that implicates acetamido participation. **J. Am. Chem. Soc.** 118: 6804-6805.

- Koshland, D.E. (1953). Stereochemistry and the mechanism of enzymatic reactions. **Biological Reviews**. 28: 416-436.
- Kramer, E.B. and Farabaugh, P.J. (2007). The frequency of translational misreading errors in *E. coli* is largely determined by tRNA competition. **RNA**. 13: 87-96.
- Laemmli, U.K. (1970). Cleavage of structural proteins during the assembly of the head of bacteriophage T4. **Nature**. 227: 680-685.
- Laskowski, R.A., MacArthur, M.W., Moss, D.S., and Thornton, J.M. (1993). PROCHECK, a program to check the stereochemical quality of protein structures. **J. Appl. Crystallogr.** 26: 283-291.
- Leah, R., Kigel, J., Svendsen, I., and Mundy, J. (1995). Biochemical and molecular characterization of a barley seed β -glucosidase. **J. Biol. Chem.** 270: 15789-15797.
- Legler, G. (1990). Glycoside hydrolases: mechanistic information from studies with reversible and irreversible inhibitors. **Adv. Carbohydr. Chem. Biochem.** 48: 319-384.
- Lieshout, J.V., Fajjes, M., Nieto, J., Oost, J.V., and Planas, A. (2004). Hydrolase and glycosynthase activity of endo-1,3- β -glucanase from the thermophile *Pyrococcus furiosus*. **Archaea**. 1: 285-292.
- Ly, H.D. and Withers, S.G. (1999). Mutagenesis of glycosidases. **Annu. Rev. Biochem.** 68: 487-522.
- Mackenzie, L.F., Wang, Q., Warren, R.A.J., and Withers, S.G. (1998). Glycosynthases: mutant glycosidases for oligosaccharide synthesis. **J. Am. Chem. Soc.** 120: 5583-5584.

- MacLeod, A.M., Tull, D., Rupitz, K., Warren, R.A.J., and Withers, S.G. (1996). Mechanistic consequences of mutation of active site carboxylates in a retaining β -1,4-glycanase from *Cellulomonas fimi*. **Biochemistry**. 35: 13165-13172.
- Mayer, C., Jakeman, D.L., Mah, M., Karjala, G., Gal, L., Warren, R.A.J., and Withers, S.G. (2001). Directed evolution of new glycosynthases from *Agrobacterium* β -glucosidase: a general screen to detect enzymes for oligosaccharide synthesis. **Chem. Biol.** 8: 437-443.
- Mayer, C., Zechel, D.L., Reid, S.P., Warren, R.A.J., and Withers, S.G. (2000). The E358S mutant of *Agrobacterium* sp. β -glucosidase is a greatly improved glycosynthase. **FEBS. Lett.** 466: 40-44.
- Michelin, K., Wajner, A., and Goulart, L.S. (2004). Biochemical study on β -glucosidase in individuals with Gaucher's disease and normal subjects. **Clin. Chem. Acta.** 343: 145-153.
- Mizutani, M., Nakanishi, H., Ema, J., Ma, S.J., Noguchi, E., Inohara-Ochiai, M., Fukuchi-Mizutani, M., Nakao, M., and Sakata, K. (2002). Cloning of beta-primeverosidase from tea leaves, a key enzyme in tea aroma formation. **J. Plant Physiol.** 130: 2164-2176.
- Moracci, M., Trincone, A., and Rossi, M. (2001). Glycosynthase: new enzymes for oligosaccharide synthesis. **J. Mol. Catal. B: Enzyme.** 11: 155-163.
- Müllegger, J., Jahn, M., Chen, H.M., Warren, R.A.J., and Withers, S.G. (2005). Engineering of a thioglycoligase: randomized mutagenesis of the acid-base residue leads to the identification of improved catalysis. **Protein Eng. Des. Sel.** 18: 33-40.

- Müllegger, J., Chen, H., Chan, W.Y., Reid, S.P., Jahn, M., Warren, R.A.J., Salleh, H.M., and Withers, S.G. (2006). Thermostable glycosynthases and thioglycoligases derived from *Thermotoga maritima* β -glucuronidase. **Chem. Bio. Chem.** 7: 1028-1030.
- Murshudov, G.N., Lebedev, A., Vagin, A.A., Wilson, K.S., and Dodson, E.J. (1999). Efficient anisotropic refinement of macromolecular structures using FFT. **Acta Crystallogr. D.** 55: 247-255.
- Naim, H.Y. (2001). Molecular and cellular aspects and regulation of intestinal lactase-phlorizin hydrolase. **Histol. Histopathol.** 16: 553-561.
- Namchuck, N.M. and Withers, S.G. (1995). Mechanism of *Agrobacterium* β -glucosidase: kinetic analysis of the role of noncovalent enzyme/substrate interactions. **Biochemistry.** 34: 16194-16202.
- Nashiru, O., Zechel, D.L., Stoll, D., Mohammadzadeh, T., Warren, R.A., and Withers, S.G. (2001). β -Mannosynthase: synthesis of β -mannosides with a mutant β -mannosidase. **Angew. Chem. Int. Ed. Engl.** 40: 417-420.
- Naumoff, D.G. (2011). Hierarchical classification of glycoside hydrolases. **Biochem. (Moscow).** 76: 622-635.
- Navaza, J. (1994). AMoRe: an automated package for molecular replacement. **Acta Crystallogr. A.** 50: 157-163.
- Noguchi, J., Hayashi, Y., Baba, Y., Zkino, O., and Kimura, M. (2008). Crystal structure of the covalent intermediate of human cytosolic β -glucosidase. **Biochem. Biophys. Res. Comm.** 374: 549-552.

- Opassiri, R., Ketudat Cairns, J.R., Akiyama, T., Wara-Aswapati, O., Svasti, J., and Esen, A. (2003). Characterization of a rice β -glucosidase gene highly expressed in flower and germinating shoot. **Plant Sci.** 165: 627-638.
- Opassiri, R., Hua, Y., Wara-Aswapati, O., Akiyama, T., Svasti, J., Esen, A., and Ketudat Cairns, J.R. (2004). β -Glucosidase, exo- β -glucanase and pyridoxine transglucosylase activities of rice BGlu1. **Biochem. J.** 379: 125-131.
- Opassiri, R., Pomthong, B., Onkoksoong, T., Akiyama, T., Esen, A., and Ketudat Cairns, J. R. (2006). Analysis of rice glycosyl hydrolase family 1 and expression of Os4bglu12 beta-glucosidase. **BMC Plant Biol.** 33.
- Otwinowski, Z. and Minor, W. (1997). Processing of X-ray diffraction data collected in oscillation mode. **Methods Enzymol.** 276: 307-326.
- Parker, J. (1989). Errors and alternatives in reading the universal genetic code. **Microbiol. Rev.** 53: 273-298.
- Pengthaisong, S., Chen, C.-F., Withers, S.G., Kuaprasert, B., and Ketudat Cairns, J.R. (2012). Rice BGlu1 glycosynthase and wild type transglycosylation activities distinguished by cyclophellitol inhibition. **Carbohydr. Res.** 352:51-59.
- Perugino, G., Trincone, A., Rossi, M., and Moracci, M. (2004). Oligosaccharide synthesis by glycosynthases. **Trends Biotechnol.** 22: 31-37.
- Prade, H., Mackenzie, L.F., and Withers, S.G. (1998). Enzymatic synthesis of disaccharides using *Agrobacterium* sp. β -glucosidase. **Carbohydr. Res.** 305: 371-381.
- Rakić, B. and Withers, S.G. (2009). Recent developments in glycoside synthesis with glycosynthases and thioglycoligases. **Aust. J. Chem.** 62: 510-520.

- Rempel, B.P. and Withers, S.G. (2008). Covalent inhibitors of glycosidases and their applications in biochemistry and biology. **Glycobiology**. 18: 570-586.
- Ross, P., Mayer, R., and Benziman, M. (1991). Cellulose biosynthesis and function in bacteria. **Microbiol. Rev.** 55: 35-58.
- Sanz-Aparicio, J., Hermoso, J.A., Martinez-Ripoll, M., Lequerica, J.L., and Polaina, J. (1998). Crystal structure of β -glucosidase A from *Bacillus polymyxa*: insights into the catalytic activity in family 1 glycosyl hydrolases. **J. Mol. Biol.** 275: 491-502.
- Shaikh, F.A. and Withers, S.G. (2008). Teaching old enzymes new tricks: engineering and evolution of glycosidases and glycosyl transferases for improved glycosides synthesis. **Biochem. Cell Biol.** 86: 169-177.
- Shawn, J. and Skerrett, M.D. (2004). Lysozyme in pulmonary host defense new tricks for an old dog. **Am. J. Respir. Crit. Care Med.** 169: 435-436.
- Sinnott, M.L. (1990). Catalytic mechanisms of enzymatic glycosyl transfer. **Chem. Rev.** 90: 1171-1202.
- Skriver, K., Olsen, F.L., Rogers, J.C., and Mundy, J. (1991). Cis-acting DNA elements responsive to gibberellin and its antagonist abscisic acid. **Proc. Natl. Acad. Sci. U. S. A.** 88: 7266-7270.
- Stick, R.V., Stubbs, K.A., and Watts, A.G. (2004). Modifying the regioselectivity of glycosynthase reactions through changes in the acceptor. **Aust. J. Chem.** 57: 779-786.
- Street, I.P., Kempton, J.B., and Withers, S.G. (1992). Inactivation of a β -glucosidase through the accumulation of a stable 2-deoxy-2-fluoro- α -D-

- glucopyranosylenzyme intermediate: a detailed investigation. **Biochemistry**. 31: 9970-9978.
- Sue, M., Yamazaki, K., Yajima, S., Nomura, T., Matsukawa, T., Iwamura, H., and Miyamoto, T. (2006). Molecular and structural characterization of hexameric β -D-glucosidases in wheat and rye. **Plant. Physiol.** 141: 1237-1247.
- Sugimura, M., Nishimoto, M., and Kitaoka, M. (2006). Characterization of glycosynthase mutants derived from glycosyl hydrolase family 10 xylanases. **Biosci. Biotechnol. Biochem.** 70: 1210-1215.
- Sulzenbacher, G., Shareck, F., Morosoli, R., Dupont, C., and Davies, G.J. (1997). The *Streptomyces lividans* family 12 endoglucanase: construction of the catalytic core, expression, and X-ray structure at 1.75 Å resolution. **Biochemistry**. 36: 16032-16039.
- Tai, V.W., Fung, P.H., Wong, Y.S., and Shing, T.K. (1995). Kinetic studies on cyclophellitol analogues--mechanism-based inactivators. **Biochem. Biophys. Res. Commun.** 213: 175-80.
- Terwisscha van Scheltinga, A.C., Armad, S., Kalk, K.H., Isogai, A., Henrissat, B., and Dijkstra, B. (1995). Stereochemistry of chitin hydrolysis by a plant chitinase/lysozyme and x-ray structure of a complex with allosamidin: evidence for substrate assisted catalysis. **Biochemistry**. 34: 15619-15623.
- Thiem, J. (1995). Application of enzymes in synthetic carbohydrate chemistry. **FEMS Microbiol. Rev.** 16: 193-211.
- Trimbur, D.E., Warren, R.A.J., and Withers, S.G. (1992). Region-directed mutagenesis of residues surrounding the active site nucleophile in β -glucosidase from *Agrobacterium faecalis*. **J. Biol. Chem.** 267: 10248-10251.

- Trincone, A., Perugino, G., Rossi, M., and Moracci, M. (2000). A novel thermophilic glycosynthase that effects branching glycosylation. **Bioorg. Med. Chem. Lett.** 10: 365-368.
- Vallmitjana, M., Ferrer-Navarro, M., Planell, R., Abel, M., Ausin, C., Querol, E., Planas, A., and Pérez-Pons, J.A. (2001). Mechanism of the family 1 β -glucosidase from *Streptomyces* sp: Catalytic residues and kinetic studies. **Biochemistry.** 40: 5975-5982.
- Varrot, A., Yip, V.L., Li, Y., Rajan, S.S., Yang, X., Anderson, W.F., Thompson, J., Withers, S.G., and Davies, G.J. (2005). NAD⁺ and metal-ion dependent hydrolysis by family 4 glycosidases: structural insight into specificity for phospho-beta-D-glucosides. **J. Mol. Biol.** 346: 423-435.
- Verdoucq, L., Czjzek, M., Moriniere, J., Bevan, D.R., and Esen, A. (2003). Mutational and structural analysis of aglycone specificity in maize and sorghum β -glucosidases. **J. Biol. Chem.** 278: 25055-25062.
- Verdoucq, L., Morinière, J., Bevan, D.R., Esen, A., Vasella, A., Henrissat, B., and Czjzek, M. (2004). Structural determinants of substrate specificity in family 1 β -glucosidases: Novel insights from the crystal structure of sorghum dhurrinase-1, a plant β -glucosidase with strict specificity, in complex with its natural substrate. **J. Biol. Chem.** 279: 31796-31803.
- Vetter, J. (2000). Plant cyanogenic glycosides. **Toxicon.** 38: 11-36.
- Wang, Q., Graham, R.W., Trimbur, D., Warren, R.A.J., and Withers, S.G. (1994). Changing enzymatic reaction mechanisms by mutagenesis: Conversion of a retaining glucosidase to an inverting enzyme. **J. Am. Chem. Soc.** 116: 11594-11595.

- Wang, Q., Trimbur, D., Graham, R., Warren, R.A.J., and Withers, S.G. (1995). Identification of the acid/base catalyst in *Agrobacterium faecalis* β -glucosidase by kinetic analysis of mutants. **Biochemistry**. 34: 14554-14562.
- Watts, A.G., Damager, I., Amaya, M.L., Buschiazzo, A., Alzari, P., Frasch, A.C., and Withers, S.G. (2003). *Trypanosoma cruzi* trans-sialidase operates through a covalent sialyl-enzyme intermediate: tyrosine is the catalytic nucleophile. **J. Am. Chem. Soc.** 125: 7532-7533.
- Wells, L., Gao, Y., Mahoney, J.A., Vosseller, K., Chen, C., Rosen, A., and Hart, G.W. (2002). Dynamic O-glycosylation of nuclear and cytosolic proteins: further characterization of the nucleocytoplasmic β -N-acetylglucosaminidase, O-GlcNAcase. **J. Biol. Chem.** 277: 1755-1761.
- Wiesmann, C., Hengstenberg, W., and Schulz, G.E. (1997). Crystal structures and mechanism of 6-phospho- β -galactosidase from *Lacococcus lactis*. **J. Mol. Biol.** 269: 851-860.
- Wilkinson, S.M., Liew, C.W., Mackay, J.P., Salleh, H.M., Withers, S.G., McLeod, M.D. (2008). *Escherichia coli* glucuronylsynthase, an engineered enzyme for the synthesis of beta-glucuronides. **Org. Lett.** 10: 1585-1588.
- Williams, S.J. and Withers, S.G. (2000). Glycosyl fluorides in enzymatic reactions. **Carbohydr. Res.** 327: 27-46.
- Williams, S.J. and Withers, S.G. (2002). Glycosynthases: mutant glycosidases for glycoside synthesis. **Aus. J. Chem.** 55: 3-12.
- Withers, S.G., Street, I.P., Bird, P., and Dolphin, D.H. (1987). 2-Deoxy-2-fluoroglucosides: A novel class of mechanism-based glucosidase inhibitors. **J. Am. Chem. Soc.** 109: 7530-7531.

- Withers, S.G. and Street, I.P. (1988). Identification of a covalent α -D-glucopyranosyl enzyme intermediate formed on a β -glucosidase. **J. Am. Chem. Soc.** 110: 8551- 8553.
- Withers, S.G., Warren R.A.J., Street, I.P., Rupitz, K., Kempton, J.B., and Aebersold, R. (1990). Unequivocal demonstration of the involvement of a glutamate residue as a nucleophile in the mechanism of retaining glycosidase. **J. Am. Chem. Soc.** 112: 5887-5889.
- Withers, S.G. and Umezawa, K. (1991). Cyclophellitol: a naturally occurring mechanism-based inactivator of beta-glucosidases. **Biochem. Biophys. Res. Commun.** 177: 532-537.
- Withers, S.G. and Aebersold, R. (1995). Approaches to labeling and identification of active site residues in glycosidases. **Prot. Sci.** 4: 361-371.
- Yokoyama, M. (2000). Methods of synthesis of glycosyl fluorides. **Carbohydr. Res.** 327: 5-14.
- Zagrobelny, M., Bak, S., and Møller, B.L. (2008) Cyanogenesis in plants and arthropods. **Phytochemistry.** 69: 1457-1468.
- Zechel, D.L. and Withers, S.G. (2000). Glycosidase mechanisms: anatomy of a finely tuned catalyst. **Acc. Chem. Res.** 33: 11-18.
- Zhang, L., Bharadwaj, A.G., Casper, A., Barkley, J., Barycki, J.J., and Simpson, M.A. (2009). Hyaluronidase activity of human Hyal1 requires active site acidic and tyrosine residues. **J. Biol. Chem.** 284: 9433-9442.
- Zhou, H., Yu, Z., Hu, Y., Tu, J., Zou, W., Peng, Y., Zhu, J., Li, Y., Zhang, A., Yu, Z., Ye, Z., Chen, H., and Jin, M. (2009). The special neuraminidase stalk-motif

responsible for increased virulence and pathogenesis of H5N1 influenza A virus. **PLoS One.** 4: e6277.

Zopf, D. and Roth, S. (1996). Oligosaccharide anti-infective agents. **Lancet.** 347: 1017-1021.



APPENDICES



APPENDIX A

MOLECULAR MASS OF TRANGLUCOSYLATION

PRODUCTS SYNTHESIZED BY THE RICE BGLU1

E386G USING α -GLCF AND *PNPC2*

The soluble products of the reaction at the 1:1 α -GlcF donor to *pNPC2* acceptor substrate ratio were synthesized by rice BGlU1 E386G and analyzed by HPLC. The selected ion chromatograms of molecular mass [Mass + ^{35}Cl] $^{-}$ of each eluted compound was confirmed by mass spectrometry (Figure A1). However, the small amounts of longer *pNP*-oligosaccharide products (*pNPC8* and *pNPC9*), which could not be confirmed by mass spectrometry, were identified only their relative positions of peaks detected by the UV absorbance at 300 nm. The mass spectra of molecular mass [Mass + ^{35}Cl] $^{-}$ corresponding to retention time of each eluted compound was confirmed by mass spectrometry in Figure A2.

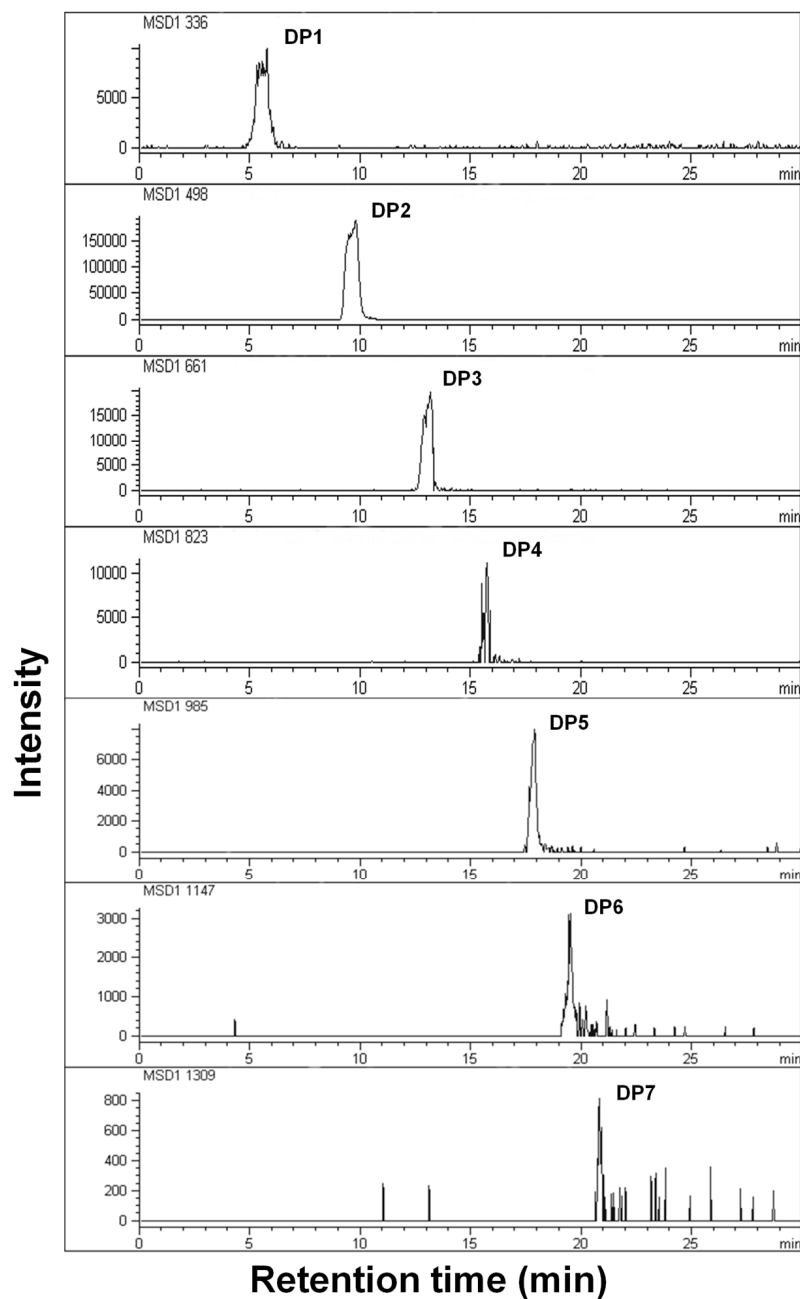


Figure A1 Selected ion chromatograms of products synthesized by the rice BGlu1 E386G using α -GlcF and *p*NPC2. The selected ion chromatograms of molecular masses [Mass + ³⁵Cl]⁻ of the *p*NP-oligosaccharide products, which ranged from DP 1-7 were analyzed by mass spectrometry. DP 1 (*p*NPGlc, 336 *m/z*), DP 2 (*p*NPC2, 498 *m/z*), DP 3 (*p*NPC3, 661 *m/z*), DP 4 (*p*NPC4, 823 *m/z*), DP 5 (*p*NPC5, 985 *m/z*), DP 6 (*p*NPC6, 1147 *m/z*), and DP 7 (*p*NPC7, 1309 *m/z*).

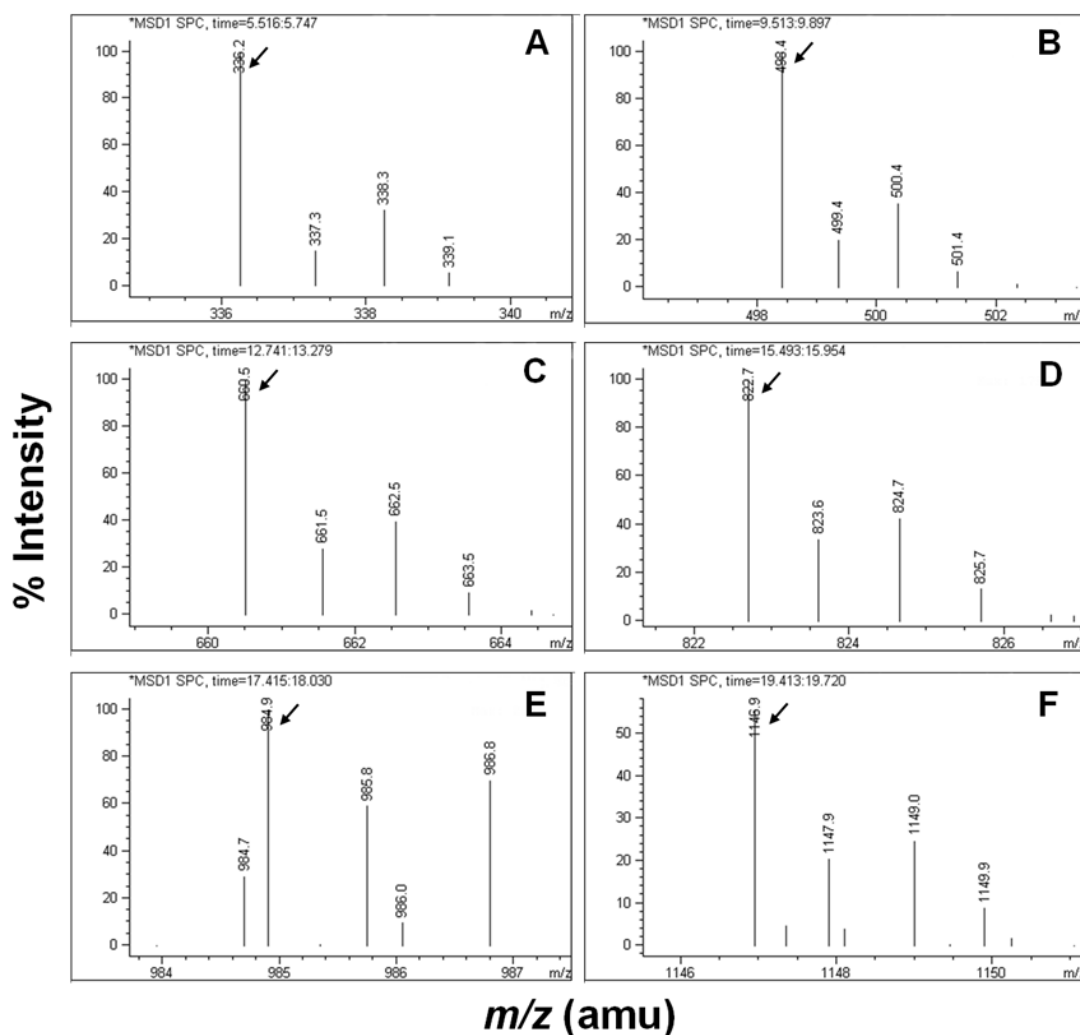


Figure A2 Mass spectra of products synthesized by the rice BGlu1 E386G using α -GlcF and p NPC2. The molecular masses $[\text{Mass} + {}^{35}\text{Cl}]^-$ of the p NP-oligosaccharide products (arrow), which ranged from DP 1-9 were analyzed by mass spectrometry. DP 1 (p NPGlc, 336 m/z), DP 2 (p NPC2, 498 m/z), DP 3 (p NPC3, 661 m/z), DP 4 (p NPC4, 823 m/z), DP 5 (p NPC5, 985 m/z), DP 6 (p NPC6, 1147 m/z), DP 7 (p NPC7, 1309 m/z), DP 8 (p NPC8, 1471 m/z), and DP 9 (p NPC9, 1633 m/z).

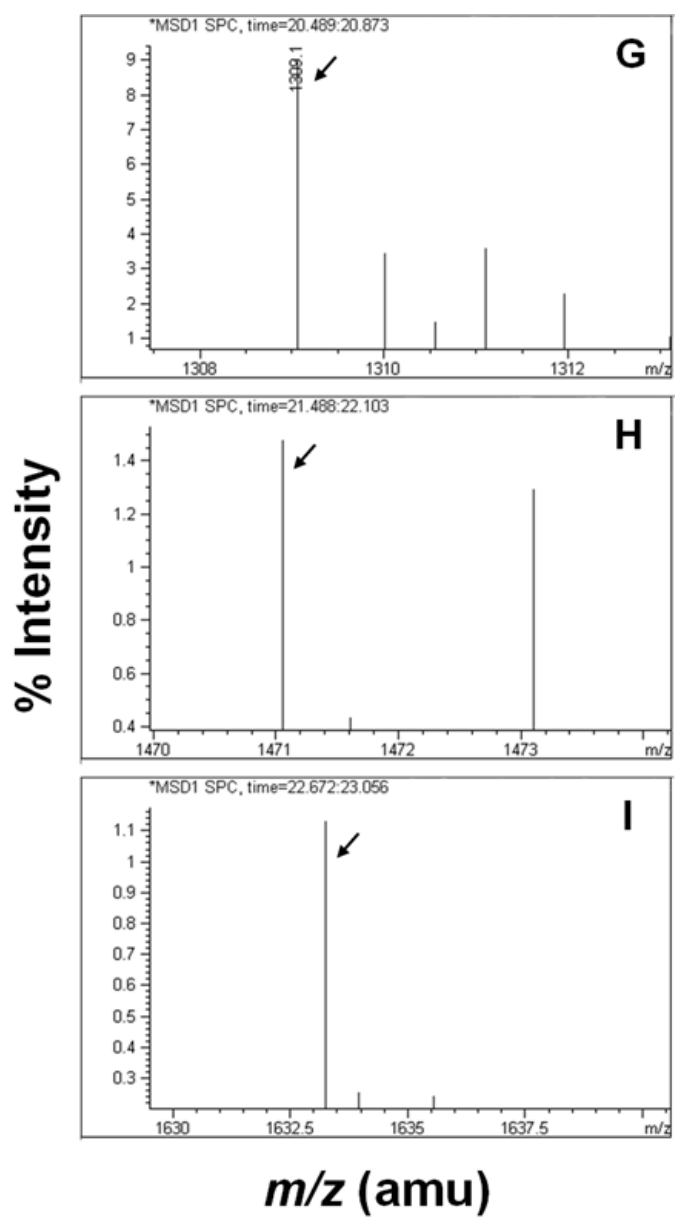


Figure A2 Mass spectra of products synthesized by the rice BGlu1 E386G using α -GlcF and *pNPC2* (continued).

APPENDIX B

PUBLICATIONS

1. Publications from Ph.D. Thesis

- 1) **Pengthaisong, S.**, Withers, S.G., Kuaprasert, B., Svasti, J., and Ketudat Cairns, J. R. (2012). The role of the oligosaccharide binding cleft of rice BGlul in hydrolysis of cellooligosaccharides and in their synthesis by rice BGlul glycosynthase. *Protein Sci.*, 21: 362-372.*

*Selected for Cover Picture and Research Highlight

- 2) **Pengthaisong, S.**, Chen, C.-F., Withers, S.G., Kuaprasert, B., Svasti, J., and Ketudat Cairns, J.R. (2012). Rice BGlul glycosynthase and wild type transglycosylation activities distinguished by cyclophellitol inhibition. *Carbohydr. Res.* 352: 51-59.

2. Other international publications

- 1) Ketudat Cairns, J.R., **Pengthaisong, S.**, Luang, S., Sansenya, S., Tankrathok, A., and Svasti, J. (2012). Protein-carbohydrate interactions leading to hydrolysis and transglycosylation in plant glycoside hydrolase family 1 enzymes. *J. Appl. Glycosci.* Accepted January 30, 2012.
- 2) Chuenchor, W., **Pengthaisong, S.**, Robinson, R.C., Yuvaniyama, J., Svasti, J., and Ketudat Cairns, J.R. (2011). The structural basis of oligosaccharide binding by rice BGlul beta-glucosidase. *J. Struct. Biol.* 173: 169-179.

- 3) Kuntothom, T., Raab, M., Tvaroska, I., Fort, S., **Pengthaisong, S.**, Cañada, F.J., Calle, L., Jimenez-Barbero, J., Ketudat Cairns, J.R., and Hrmova, M. (2010). Binding of β -D-glucosides and β -D-mannosides by rice and barley β -glycosidases with distinct substrate specificities. *Biochemistry*. 49: 8779-8793.
- 4) Chuenchor, W., **Pengthaisong, S.**, Robinson, R.C., Yuvaniyama, J., Oonant, W., Bevan, D.R., Esen, A., Chen, C.-J., Opassiri, R., Svasti, J., and Ketudat Cairns, J.R. (2008). Structural insights into rice BGlu1 β -glucosidase oligosaccharide hydrolysis and transglycosylation. *J. Mol. Biol.* 377: 1200-1215.
- 5) Chuenchor, W., **Pengthaisong, S.**, Yuvaniyama, J., Opassiri, R., Svasti, J., and Ketudat Cairns, J.R. (2006). Purification, crystallization and preliminary X-ray analysis of rice BGlu1 β -glucosidase with and without 2-deoxy-2-fluoro- β -D-glucoside inhibitor. *Acta Crystallogr. F* 62: 798-801.

CURRICULUM VITAE

NAME	Miss Salila Pengthaisong
DATE OF BIRTH	December 3, 1975
PLACE OF BIRTH	Nakhon Ratchasima, Thailand
EDUCATION	
2007- 2012	School of Biochemistry, Institute of Science, Suranaree University of Technology, Nakhon Ratchasima, Thailand Ph.D. in Biochemistry
1998-2001	Biochemistry Department, Khon Kaen University, Khon Kaen, Thailand M.Sc. in Biochemistry
1994-1998	Biochemistry Department, Khon Kaen University, Khon Kaen, Thailand B.Sc. in Biochemistry
FELLOWSHIP	
2008- 2012	Graduate student from Synchrotron Light Research Institute (Public Organization), Thailand